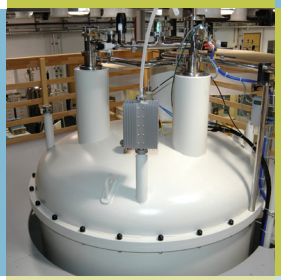

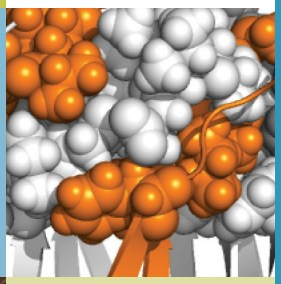

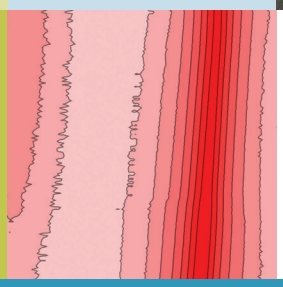

The UK 850 MHz Solid-State NMR Facility

Annual Report 2014

The UK 850 MHz Solid-State NMR Facility

In **5** years of operation:

1586 days have been allocated to

47 PIs from **22** different UK institutions

with **2290** days being requested.

Attendees at the 2014 Annual Symposium that took place at the University of Warwick on Thursday 3rd April.

Contents

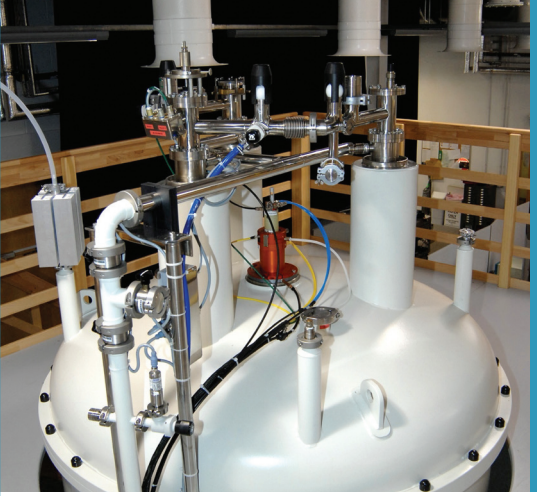

Introduction

This is our fifth annual report describing the broad range of high-quality research that continues to be carried out at the UK 850 MHz Solid-State NMR Facility. The Facility was originally funded for five years by a grant from EPSRC with a 10% contribution from BBSRC and additional funding from the University of Warwick and the European Regional Development Fund. In 2014, the original grant was extended by a further 12 months to January 2015, bringing the total grant value to almost £4M. The use of high magnetic fields in NMR spectroscopy brings increases in both sensitivity and resolution, and so the 850 MHz Facility enables experiments to be performed that are impossible at lower fields. Since its inception, the Facility has proved a valuable shared resource for the UK science community, with visiting researchers from more than 20 different institutions using the 850 MHz spectrometer for solid-state NMR studies in a range of disciplines, including chemistry, material science, Earth sciences, biology and physics.

At the fourth annual symposium in 2014, there were over 60 registered participants with 11 talks by graduate students, postdoctoral researchers and principal investigators from 9 different institutions. This meeting provides an excellent opportunity for the user community to discuss new advances in solid-state NMR and its applications and gives graduate students in the field a forum in which to present their work and meet their peers.

In April 2015, a contract was signed with UKSBS (Shared Business Services) to operate a high-field solid-state NMR facility on behalf of the UK community for a further period of three plus two years, with funding provided by EPSRC with a contribution from BBSRC. Note that this year's annual report includes new pages (55 to 60) whose content is aligned with the reporting procedure for EPSRC-funded mid-range facilities.

We hope you enjoy reading about the new and exciting science taking place at the UK 850 MHz Solid-state NMR Facility, and we look forward to welcoming both new and experienced users during the next year.

Further details of the Facility can be found on our website: **http://go.warwick.ac.uk/850mhz/**

The National Management Committee

Sharon E Ashbrook
(St Andrews)

Steven P Brown
(Chair, Warwick)

Melinda J Duer
(Cambridge)

Ray Dupree
(Warwick)

Robin K Harris
(Durham)

Mark E Smith
(Lancaster)

Jeremy J Titman
(Nottingham)

Stephen Wimperis
(Glasgow)

Organization and Management of the Facility

The UK 850 MHz solid-state NMR Facility was established with the aid of several linked research grants from EPSRC. The eight investigators on the grant comprise the National Management Committee (NMC) which determines the strategic objectives for the Facility and the procedures by which these are to be achieved. The NMC meets twice a year, communicating informally more frequently as the need arises. The operation of the Facility is the responsibility of the Local Management Team (LMT) comprising the Facility Manager (FM) who is an *ex-officio* member of the NMC and the Warwick-based NMC chair. The duties of the Facility Manager include maintaining the instrumentation and assisting visitors with their experiments. The management of the Facility is overseen by the International Advisory Board (IAB) which is made up of three eminent solid-state NMR spectroscopists from overseas: Chris Jaroniec (Ohio), Dominique Massiot (Orléans) and Roderick Wasylishen (Alberta). The terms of reference of the NMC and IAB, the remit of the LMT and the duties of the FM are available on the Facility website.

Time Allocation Process

All UK academics who are eligible to apply for Research Council funding, as well as UK researchers of similar standing in industry, may apply for an allocation of spectrometer time at the Facility. Users are expected to run their own experiments with the assistance of the Facility Manager, so personnel with previous solid-state NMR experience should be identified to visit the Facility and carry out the research (inexperienced users should contact the Facility Manager in advance, to agree a collaborative arrangement with the Facility Manager relating to the Facility Manager's role in carrying out the experiments). A minimum of 80% of the available time is allocated by an independent Time Allocation Panel (TAP) that comprises three UK scientists, including one member of the NMC, as well as the Facility Manager in an *ex-officio* capacity. The balance is allocated by the NMC and is used for fast-track applications, measurements referred from the EPSRC solid-state NMR service, the Facility Manager's designated research time, to compensate users who were unable to take up their allocated time because of instrument downtime, and a small number of maintenance days. Members of the TAP normally serve for a two-year term.

There are two allocation rounds each year for time, each covering a six-month period, starting in either February or August, corresponding to deadlines of November 30th and May 31st. Previous users of the Facility are notified of upcoming deadlines by email. Previous time allocations and instructions for applicants are given on the Facility website. The main criterion for allocating time is overall scientific merit, as well as the quality of the case made for high-field solid-state NMR. Where appropriate, the TAP will consider additional factors, such as the quality of publications arising from previous allocations of time and whether the research is supported by peer-reviewed grants or involves students funded by EPSRC or BBSRC. The TAP is charged with ensuring that the balance of the allocated time broadly reflects the research objectives of the original grant and with providing feedback for unsuccessful applicants. During the TAP meeting, the Facility Manager gives advice on the feasibility of the proposed experiments and the spectrometer time required.

The maximum time that can be requested by an individual applicant during any allocation round is 28 days, but this can be split between several applications. It is a condition that the Facility is mentioned in any publication arising wholly or partly from an allocation of time. Furthermore, a user report must be produced by the original applicant no later than the 7th of the month following the end of the specific six-month time-allocation period, i.e., 7th February or 7th August. Applications are not accepted from users who have outstanding reports from previous allocations of time. The code for all NMR pulse sequences implemented by users on the Facility's spectrometer must be deposited in a shared database. If the experiment is a new one, the code will only be made available to other users after the pulse sequence has been published. Reasonable travel costs associated with the use of the facility will be paid to academic users. The Facility rents accommodation on the University of Warwick campus for use by Facility visitors.

TAP membership (2014): Chair: Sharon Ashbrook, St. Andrews; non-NMC members: Paul Hodgkinson, Durham, Phil Williamson, Southampton (up to February 2014 round) and Mark Pfuhl, Kings College (for the August 2014 round onwards).

What is the Facility?

UK 850 MHz Solid-State NMR Facility Probes

No	Probe
1	1.3 mm probe HXY (+^{19}F) conventional insert design H13863
2	2.5 mm HXY DBB (double-broadband) H13856
3	2.5 mm HX (+^{19}F) H13889
4	2.5 mm HFX H13894
5	3.2 mm HXY DBB (double-broadband) H13857
6	3.2 mm HXY low E field for biosolids LLC H13900
7	3.2 mm HXY conventional insert design H13888
8	4 mm HXY conventional insert design (+^{19}F) H13694
9	4 mm HX (low gamma) H13892
10	7 mm X (low gamma) H13895
11	Static
12	1 mm HX (produced by Jeol)
13	DOR probe (produced by Samoson group, Tallinn, Estonia)

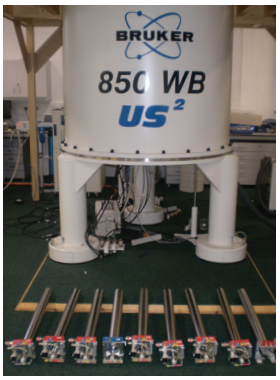

850 MHz spectrometer and probes. Probes 1 to 11 were supplied by Bruker. Maximum MAS frequencies: 4 mm probes 15 kHz; 3.2 mm probes 24 kHz, 2.5 mm probes 35 kHz; 1.3 mm probe 65 kHz. All 3.2 mm and 4 mm MAS probes are equipped with DVT stators and can operate between –140 °C and + 150 °C.

Probe usage 2010 and 2014

Year 1 to Year 5 (Round 1 to Round 10)

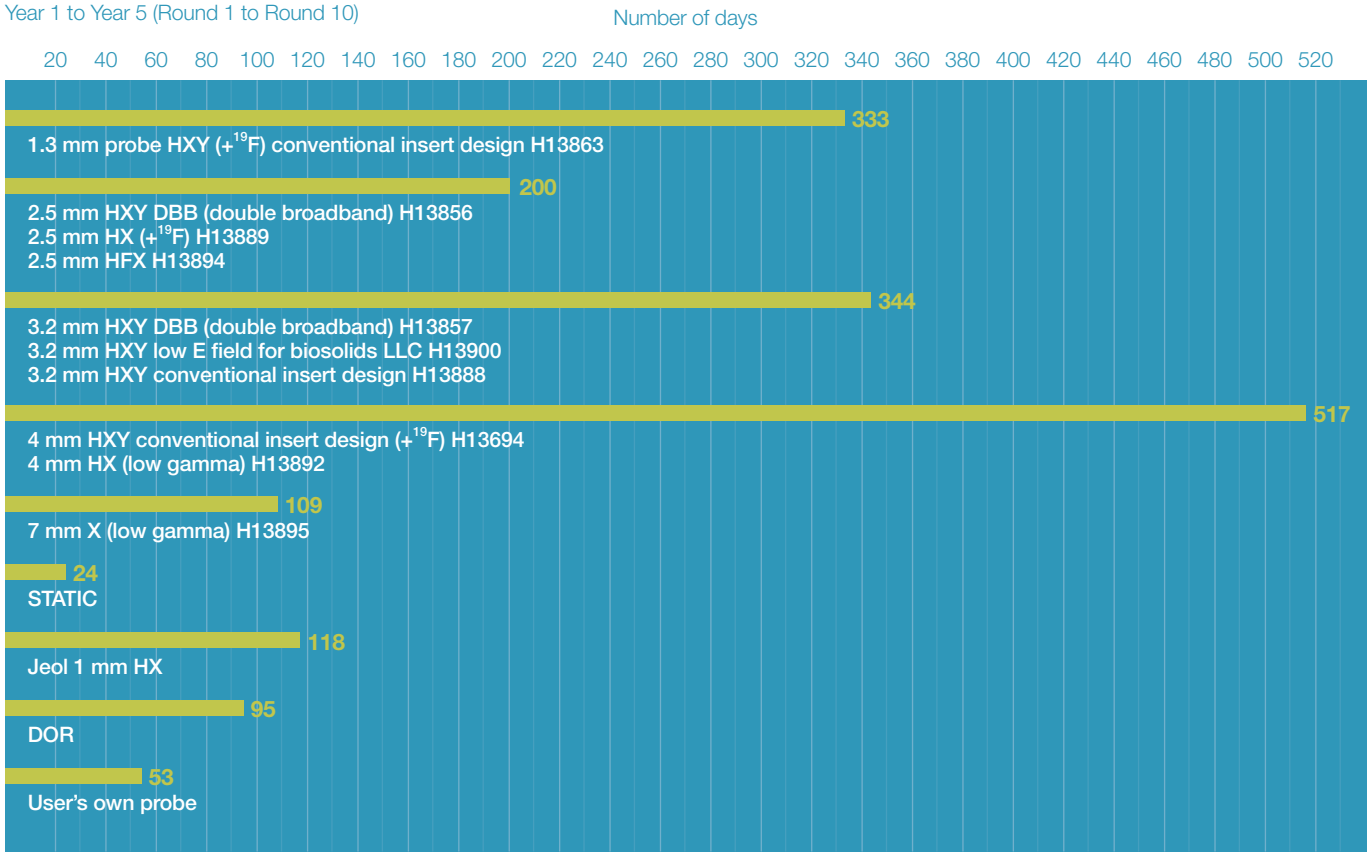

Nuclei tested in Double Resonance Mode

Probe in double Resonance mode	Mode	X-Nucleus: ^{31}P	^{7}Li	^{119}Sn	^{87}Rb	^{11}B	^{71}Ga	^{65}Cu	^{23}Na	^{27}Al	^{13}C	^{79}Br	^{93}Nb	^{45}Sc	^{69}Ga	^{59}Co	^{127}I	^{29}Si	^{77}Se	^{2}H	^{6}Li	^{139}La	^{17}O	^{133}Cs	^{137}Ba	^{15}N	^{35}Cl	^{91}Zr	^{33}S	^{14}N	^{43}Ca	^{67}Zn	^{25}Mg	^{89}Y	^{39}K	^{87}Sr	^{183}W	^{73}Ge
1.3 mm HXY (+^{19}F) conventional insert design	DR ^{1}H-X DR ^{19}F-X ●	■	■	★	★	★	■	★	★	★ ■	■	■	■	■	■	★	★	★	★	★	★	★	■	★	★	■	★	★	★	■								
2.5 mm HX (+^{19}F) 2.5 mm HFX 2.5mm HXY DBB	DR ^{1}H-X DR ^{19}F-X ●	■	★	★	■	★	■	★	★	■ ■	■ ■	■	★	■	■	★	★	★	■	■	★	★	■	★	★	■	★	★	★	■	★	★	■	★	■			
3.2 mm HXY low E field for biosolids LLC	DR ^{1}H-X				★	★	★	★	★	★	■	■	★	★	★			★		★	★		★		★	■	★		★	★								
3.2 mm HXY conventional insert design 3.2mm HXY DBB	DR ^{1}H-X				■	■	■	★	■	■	■	■	★	★	★	★	★	■	★	★	★	★	■	★	★	■	■	★	★	■								
4 mm HXY conventional insert design (+^{19}F)	DR ^{1}H-X DR ^{19}F-X ●	■	★	■	★	★	★	★	■	■	■ ■	■	★	★	★	★	■	■	■	★	★	★	★	★	★	■ ■	★	★	★	★								
4 mm HX (low gamma)	DR ^{1}H-X										■	■	■	★	■	■	★	■	★	■	■	★	■	■	★	■	★	★	■	■	■	■	■	■	■	■	★	★
7 mm X (low gamma)	X																						★	★	■	★	■	■	■	■	■	★	★	■	■	■	■	■
Static	X	■	★	★	★	■	■	■	★	★	■	★	■	★	■	★	★	★	★	■	★	■	★	★	★	★	■	★	★	■	★	★	★	★	■	★	★	★
DOR	X				■	■	■	★	■	■	★	★	★	★	★	★	★	★	★	★	★	★	■	★	★	★	★	★	★	★	■	■	★	★				
Jeol 1 mm HX	DR ^{1}H-X		■	★	■	★	■	★	■	★	■	★	■	★	★	★	★	★	★	★	★	★	★	★	★	■	★	★	★	■								

■ *Experiments performed at the facility to date*

★ *Bench tests indicate should be possible*

● *Other ^{19}F-X DR combinations have not yet been investigated*

For triple-resonance capabilities, refer to the facility website

Time Allocation

451 days requested by 23 PIs from 13 different institutions (Cambridge, Cardiff, Glasgow, King's College London, Lancaster, Liverpool, Nottingham, Oxford, Sheffield, Strathclyde, Southampton, St Andrews and Warwick). 316 days allocated by the Time Allocation Panel.

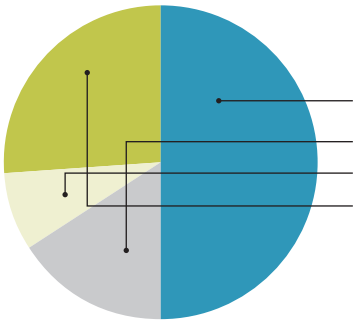

Requested time

Outside Warwick and non-NMC **50%**
NMC outside Warwick **16%**
Warwick NMC **8%**
Warwick non-NMC **26%**

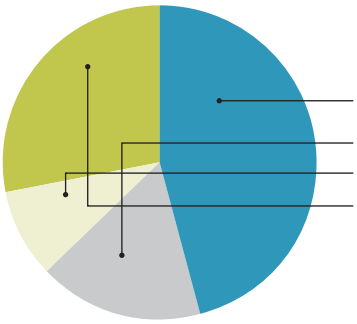

Allocated time

Outside Warwick and non-NMC **46%**
NMC outside Warwick **17%**
Warwick NMC **9%**
Warwick non-NMC **28%**

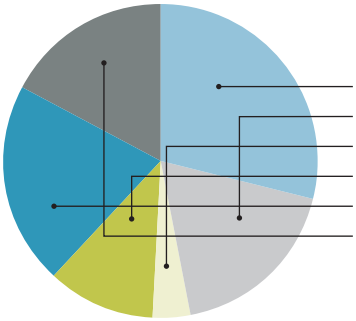

Requested time

Advanced materials **29%**
Bio-materials **18%**
Energy materials **4%**
Methods development **11%**
Proteins **21%**
Pharmaceuticals and self assembly **17%**

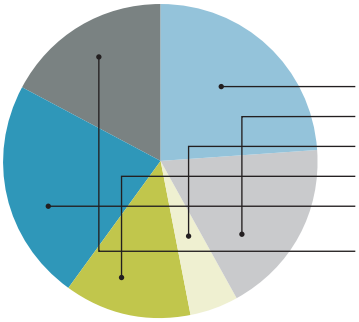

Allocated time

Advanced materials **24%**
Bio-materials **18%**
Energy materials **5%**
Methods development **13%**
Proteins **23%**
Pharmaceuticals and self assembly **17%**

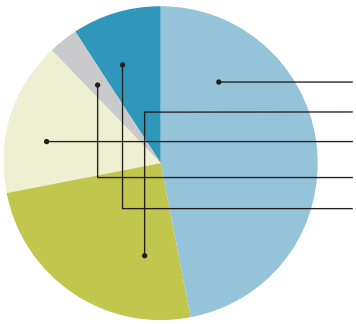

Requested time

EPSRC **47%**
BBSRC **25%**
Other agencies **16%**
Industrial **3%**
No external funding **9%**

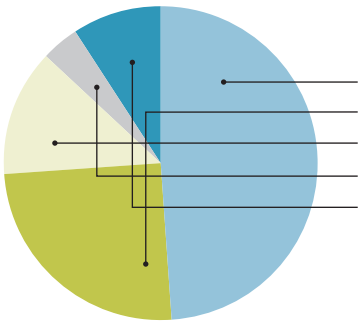

Allocated time

EPSRC **49%**
BBSRC **25%**
Other agencies **13%**
Industrial **4%**
No external funding **9%**

Projects with more than one funding source were counted only once. Other agencies that are funding facility users are: British Heart Foundation, Leverhulme Trust, Royal Society, Wellcome Trust, ERC, EU, agencies from Australia, Chile, France, Iraq and Sweden as well as industry (Agilent, AWE, Bruker, GSK, Johnson Matthey, Nissan, Sasol).

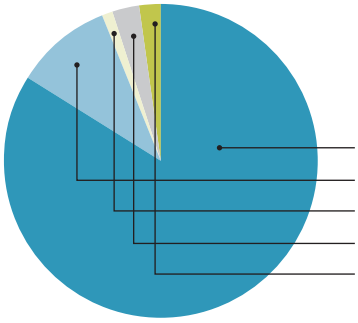

Spectrometer time

Feb 1 2014 – Jan 4 2015
(the facility operates 24 hours a day, 7 days a week)

TAP allocated days **84%**
Facility manager research **10%**
Maintenance **1%**
Fast track **3%**
Compensation **2%**

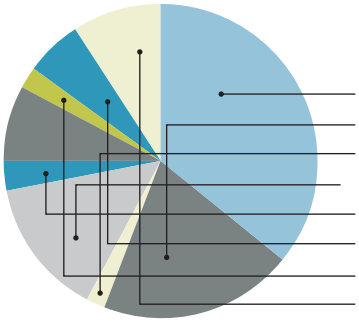

Facility users

Feb 1 2014 – Jan 4 2015

PIs **23**
EPSRC PhD students* **13**
BBSRC PhD students **1**
Other PhD students** **9**
Industrial PhD **2**
PDRAs*** **5**
UG student **1**
Research staff **4**
Overseas collaborators **6**

* *5 students partially funded by industry*
** *3 overseas (Chile, EU, Iraq), 1 British Heart Foundation, 5 UK university funding*
*** *1 BBSRC, 2 EPSRC, 2 Leverhulme Trust*

Results from User Questionnaire Feb 2014 – Jan 2015

Facility users are asked to complete feedback questionnaires which contain a series of questions and provide the opportunity for visitors to make comments and suggestions. The responses are graded from 1 (least satisfied) to 5 (most satisfied). The average scores are based on the responses from 12 PIs and 25 visitors for visits over the period February 2014 to January 2015.

Section 1 to be completed by the PI

Application for time

1 Ease of application process
2 Transparency of application process
3 Feedback on any unsuccessful time request

Scheduling of time awarded

4 Scheduling of your time by the facility

Overall impact

5 Quality of results obtained

Section 2 to be completed by the visitor

Accommodation

6 Ease of arranging accommodation
7 Quality of accommodation
8 Location of accommodation

At the 850 MHz Facility

9 Support from the Facility Manager upon arrival
10 Support from the Facility Manager throughout your visit
11 Quality of the NMR facilities
12 Quality of the sample preparation area and storage facilities
13 Ease of access to the facility out of hours
14 Your overall time at the facility

Post visit experience

15 Arrangements for accessing data
16 Arrangements for returning any samples
17 Reimbursement of expenses

Average scores from feedback questionnaires over period Feb 2014 – Jan 2015

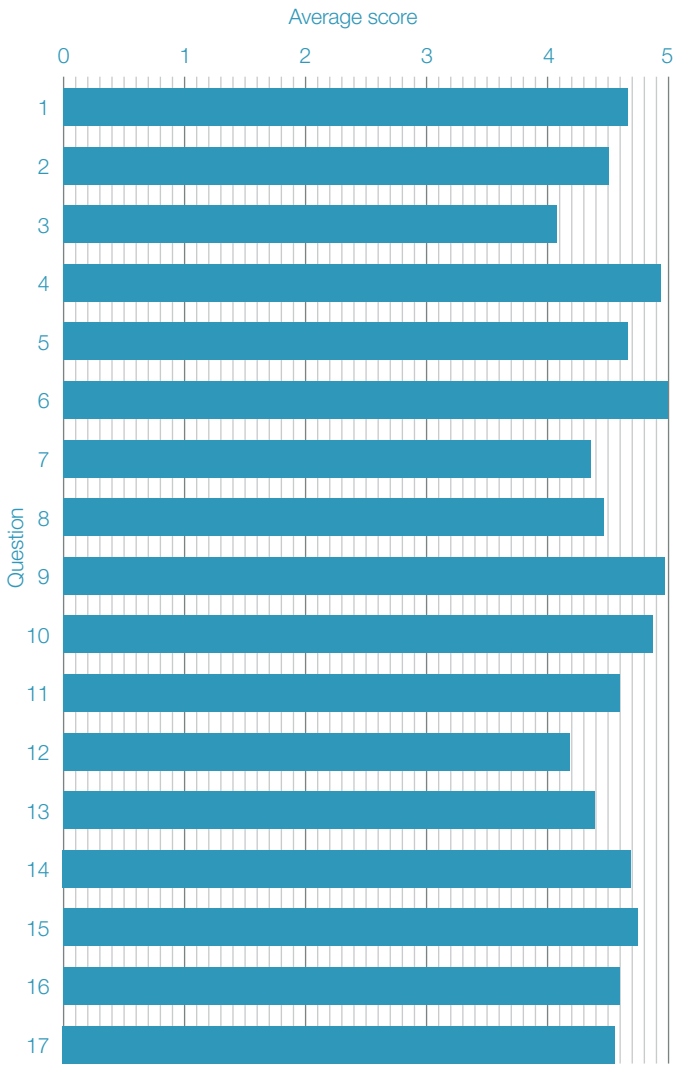

UK 850 MHz Solid-State NMR Facility 4th Annual Symposium

Thursday April 3rd 2014
Millburn House, University of Warwick
Symposium Organiser: Ray Dupree

List of talks

1 ***Probing the Molecular Architecture of Plant Cell Walls Using 2D and 3D ^{13}C NMR***
Paul Dupree *(University of Cambridge)*

2 ***A Multinuclear NMR Study of $Sr_2Sc_{2-x}Ga_xO_5$ Perovskite Fuel Cell Materials and Rare-Earth Containing GeS_2-Ga_2S_3 Chalcogenide Glasses for Bright Fibre Laser Devices***
Stephen Day *(University of Warwick)*

3 ***High-Resolution Natural Abundance ^{33}S STMAS NMR Study of Ettringite***
Akiko Sasaki *(University of Glasgow)*

4 ***Progress in First Principles Calculations of NMR Parameters: Heavy Atoms, Processing and Visualisation***
Jonathan Yates *(University of Oxford)*

5 ***A Solid-State NMR Journey (Why I Wish I Had Access to 850 MHz 35 Years Ago)***
Robin Harris *(Durham University)*

6 ***Solid-State NMR of Nanomolar Quantities of Protein Complexes at 60-100 kHz Magic Angle Spinning***
Jonathan Lamley *(University of Warwick)*

7 ***New Materials for Optical Fibres: Understanding the Effect of Modifier on Tellurite Glass Structure***
Emma Barney *(University of Nottingham)*

8 ***Advanced Cements for Nuclear Waste Immobilisation – New Structural Insights***
John Provis *(University of Sheffield)*

9 ***Monitoring the Electrochemical Processes in the Lithium-Air Battery by Solid-State NMR Spectroscopy***
Michal Leskes *(University of Cambridge)*

10 ***Exploiting the ^{31}P Chemical Shift Anisotropy of Aluminophosphates***
Scott Sneddon *(University of St Andrews)*

11 ***From Order to Disorder, Structure to Properties from Solid-State NMR***
Dominique Massiot *(CNRS, France)*

Publications 2014

Cation Substitution in β-tricalcium Phosphate Investigated using Multi-Nuclear, Solid-State NMR
A.T. Grigg, M. Mee, P.M. Mallinson, S.K. Fong, Z. Gan, R. Dupree, D. Holland
Journal of Solid State Chemistry, 212, 227-236 (2014)

A Hexameric Peptide Barrel as Building Block of Amyloid-β Protofibrils
C. Lendel, M. Bjerring, A. Dubnovitsky, R.T. Kelly, A. Filippov, O.N. Antzutkin, N. Chr. Nielsen, T. Hard
Angewandte Chemie International Edition, 53, 12756-12760 (2014)

Solid-State NMR of a Protein in a Precipitated Complex with a Full-Length Antibody
J.M. Lamley, D. Iuga, C. Öster, H.-J. Sass, M. Rogowski, A. Oss, J. Past, A. Reinhold, S. Grzesiek, A. Samoson, J.R. Lewandowski
J. Am. Chem. Soc., 136, 16800-16806 (2014)

A $G_4{\cdot}K^+$ Hydrogel Stabilized by an Anion
G.M. Peters, L.P. Skala, T.N. Plank, B.J. Hyman, G.N.M. Reddy, A. Marsh, S.P. Brown, J.T. Davis
J. Am. Chem. Soc., 136, 12596-12599 (2014)

Expression and Purification of the Aortic Amyloid Polypeptide Medin
H.A. Davies, M.C. Wilkinson, R.P. Gibson, D.A. Middleton
Protein Expression and Purification, 98, 32-37 (2014)

Characterization of Structural Disorder in γ-Ga_2O_3
H.Y. Playford, A.C. Hannon, M.G. Tucker, D.M. Dawson, S.E. Ashbrook, R.J. Kastiban, J. Sloan, R.I. Walton
J. Phys. Chem. C, 118, 16188-16198 (2014)

Fluorine Speciation as a Function of Composition in Peralkaline and Peraluminous Na_2O–CaO–Al_2O_3–SiO_2 Glasses: A Multinuclear NMR Study
A. Baasner, B.C. Schmidt, R. Dupree, S.L. Webb
Geochim. Cosmochim. Acta, 132, 151-169 (2014)

A 3D Experiment that Provides Isotropic Homonuclear Correlations of Half-Integer Quadrupolar Nuclei
D. Iuga, D. Holland, R. Dupree
Journal of Magnetic Resonance, 246, 122-129 (2014)

Highly Efficient Chiral Resolution of DL-Arginine by Cocrystal Formation Followed by Recrystallization under Preferential-Enrichment Conditions
S. Iwama, K. Kuyama, Y. Mori, K. Manoj, R.G. Gonnade, K. Suzuki, C.E. Hughes, P.A. Williams, K.D.M. Harris, S. Veesler, H. Takahashi, H. Tsue, R. Tamura
Chemistry - A European Journal, 20, 10343-10350 (2014)

"CLASSIC NMR": A New In-Situ NMR Strategy for Mapping the Time-Evolution of Crystallization Processes by Combined Liquid-State and Solid-State Measurements
C.E. Hughes, P.A. Williams, K.D.M. Harris
Angewandte Chemie International Edition, 53, 8939-8943 (2014)

A Solid-State NMR Study of the Immobilization of α-Chymotrypsin on Mesoporous Silica
N.E. Faure, P.J. Halling, S. Wimperis
Journal of Physical Chemistry C, 118, 1042-1048 (2014)

Citrate Bridges Between Mineral Platelets in Bone
E. Davies, K.H. Müller, W.C. Wong, C.J. Pickard, D.G. Reid, J.N. Skepper, M.J. Duer
Proceedings of the National Academy of Sciences of the United States of America, 111, E1354-E1363 (2014)

Motional Timescale Predictions by Molecular Dynamics Simulations: Case Study using Proline and Hydroxyproline Sidechain Dynamics
A.E. Aliev, M. Kulke, H.S. Khaneja, V. Chudasama, T.D. Sheppard, R.M. Lanigan
Proteins: Structure, Function and Bioinformatics, 82, 195-215 (2014)

Water Scaffolding in Collagen: Implications on Protein Dynamics as Revealed by Solid-State NMR
A.E. Aliev, D. Courtier-Murias
Biopolymers, 101, 246-256 (2014)

Concise NMR Approach for Molecular Dynamics Characterizations in Organic Solids
A.E. Aliev, D. Courtier-Murias
Journal of Physical Chemistry A, 117, 7855-7862 (2014)

In addition, users reported 48 talks and 28 posters at conferences and seminars in 2014, where results obtained at the UK 850 MHz Solid-State NMR Facility were presented.

Theses 2014

Student	Department	University	Supervisor	Title	Date
PhD Theses					
Daniel Dawson	Chemistry	St Andrews	Sharon E Ashbrook	*'Combined Theoretical and Experimental Investigations of Porous Crystalline Materials'*	Mar 2014
Philip Andrew Williams	Chemistry	Cardiff	Kenneth D M Harris	*'In-Situ Studies of Crystallization Processes and Other Aspects of Polymorphism'*	Dec 2014
MSc Thesis					
Rebecca Katherine Karbo Yue	Chemistry	Durham	Paul Hodgkinson	*'Diffraction and Solid-State NMR Studies of Inorganice Framework Materials'*	Feb 2014

The UK 850 MHz Solid-State NMR Facility PhD Travel Fund

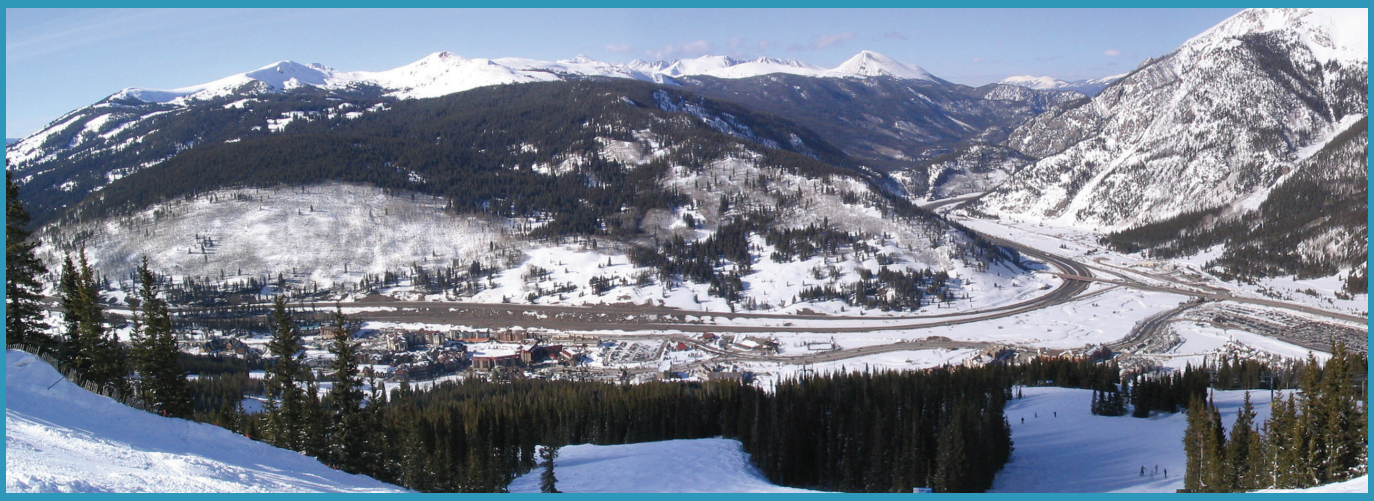

Copper Mountain, Colarado, USA. Setting for the 56th Annual Rocky Mountain Conference on Magnetic Resonance in July 2014. © DebateLord

Supported by Bruker

The UK 850 MHz Solid-State NMR Facility PhD travel fund supported by Bruker provides funding for: (a) attendance at an internationally recognised, high-profile conference where a PhD student presents results he/she obtained at the 850 MHz Facility, or (b) a "start-up" visit to another lab to learn new methods to be implemented at the 850 MHz Facility. For further details see: **http://go.warwick.ac.uk/850mhz/travel_fund/**

2014 Awards

Jonathan Lamley (University of Warwick) awarded £800 to attend the 55th Experimental Nuclear Magnetic Resonance Conference (ENC) in Boston, USA (March 2014) and present a poster entitled *Solid-State NMR of Nanomolar Quantities of Protein Complexes at 60-100 kHz Magic Angle Spinning.*

Henri Colaux (University of St Andrews) awarded £1000 to attend the 56th Annual Rocky Mountain Conference on Magnetic Resonance in Copper Mountain, USA (July 2014) and present a poster entitled *Assessing the Performance of the Computationally Optimised FAM-N Conversion Pulses for MQMAS Experiments Under Challenging Conditions.*

Nicole Fauré (University of Glasgow) awarded £1000 to attend the 56th Annual Rocky Mountain Conference on Magnetic Resonance in Copper Mountain, USA (July 2014) and present a poster entitled *Solid-State NMR Studies of Immobilised Enzyme Systems.*

Akiko Sasaki (University of Glasgow) awarded £1000 to attend the 56th Annual Rocky Mountain Conference on Magnetic Resonance in Copper Mountain, USA (July 2014) and give a talk entitled *A Natural Abundance ^{33}S STMAS NMR Study of Ettringite.*

Stephen Day (University of Warwick) awarded £550 to attend the SMARTER 4 conference in Durham (September 2014) and present a poster entitled *A Multinuclear NMR Study of $Sr_2Sc_{2-y}Ga_yO_5$ Perovskite Fuel Cell Materials.*

Conference Publicity Support

2014 Awards

In order to facilitate the publicising of the capabilities of solid-state NMR to new users, the UK 850 MHz Solid-State NMR Facility offers support for PIs or PDRAs to present results at UK conferences. For further details see: **http://go.warwick.ac.uk/850mhz/conference-publicity-funding/**

Colan Hughes (Cardiff University) awarded £400 to attend the 45th British Association for Crystal Growth Annual Conference in Leeds (July 2014) and give a talk entitled *"CLASSIC" NMR: A New Methodology to Study Crystallization.*

Emma Barney (University of Nottingham) awarded £225 to attend the Society of Glass Technology Annual Conference in Durham (November 2014) and give a talk entitled *New Materials for Optical Fibres: Using NMR to Understanding the Effect of Modifier on Tellurite Glass Structure.*

The UK 850 MHz Solid-State NMR Facility User Reports

Structure of Amyloid-β Oligomers from Solid-State NMR

Christofer Lendel,[1] Morten Bjerring,[2] Robert T. Kelly,[3] Józef R. Lewandowski,[4] Andrei V. Filippov,[5] Dinu Iuga,[3] Anatoly Dubnovitsky,[1] Niels Chr. Nielsen,[2] Torleif Härd[1] and Oleg N. Antzutkin[3,5]

[1]*Department of Molecular Biology, Swedish University of Agricultural Sciences, Uppsala, Sweden*

[2]*Interdisciplinary Nanoscience Center and Department of Chemistry, Aarhus University, Aarhus, Denmark*

[3]*Department of Physics, University of Warwick*

[4]*Department of Chemistry, University of Warwick*

[5]*Chemistry of Interfaces, Luleå University of Technology, Luleå, Sweden*

Overview

It has been suggested that amyloidogenic proteins are prone to form small aggregates, so called oligomers, which may incorporate into biological membranes resulting in cellular dysfunction and cell death.[1] Oligomers of amyloidogenic proteins are considered to be transient intermediates on the way to their further aggregation towards amyloid fibrils. For full-length variants of Aβ ($Aβ_{(1-40)}$ and $Aβ_{(1-42)}$) in the course of this aggregation cascade both secondary and tertiary structures in aggregates are changing, e.g. from *intra*-molecular anti-parallel β-hairpin structure in Aβ monomers[2] towards *inter*-molecular parallel β-sheet structures in amyloid fibrils.[3] Determination of the atomic-level resolution supramolecular structure of transient Aβ oligomers is currently a very hot topic of research. However, preparation of homogeneous samples of Aβ oligomers for structural studies is a big challenge, because of their transient nature: Oligomers and protofibrils of wild type Aβ are inherently unstable and ultimately form amyloid fibrils. The issue of oligomer/protofibril instability has been addressed by engineering a variant of Aβ (abbreviated as Aβcc)[4] that forms oligomers and protofibrils, but which cannot form amyloid fibrils. In Aβcc, alanine residues at positions 21 and 30, which have spatially close CH_3 groups in the structure of the Aβ monomer[2] are replaced by cysteines, so that a disulphide bond locks the peptide in a conformation that is incompatible with fibril formation and aggregation is, therefore, arrested at the oligomer/protofibril state.[4]

Supramolecular Structure of $Aβ_{(1-42)}$cc Oligomers

Protofibrils formed by $Aβ_{(1-42)}$cc (Figure 1D) are indistinguishable from wild type $Aβ_{42}$ protofibrils with respect to many properties: size and morphology as observed by electron microscopy and atomic force microscopy; binding of conformation specific antibodies and the ANS dye; circular dichroism and infrared spectra; the ability to induce apoptosis in neuroblastoma cell lines; and the ability to attenuate spontaneous synaptic activity in primary neurons.[4] Very recently, we reported an atomic-level resolved structural model of $Aβ_{(1-42)}$cc oligomers using structural constraints obtained from a range of solid-state NMR experiments (including data obtained at the UK 850 MHz solid-state NMR Facility) on uniformly and selectively ^{13}C and ^{15}N labelled peptides.[5] A variety of $Aβ_{(1-42)}$cc peptides with selective labelling using U-^{13}C,^{15}N-amino acids were synthesised using Fmoc solid phase peptide synthesis and purified by HPLC at LTU, Sweden. Recombinant U-^{13}C,^{15}N-$Aβ_{(1-42)}$cc and oligomers were prepared at SLU, Sweden. The 850 MHz NMR spectrometer has proven very useful for 2D ^{13}C-^{13}C and ^{13}C-^{15}N NMR experiments, because of the higher sensitivity and improved resolution. A hexameric peptide barrel structure (Figures 1B-1C) based on both *intra*-molecular β-hairpin and *inter*-molecular β-sheet structures (Figure 1A) was obtained using a range of *intra*- and *inter*-molecular NMR structural constraints and the Rosetta software molecular modelling of the set of structures.[5] Previously, it has been shown that Aβcc oligomers have a considerably higher cell toxicity *in vitro* compared to wild type and mutants of $Aβ_{(1-42)}$ and $Aβ_{(1-40)}$ amyloid fibrils.[4] Therefore, Aβcc oligomers are ideal systems for future drug development via studies of inhibition of oligomer's cell toxicity by oligomer-specific antibodies or/and small benign molecules, which are able to penetrate the blood-brain-barrier.

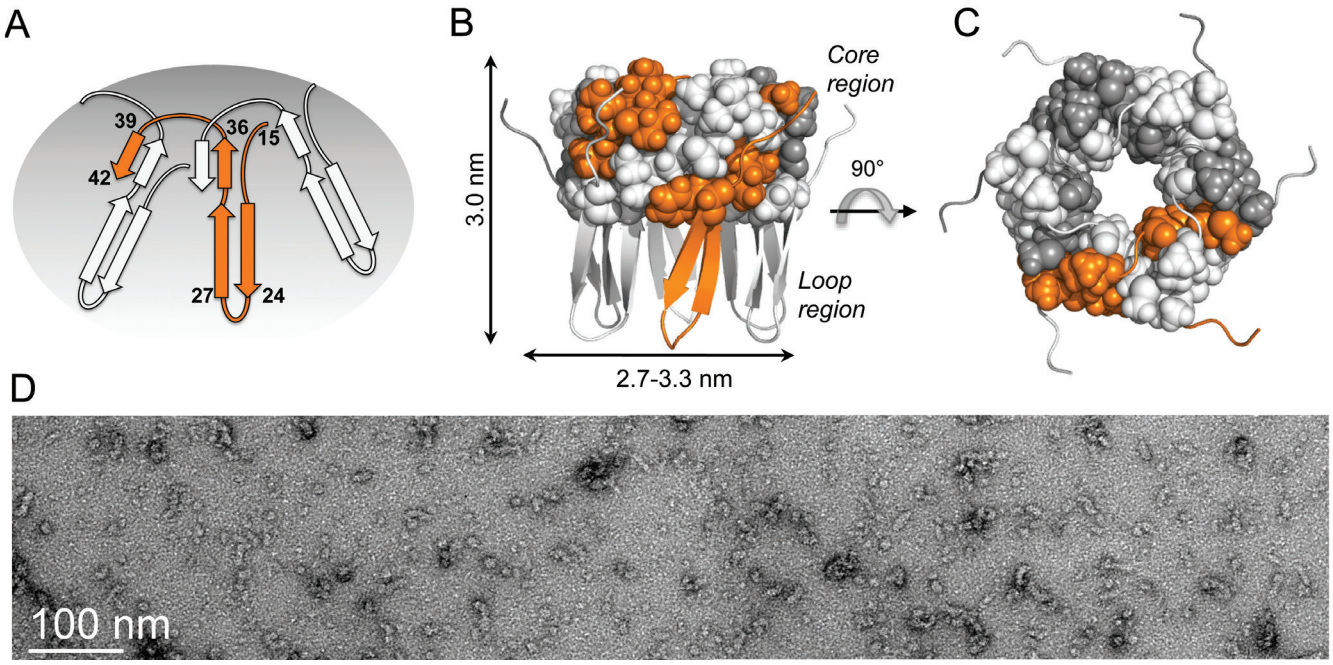

Figure 1. Models of hexameric $A\beta_{(1-42)}$cc oligomers (adapted from ref.[5]): (A) A schematic representation of the topology in $A\beta_{(1-42)}$cc oligomers. The numbers refer to the residue positions of $A\beta_{(1-42)}$cc in one of the protomers (in orange). (B, C) Dimensions of the hexameric barrel. Side chains of the hydrophobic core are shown as spheres. The image in C is rotated by 90° relative to the image in B. (D) Negatively stained TEM image of oligomers of $A\beta_{(1-42)}$cc. (The image was obtained by Dr A. Sousa and Dr R. Leapman, NIH, USA.)

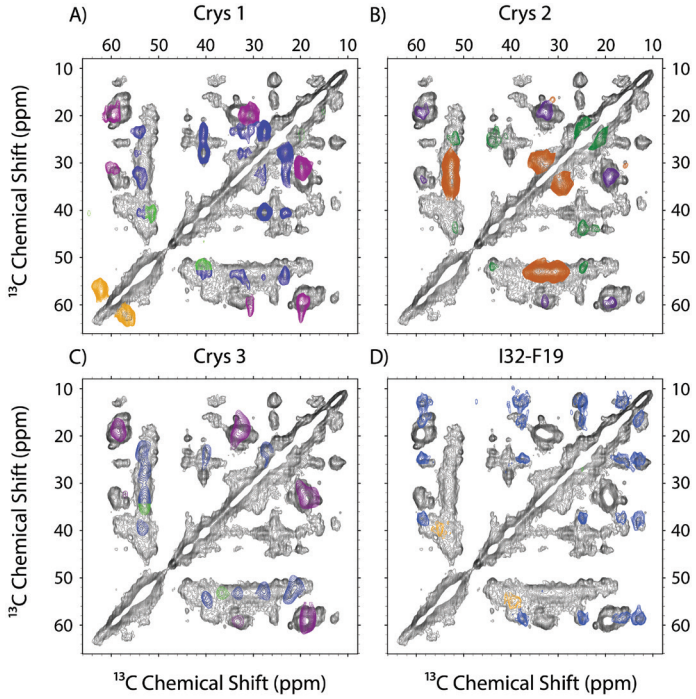

Figure 2. Overlay of 2D ^{13}C-^{13}C DARR NMR (50 ms DARR mixing time) spectra of hydrated $A\beta_{(1-42)}$cc oligomers. Grey spectrum in (A)-(D): U-^{13}C,^{15}N-$A\beta_{(1-42)}$cc oligomers sedimented in a plastic insert (600 MHz, 4 mm MAS probe, 10 kHz MAS, 2.8 s recycle delay, 41 hours). Crys1 (A), Crys2 (B), Crys3 (C) and I32-F19 (D) (coloured spectra) are oligomers from synthetic $A\beta_{(1-42)}$cc with the following U-^{13}C,^{15}N amino acid residues, respectively: (D23, V24, G25, S26, K28); (L17, V18, G29, M35); (K16, N27, V36, G37) and (I32, F19); (850 MHz, 2.5 mm MAS probe, 13 kHz MAS, dry sample weight 3.5-7 mg, 2.5-4 s recycle delay, 20-39 hours) (Adapted from the PhD thesis of R.T. Kelly, University of Warwick, 2015).

References

1. Selkoe, D. J. *Nat. Cell Biol.* **2004**, *6*, 1054.
2. Hoyer, W.; Gronwall, C.; Jonsson, A.; Stahl, S.; Härd, T. *Proc. Nat. Acad. Sc. U.S.A.* **2008**,*105*, 5099.
3. Antzutkin, O. N.; Balbach J. J.; Leapman, R. D.; Rizzo, N. W.; Reed, J.; Tycko, R. *Proc. Nat. Acad. Sc. U.S.A.* **2000**, *97*, 13045.
4. Sandberg, A.; Luheshi, L. M.; Sollvander, S.; de Barros, T. P.; Macao, B.; Knowles, T. P. J.; Biverstål, H.; Lendel, C.; Ekholm-Petterson, F.; Dubnovitsky, A.; Lannfelt, L.; Dobson, C. M.; Härd, T. *Proc. Natl. Acad. Sc. U.S.A.* **2010**, *107*, 15595.
5. Lendel, C.; Bjerring, M.; Dubnovitsky, A.; Kelly, R. T.; Filippov, A.; Antzutkin, O. N.; Nielsen, N. C.; Härd, T. *Angew. Chem. Int. Ed.* **2014**, *53*, 12756.

^{25}Mg MQMAS Signal Enhancement Using "FAM-N" Pulses

Henri Colaux, Daniel M. Dawson and Sharon E. Ashbrook

School of Chemistry and EaStCHEM, University of St Andrews

Overview

Although quadrupolar nuclei comprise 75% of all NMR-active nuclei, they are not as commonly studied as nuclei with spin $I = 1/2$, due to the presence of second-order quadrupolar broadening, which can only be reduced (rather than averaged to zero) under magic-angle spinning (MAS). The multiple-quantum (MQ) MAS[1] technique has established itself as one of the most popular methods to resolve lineshapes broadened by the second-order quadrupolar interaction, as it can separate the components of the signal according to their respective quadrupolar coupling constants, C_Q, and isotropic chemical shifts, δ_{iso}, without the need for specialist hardware. Nonetheless, the application of MQMAS is hindered by its inherent low sensitivity, which can lead to long acquisition times and restricts the samples that can be studied on a reasonable timescale. A number of methods have been developed to improve the efficiency of the conversion of multiple- to single-quantum coherences.[2-4] Despite providing signal improvement, these methods typically require additional optimisation, making them unsuitable for challenging systems where NMR sensitivity is already very low.

We have recently developed an alternative approach, using computationally pre-optimised composite pulses, termed FAM-N,[5] consisting of a succession of N subsequent and oppositely phased pulses, optimised independently using a program built on MATLAB and SIMPSON.[6] As shown in Figure 1, this high-throughput approach involves the optimisation initially of a single pulse. A second pulse is then added (with opposite phase) and the duration that provides the most efficient transfer determined. The duration of the previous pulse is then incrementally varied and the procedure repeated until a decrease in efficiency is observed. Additional pulses are added and the optimisation repeated until maximum coherence transfer is obtained. We have demonstrated the efficiency of FAM-N pulses in simulation and, most importantly, their experimental implementation with little or no reoptimisation.[5] This latter point is particularly important when considering experiments on very challenging nuclei, where optimisation of complicated pulses (or, indeed, simple ones) is either very time consuming or, sometimes, simply not possible. This is the often the case for "low-γ" nuclei, such as ^{25}Mg ($I = 5/2$), which exhibit inherently low sensitivity and significant quadupolar broadening. For ^{25}Mg, these challenges are exacerbated by its low natural abundance (10%) and the low radiofrequency field strengths typically available. For such systems, sensitivity enhancements such as that provided by FAM-N are vital, and optimisation is difficult.

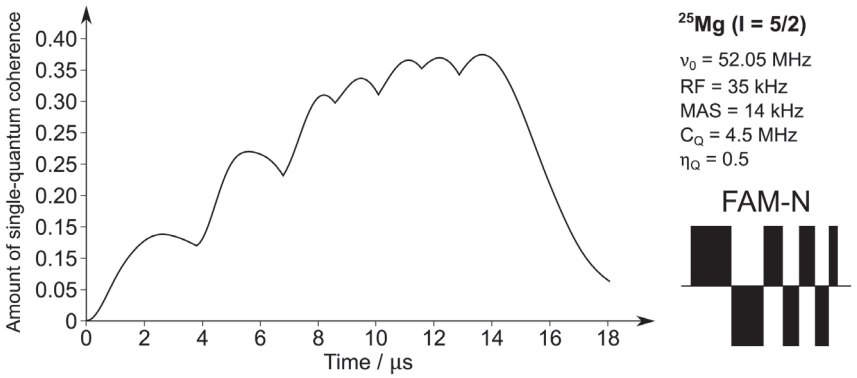

Figure 1. Illustration of the generation of a FAM-N pulse (N = 7), optimised for efficient conversion of triple- to single-quantum coherences for ^{25}Mg in forsterite.

In an attempt to investigate the applicability of FAM-N when no pulse optimisation is possible, we have studied ^{25}Mg in two mineral samples: brucite ($Mg(OH)_2$) and forsterite (α-Mg_2SiO_4).

Results

Brucite contains only one distinct Mg site with a C_Q value of 3.1 MHz.[7] The relatively low C_Q value enables spectra to be acquired in a reasonable timescale and the effect of FAM-N pulses to be assessed. ^{25}Mg triple-quantum filtered MAS NMR spectra have been recorded (Figure 2) for brucite using a single pulse (blue line) and FAM-N (red line) for the conversion from triple- to single-quantum coherences. A significant enhancement in integrated intensity is observed, although a lineshape change is also apparent.

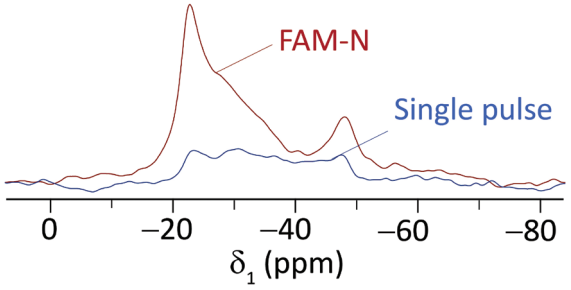

Figure 2. ^{25}Mg (20.0 T, ν_1 = 31.5 kHz, MAS rate = 12.5 kHz) triple-quantum filtered MAS spectrum of brucite, acquired at natural abundance levels using a single pulse (blue line) and a FAM-N pulse (red line, taken directly from simulation without any experimental reoptimisation) for triple- to single-quantum conversion.

The acquisition of ^{25}Mg MQMAS NMR experiments on forsterite is known to be very challenging, with early measurements exploiting dynamic polarization techniques.[8] Forsterite has two Mg sites with C_Q values of 4.2 MHz (Mg1) and 5.1 MHz (Mg2).[7] The FAM-N enhanced MQMAS spectrum is presented Figure 3. Even though signal was successfully observed in just two days of acquisition, only Mg1 is clearly visible. However, simulations show that Mg2 will be observed if higher signal-to-noise could be obtained in a longer experiment.

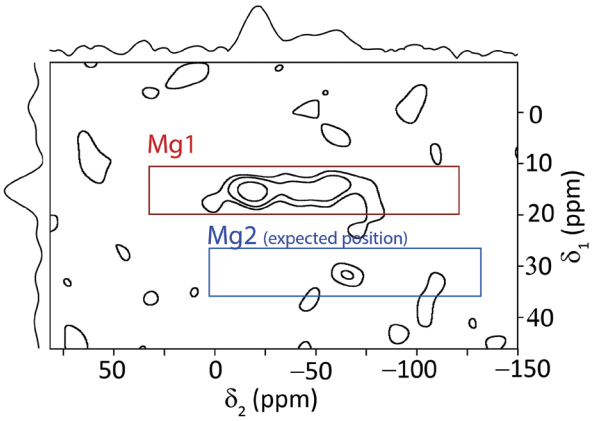

Figure 3. ^{25}Mg (20.0 T, ν_1 = 35 kHz, MAS rate = 14 kHz) MQMAS spectrum of forsterite, acquired at natural abundance levels using a FAM-N conversion pulse (taken directly from simulation without any experimental reoptimisation).

References

1. Frydman, L.; Harwood, L. *J. Am. Chem. Soc.* **1995**, *117*, 5367.
2. Madhu, P.; Goldbourt, A.; Frydman, L. and Vega, *S. Chem. Phys. Lett.* **1999**, *307*, 41.
3. Gan, Z.; Kwak, H. *J. Magn. Reson*, **2004**, *168*, 346.
4. Kentgens, A.; Verhagen, R. *Chem. Phys. Lett.* **1999**, *300*, 435.
5. Colaux, H.; Dawson, D. M.; Ashbrook, S. E. *J. Phys. Chem.* A **2014**, *118*, 6018.
6. Bak, M.; Rasmussen, J. T.; Nielsen, N. C. *J. Magn. Reson.* **2000**, *147*, 296.
7. Pallister, P. J.; Moudrakovski, I. L.; Ripmeester, J. A. *Phys. Chem. Chem. Phys.* **2009**, *11*, 11487.
8. Derighetti, B.; Hafner, S.; Marxer H.; Rager H. *Phys. Lett. A* **1978,** *66*, 150.

^{17}O and ^{71}Ga NMR Studies of New Ga-Based Langasite Fast Ion Conductors

Frédéric Blanc, Maria Diaz-Lopez, Matthew S. Dyer, John B. Claridge and Matthew J. Rosseinsky

Department of Chemistry, University of Liverpool

Overview

Polyhedral frameworks-based oxides containing cations that can tolerate increased coordination number have shown remarkable flexibility, enabling the accommodation of excess oxygen in the crystal structure and the incorporation of interstitial oxygens responsible for high ionic conductivity.[1] The typical example of this family of compounds is the melilite structure $La_{1.54}Sr_{0.46}Ga_3O_{7.17}$ which shows very fast oxide ion conductivity in the range of 0.02 – 0.1 S.cm^{-1} over the 600 – 900 °C temperature range.[1] Three-dimensional structures based on a tetrahedral network are also potential extra oxygen hosts and we have found that the langasite structure $La_3Ga_5GeO_{14}$ (Figure 1a) which has the key crystal chemical features demanded for network deformation can accommodate over 5% of extra oxygen by hypervalent doping with Ge^{4+} in place of Ga^{3+}; that is a structure of the type $La_3Ga_{5-x}Ge_{1+x}O_{14+x/2}$ with $0 \le x \le 1.5$ (Diaz-Lopez, M.; Dyer, M. S.; Shin, J. F.; Ming, L.; Blanc, F.; Claridge, J. B.; Rosseinsky, M. J. in preparation). Insight into the location of the Ga (and Ge) sites in the structure and direct observation of additional interstitial oxygens are achieved by high field ^{71}Ga and ^{17}O solid-state NMR, respectively, under various experimental conditions.

^{71}Ga Very Fast MAS Solid-State NMR of $La_3Ga_{5-x}Ge_{1+x}O_{14+x/2}$

^{71}Ga (spin I = 3/2) solid-state NMR spectra of $La_3Ga_{5-x}Ge_{1+x}O_{14+x/2}$ materials (with $0 \le x \le 1.5$) obtained at 20 T and under very fast MAS at 65 kHz are shown in Figure 1b. The ^{71}Ga spectrum of $La_3Ga_5GeO_{14}$ presents one signal at 0 ppm corresponding to the central transition (CT) of the Ga site in octahedral geometry as well as a broad signal (with a full width at half maximum of approximately 45 kHz) centred at 150 ppm and corresponding to Ga with tetrahedral geometry. Two tetrahedral Ga sites in 2d and 3f positions are present in the structure; GIPAW NMR calculations reveal that both sites have large quadrupolar coupling constants (C_Q) with values of 13.9 and 25.3 MHz calculated for the 2d and 3f sites, respectively. Only the 2d site is observed under the very fast MAS experimental conditions used to acquire the spectrum in Figure 1b, with the anticipated CT linewidth under MAS (approximately 140 kHz) of the 3f site significantly exceeding the MAS frequency.

The ^{71}Ga spectra of $La_3Ga_{5-x}Ge_{1+x}O_{14+x/2}$ materials (with $0.5 \le x \le 1.5$) reveal that upon Ge doping an additional third resonance around 100 ppm (with C_Q ~ 14 MHz) is observed, whose increase in intensity is correlated with an increase in Ge concentration. This could be assigned to a 5 coordinated Ga site based on previous work on $LaGaGe_2O_7$ (δ = 90 ppm, C_Q = 15 MHz)[2] and present GIPAW NMR calculations on $La_3Ga_4Ge_2O_{14.5}$ (δ ~ 101 ppm). This highlights a change of coordination number of Ga atoms needed to accommodate interstitials oxygens as anticipated and indicates the presence of these sites around Ga.

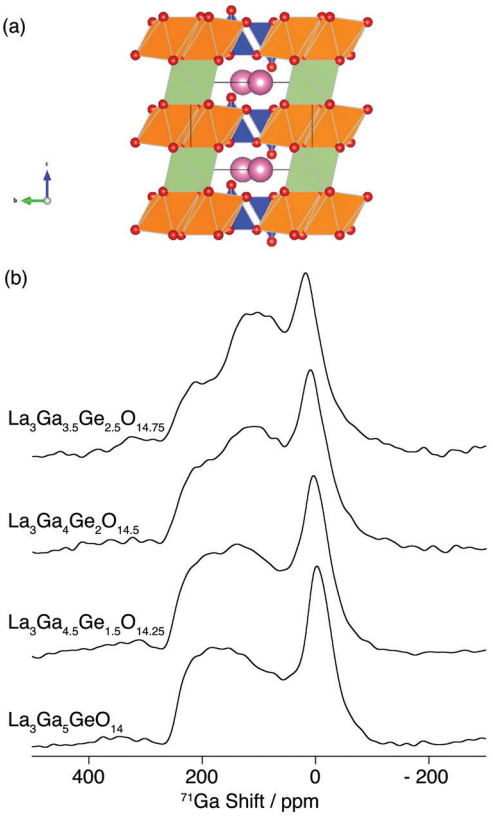

Figure 1. (a) Crystal structure of Ga-based langasite $La_3Ga_5GeO_{14}$ projected along (001) with space group P321. Decahedral La, octahedral Ga, tetrahedral 3f and tetrahedral 2d sites are shown in purple, green, orange and blue, respectively; oxygen atoms are red. (b) ^{71}Ga Hahn echo (20.0 T, 65 kHz MAS) NMR spectra of $La_3Ga_{5-x}Ge_{1+x}O_{14+x/2}$ (with $0 \le x \le 1.5$) as a function of Ge doping level. The spectra were recorded with a 2 ms DFS pulse.[3]

^{17}O MAS Solid-State NMR of ^{17}O Enriched $La_3Ga_{5-x}Ge_{1+x}O_{14+x/2}$

^{17}O (spin I = 5/2) NMR spectra of ^{17}O enriched $La_3Ga_{5-x}Ge_{1+x}O_{14+x/2}$ (prepared by gas – solid exchange reaction of $La_3Ga_{5-x}Ge_{1+x}O_{14+x/2}$ under an atmosphere of 60% enriched O_2 gas at 750 °C for 24 h) are presented in Figure 2a. The spectrum of $La_3Ga_5GeO_{14}$ presents two main resonances, which are well reproduced by the simulated spectrum based upon the ^{17}O GIPAW NMR calculations (5 different sites) and give confidence that the calculations describe accurately the experimental data. A third additional sharp resonance is also observed at approximately 70 ppm and is tentatively assigned to water bound at the surfaces of the particles. Upon Ge doping (Figure 2a), the signals clearly broaden as a result of a distribution of chemical shifts rather than quadrupolar couplings (see the ^{17}O MQMAS spectrum of $La_3Ga_4Ge_2O_{14.5}$ in Figure 2b) and this is consistent with Ga/Ge disorder. More importantly, in the two highest Ge doped samples, $La_3Ga_4Ge_2O_{14.5}$ and $La_3Ga_{3.5}Ge_{2.5}O_{14.75}$, an additional resonance is observed in the 230 – 280 ppm shift range. Assignment of this resonance is non-trivial, and so we have used the GIPAW NMR data to identify the origin of this resonance. The calculations reveal that all ^{17}O resonances with a shift larger than 240 ppm are associated with the presence of interstitials oxygens, confirming the doping strategy.

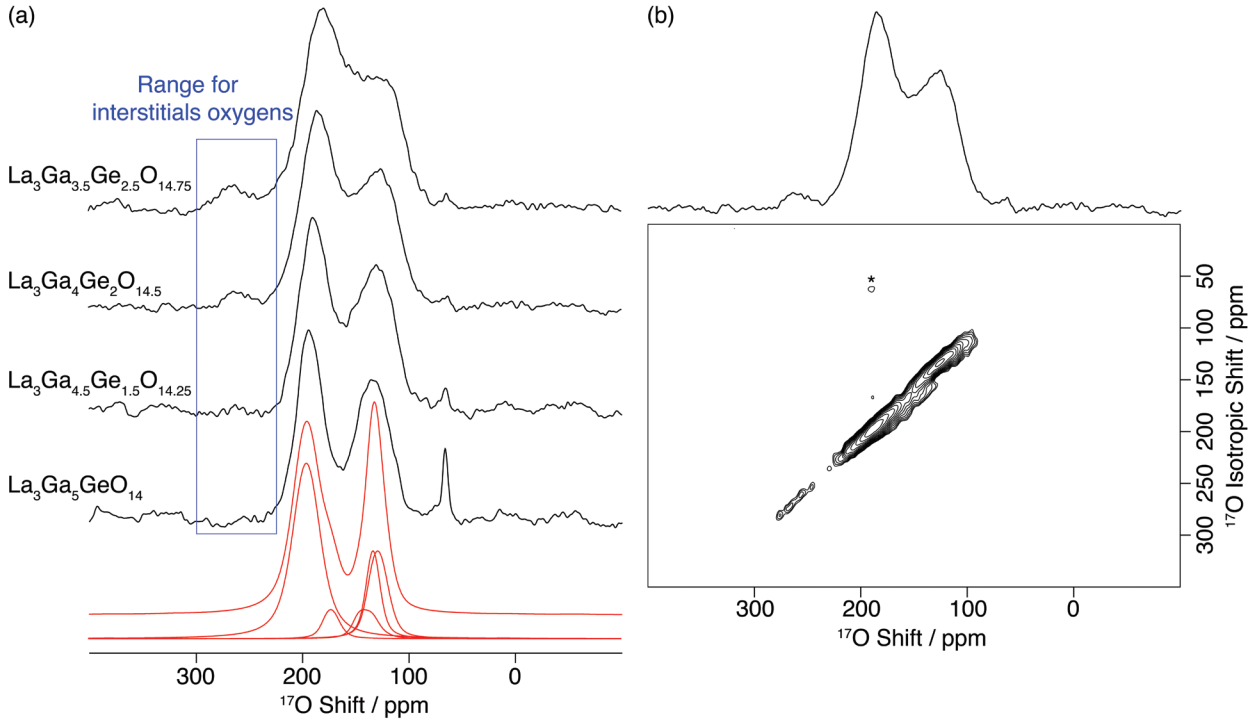

Figure 2. (a) ^{17}O (20.0 T, 22 kHz MAS) NMR spectra of ^{17}O enriched $La_3Ga_{5-x}Ge_{1+x}O_{14+x/2}$ (with $0 \leq x \leq 1.5$) as a function of Ge doping level. The blue rectangle and red lines represent the expected ^{17}O shift range of interstitials oxygens and the simulated spectra obtained from the GIPAW[4] calculations, respectively.[5] The sharp lines around 70 ppm correspond to absorbed H_2O. (b) A ^{17}O MQMAS NMR spectrum of ^{17}O enriched $La_3Ga_4Ge_2O_{14.5}$. Asterisk (*) denotes a spinning side band.

References

1. Kuang, X.; Green, M. A.; Niu, H.; Zajdel, P.; Dickinson, C.; Claridge, J. B.; Jantsky, L.; Rosseinsky, M. J. *Nat. Mat.* **2008**, *7*, 498.
2. Middlemiss, D. S.; Blanc, F.; Pickard, C. J.; Grey, C. P. *J. Magn. Reson.* **2010**, *204*, 1.
3. Iuga, D.; Schäfer, H.; Verhagen, R.; Kentgens, A. P. M. *J. Magn. Reson.* **2000**, *147*, 192.
4. Pickard, C. J.; Mauri, F. *Phys. Rev. B* **2001**, *63*, 245101.
5. Ashbrook, S. E.; Dawson, D. M. *Acc. Chem. Res.* **2013**, *46*, 1964.

Insight into Cation Coordination of Brownmillerite Ba_2InBO_5 (B = Al, Ga) by Solid-State NMR Spectroscopy

Frédéric Blanc, Christophe Didier, John B. Claridge and Matthew J. Rosseinsky

Department of Chemistry, University of Liverpool

Overview

The Brownmillerite structure of general formula $A^{2+}_2B^{3+}_2O_5$ is very well known in solid-state chemistry and is related to the perovskite structure ABO_3. Compensation of the Ba^{2+} and In^{3+} cation charges in $A^{2+}_2B^{3+}_2O_5$ requires the removal of one-sixth of the O atoms in the parent ABO_3 structure yielding a high intrinsic concentration of O vacancies, and the structure could be described as alternating layers of tetrahedral and octahedral centered polyhedra with 'staggered' or 'stacked' O vacancy arrangements (Figure 1a). $Ba_2In_2O_5$ is one of the most studied Brownmillerites as its high temperature cubic phase displays O ion conductivity,[1] albeit with average O conductivity as the vacancy ordering reduces the O mobility, along with fast proton conductivity when hydrated.[1,2] Despite the simplicity of the $Ba_2In_2O_5$ structure, its polymorphism is poorly understood and we have shown that structure characterization can be achieved with multinuclear solid-state NMR.[3,4] Other trivalent B^{3+} cations (Al^{3+}, Ga^{3+}) can be used and we have shown that a new Ba_2InGaO_5 orthorhombic phase can be prepared by a high temperature solid-state reaction.[5] ^{27}Al and ^{71}Ga NMR on Ba_2InAlO_5 and Ba_2InGaO_5, respectively, are used here to help the structural refinements and confirm the coordination number of the B^{3+} cations in both cases, owing to the well known relationship between shift and coordination number for Al and Ga atoms.[6]

^{71}Ga Static and Very Fast MAS Solid-State NMR of Ba_2InGaO_5

^{71}Ga (spin I = 3/2) solid-state NMR spectra of orthorhombic Ba_2InGaO_5 obtained at 20 T and under both static and MAS conditions are presented in Figure 1. The static spectrum was obtained using the QCPMG signal enhancement sequence allowing fast acquisition of the data as a series of narrow 'spikelets' whose manifold reproduces the frequency-domain NMR lineshape. Alternative processing obtained by adding all the echoes together yields a standard looking static NMR spectrum, which could be fitted fairly well with a single Ga environment having a shift of approximately 230 ± 30 ppm, a very large quadrupolar coupling constant (C_Q) of ~25.8 MHz and a quadrupolar asymmetry parameter (η_Q) of 0.04. The MAS spectra obtained under very fast MAS conditions, first at 65 kHz using the 1.3 mm Bruker probe and then at 78 kHz with the 1 mm JEOL probe, showed that the shift is around 220 ppm, in agreement with the static data.

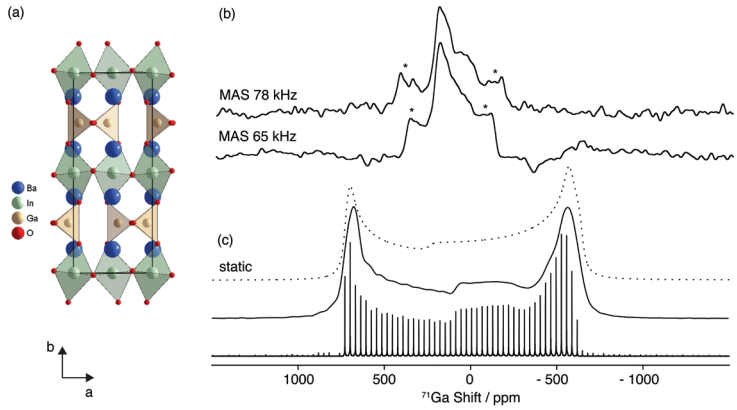

Figure 1. (a) Crystal structure of orthorhombic Brownmillerite $BaInGaO_5$,[5] showing the 'staggered' O vacancy arrangements. (b) ^{71}Ga Hahn echo (20.0 T) spectra obtained under very fast MAS conditions (78 kHz MAS using the JEOL1 mm probe, 15 h experimental time; and 65 kHz MAS using the Bruker 1.3 mm probe, 2 h experimental time). The 78 kHz spectrum was recorded with a 2 ms DFS pulse.[7] Asterisks (*) denote spinning side bands. (c) ^{71}Ga (20.0 T, static, 26 min experimental time) QCPMG NMR spectrum of $BaInGaO_5$. Both 'spikelets' and processed (by adding all the echoes followed by Fourier transformation) QCPMG spectra are shown (full line) along the best fit simulation (dashed line).

Assignment of this resonance based on the shift obtained supports the presence of a tetrahedral Ga site as undependably demonstrated by the combined X-rays and neutron refinement of the structure.[5]

^{27}Al MAS Solid-State NMR of Ba_2InAlO_5

The ^{27}Al (spin I = 5/2) NMR spectra of 2 different Ba_2InAlO_5 sample obtained by high-temperature solid-state reactions at 1250 and 1400 °C and crystallizing in a tetragonal and hexagonal phase, respectively, are presented in Figure 2. Although very different, the 1D NMR spectra of both samples show that most Al signals appear in the 50 - 90 ppm shift range, demonstrating that most of the Al sites are in a tetrahedral geometry. This is in line with the ^{71}Ga results in orthorhombic Ba_2InGaO_5 and the presence of tetrahedra Ga. An ^{27}Al MQMAS spectrum of tetragonal Ba_2InAlO_5 shows that two different Al tetrahedra are clearly visible at a shift of approximately 75 ppm and with different quadrupolar parameters (with C_Q = 10 MHz and η_Q = 0; and C_Q = 2 MHz and η_Q not determined); we have tentatively assigned these resonances to Al sites in both 'staggered' or 'stacked' O vacancy arrangements. The MQMAS data of hexagonal Ba_2InAlO_5 reveals the presence of three ^{27}Al NMR resonances at 86, 78 and approximately 75 ppm for Al ions in tetrahedra, the latter clearly showing a tail towards low frequency due to a distribution of NMR quadrupolar parameters caused by disorder.[8]

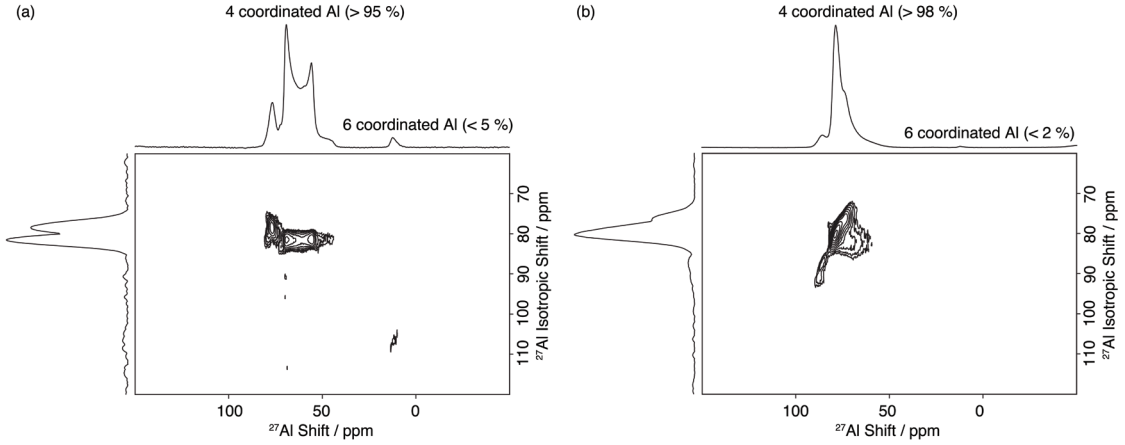

Figure 2. ^{27}Al (20.0 T, 30 kHz MAS) MQ MAS NMR spectra of (a) tetragonal and (b) hexagonal Ba_2InAlO_5. Top: semi-quantitative one pulse NMR spectra obtained with a short 30° pulse flip angle. Left: Isotropic projection along F_1.

References

1. Goodenough, J. B.; Ruizdiaz, J. E.; Zhen, Y. S. *Solid State Ionics* **1990**, *44*, 21.
2. Jayaraman, V.; Magrez, A.; Caldes, M.; Joubert, O.; Taulelle, F.; Rodriguez-Carvajal, J.; Piffard, Y.; Brohan, L. *Solid State Ionics* **2004**, *170*, 25.
3. Dervişoğlu, R.; Middlemiss, D. S.; Blanc, F.; Holmes, L. A.; Lee, Y.-L.; Morgan, D.; Grey, C. P. *Phys. Chem. Chem. Phys.* **2014**, *16*, 2597.
4. Dervişoğlu, R.; Middlemiss, D. S.; Blanc, F.; Lee, Y.-L.; Morgan, D.; Grey, C. P. *Chem. Mater.* **2015**, DOI**:** 10.1021/acs.chemmater.5b00328.
5. Didier, C.; Claridge, J. B.; Rosseinsky, M. J. *J. Solid State Chem.* **2014**, *218*, 38.
6. MacKenzie, K. J. D.; Smith, M. E. *Multinuclear Solid-State NMR of Inorganic Materials*; Pergamon Press: Oxford, 2002.
7. Iuga, D.; Schäfer, H.; Verhagen, R.; Kentgens, A. P. M. *J. Magn. Reson.* **2000**, *147*, 192.
8. Jager, C.; Kunath, G.; Losso, P.; Scheler, G. *Solid State Nucl. Magn. Reson.* **1993**, *2*, 73.

Multinuclear Solid-State NMR Characterization of Guanosine Self-Assembly

G. N. Manjunatha Reddy,[1] Gretchen M. Peters,[3] Daniel S. Cook,[2] Dinu Iuga,[1] Jeffrey T. Davis,[3] Richard I. Walton,[2] Andrew Marsh[2] and Steven P. Brown[1]

[1]*Department of Physics, University of Warwick*

[2]*Department of Chemistry, University of Warwick*

[3]*Department of Chemistry and Biochemistry, University of Maryland, USA*

Overview

Nucleobases self-assemble into supramolecular structures in organic solutions, gels, on surfaces and in the solid state.[1] Many NMR isotopes, e.g., ^{1}H, ^{7}Li, ^{11}B, ^{13}C, ^{14}N, ^{19}F, ^{23}Na, ^{29}Si, ^{39}K, ^{133}Cs, can be used in a solid-state NMR characterisation of guanosine self-assembly. This is illustrated here in, first, the characterization of guanosine-based supramolecular hydrogels,[2] and second a NMR crystallography study of ribbon-like guanosine self-assembly in the solid state.[3]

Guanosine-Based Supramolecular Hydrogels

Supramolecular hydrogels have potential applications in diverse fields such as drug delivery and tissue engineering. We study here a stable supramolecular hydrogel formed by guanosine (G **1**) and $KB(OH)_4$. As shown in Figure 1, ^{1}H-decoupled ^{11}B MAS NMR enables the distinction of guanosine borate (GB) monoester (**2**) and diesters (**3**, **4**). Specifically, it is shown that GB diester components predominantly contribute to the formation of gel-like substance while monoester components likely remain in solution.

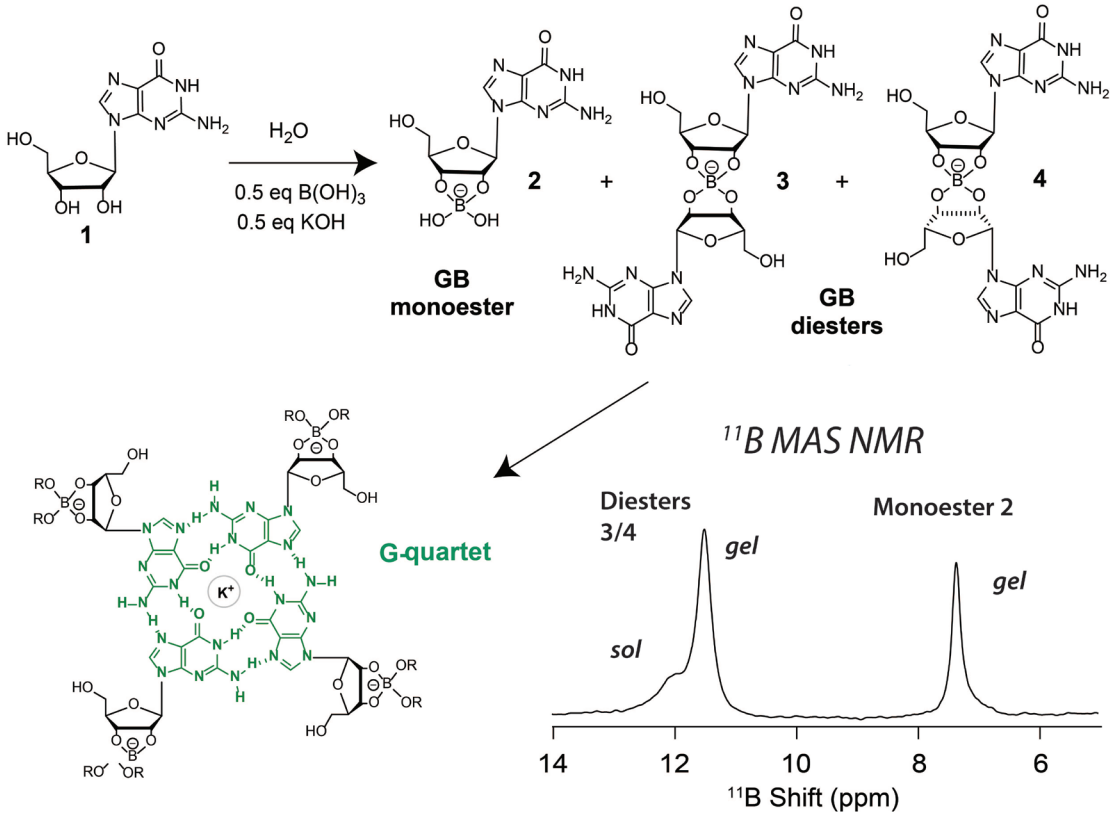

*Figure 1. Guanosine (**1**) and $KB(OH)_4$ forms GB monoester **2** and diastereomeric GB diesters **3** and **4**. ^{11}B {^{1}H-decoupled} MAS (^{1}H, 850 MHz; ^{11}B, 272.8 MHz; 5 kHz MAS; 2 hours experimental time) spectra of 2 wt % $G_4 \cdot K^+$ hydrogel.*

A NMR Crystallography Study of Ribbon-Like Self-Assembly in the Hemihydrate of 2´3´-Isopropylidineguanosine

A NMR crystallography study of the hemihydrate of 2´, 3´-*O*-isopropylidineguanosine (Gace) is presented in Figure 2c, together with powder X-ray diffraction (Figure 2a) and thermogravimetric analysis (Figure 2b).[3] ^{1}H double-quantum and ^{14}N-^{1}H HMQC spectra recorded at 850 MHz with 75 kHz MAS (using a JEOL 1 mm probe) and a ^{1}H-^{13}C refocused INEPT spectrum recorded at 500 MHz and 12.5 kHz MAS using eDUMBO-1_{22} ^{1}H homonuclear decoupling are presented. NMR chemical shieldings are calculated using the GIPAW (gauge-including projector augmented wave) method; good two-dimensional agreement between calculation and experiment is observed for ^{13}C and ^{1}H chemical shifts for directly bonded C8-H8 peaks. There are two Gace molecules in the asymmetric unit cell: differences in specific ^{1}H chemical shifts are rationalised in terms of the strength of CH-π and intermolecular hydrogen bonding interactions.

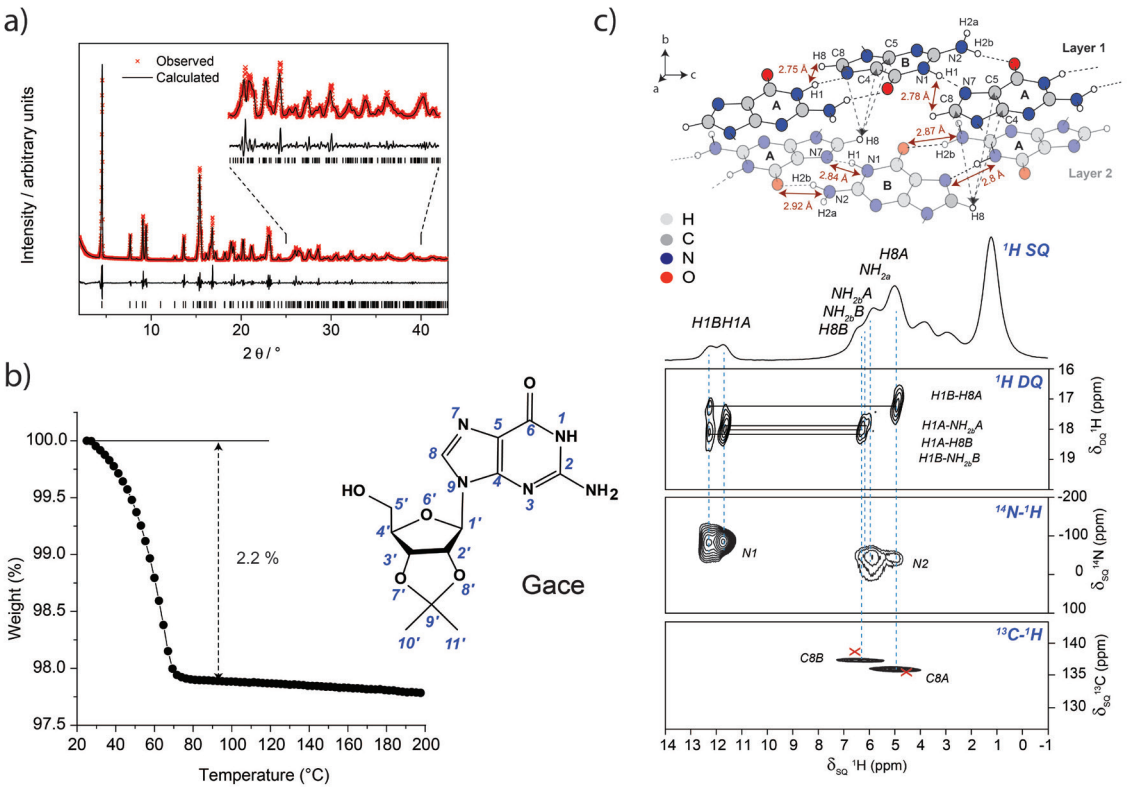

Figure 2. (a) Final profile fit to the powder XRD pattern of Gace.0.5H$_2$O (R_{wp} = 15.10% and R_p = 10.96%). (b) Thermogravimetric analysis of Gace.0.5H$_2$O. (c) A schematic representation of the crystal structure that identifies intermolecular hydrogen bonding and CH-π interactions as well as H-H proximities and spectral regions corresponding to the NH, NH$_2$ and H8 resonances extracted from (top) ^{1}H (850 MHz, 75 kHz MAS) DQ-SQ (1 τ_r of BABA recoupling, 32 transients were co-added for each of 256 t_1 FIDs corresponding to a total experimental time of 5 h), (middle) ^{14}N-^{1}H (^{1}H 850 MHz, 75 kHz MAS) HMQC (τ_{RCPL} = 12 τ_r = 160 μs, ^{14}N pulse duration was 5 μs, 128 transients were co-added for each of 48 t_1 FIDs corresponding to a total experimental time of 3 h) and (bottom) ^{13}C-^{1}H refocused INEPT (^{1}H 500 MHz, ^{13}C 126 MHz, 12.5 kHz MAS, eDUMBO-1_{22} ^{1}H homonuclear decoupling, $\tau = \tau' = 1.4$ ms, 512 transients were co-added for each of 48 t_1 FIDs corresponding to a total experimental time of 21 h, note that here the horizontal axis corresponds to the F_1 (^{1}H) dimension). Crosses (in red) are GIPAW calculated chemical shifts. The base contour level is at (top) 1%, (middle) 3% and (bottom) 12% of the maximum peak height.

References

1. Davis J. T., *Angew. Chem.* **2004**, *43*, 668.
2. Peters G. M.; Scala L. P.; Plank T. N.; Hyman B. J.; Reddy G. N. M.; Marsh A.; Brown, S. P.; Davis J. T.; *J. Am. Chem. Soc.* **2014**, *136*, 12596.
3. Reddy G. N. M.; Cook D. S.; Iuga D.; Walton R. I.; Marsh A.; Brown, S. P. *Solid State Nucl. Magn. Reson.* **2015**, *65*, 41.

Solid-State NMR on HF Encapsulated Inside a Fullerene Cage

Richard Bounds, Salvatore Mamone, Andrea Krachmalnicoff, Richard J. Whitby, Malcolm H. Levitt, Marina Carravetta

School of Chemistry, University of Southampton

Overview

A new and interesting member of the endohedral fullerene family was prepared at the University of Southampton and has HF as a guest molecule inside a fullerene.[1] We describe here the use of the 850 MHz Facility to study the ^{1}H and ^{19}F environments and the strength of the HF intramolecular interaction. We performed variable spinning measurements on this system, to characterise the anisotropic parameters. Our first study was the characterisation of the open caged fullerene denoted HF@1 for simplicity; after successfully closing the cage, we then characterised the closed HF@C_{60}.

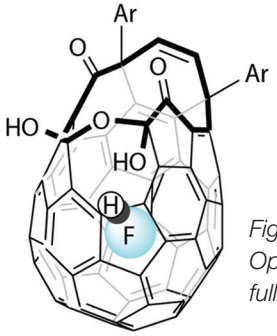

Figure 1. HF@1. Open cage fullerene with HF

^{19}F NMR to Characterise Anisotropy Parameters of Open Caged HF fullerene: Experiments and Simulations

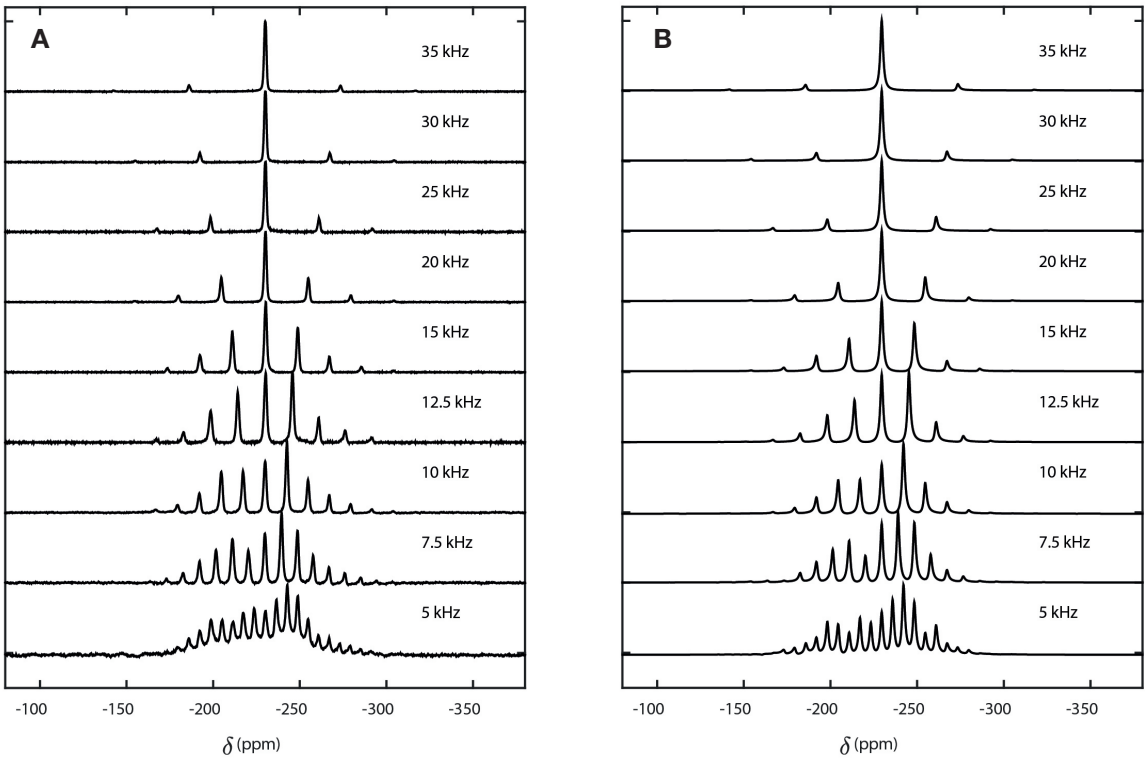

Figure 2. (A) ^{19}F MAS spectra of solid HF@1 (6.6 mg) recorded at 20.0 T and a temperature of 263 K, at the indicated spinning frequencies. The ^{19}F chemical shift scale is referenced to β-Polyvinylidene fluoride (PVDF); Each spectrum is the average of 256 coadded transients. (B) Simulated spectra (using SPINACH[2] and SIMPSON[3]) with parameters determined from best fit to experiment. The direct dipolar interaction was determined to be –7.5 ± 2.5 kHz and the ^{19}F chemical shift anisotropy was 44.1 ppm ± 1.7 ppm, with the biaxiality determined to be 0.6 ± 0.05. The major axis of the ^{19}F CSA tensor is estimated to be orientated at (α, β, γ) = (0, 90°, 0) with respect to the dipolar coupling tensor.

^{13}C, ^{1}H, ^{19}F Spectra of Closed Fullerene: $HF@C_{60}$

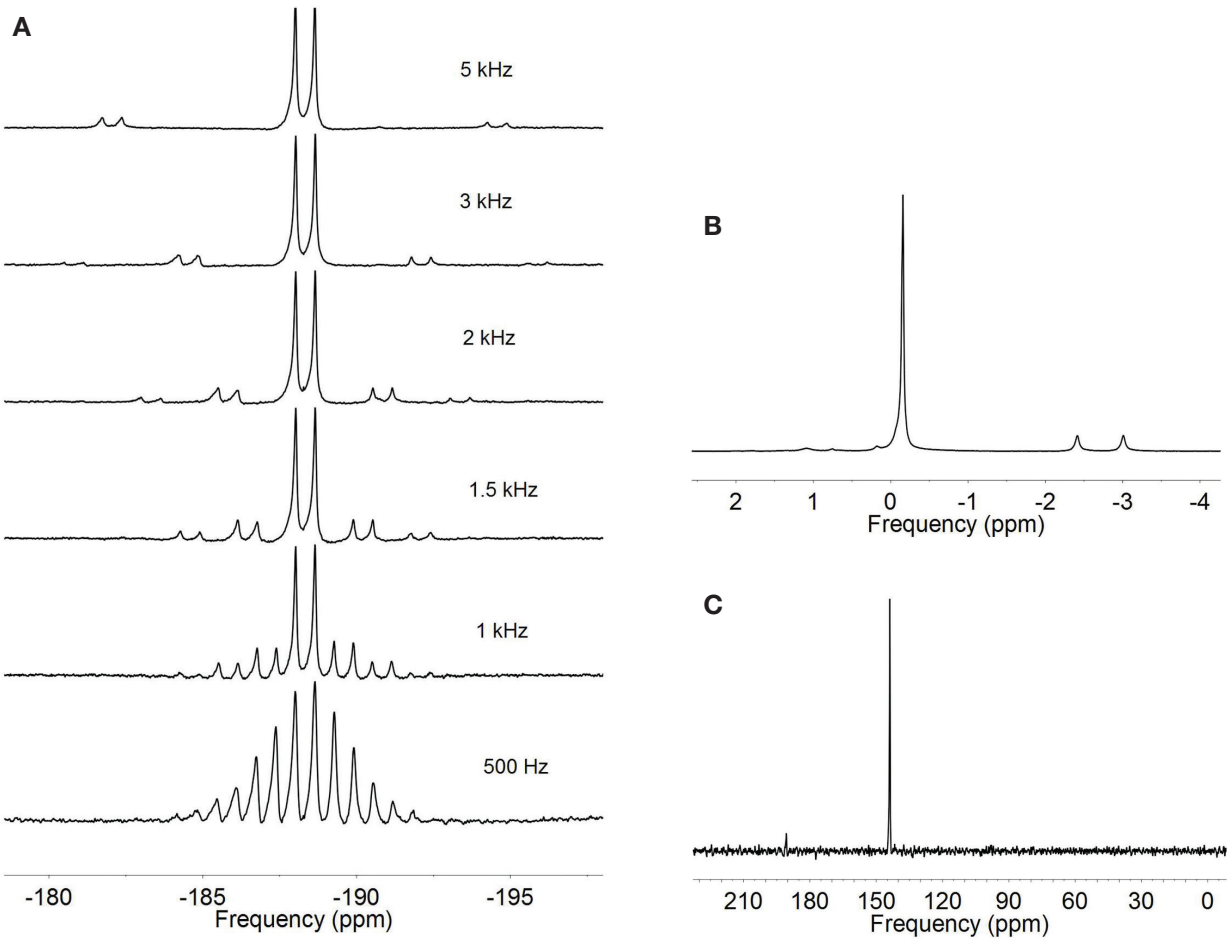

Figure 3: NMR spectra of 10 mg of $HF@C_{60}$ recorded at 20.0 T. (A) ^{19}F spectra for variable spinning frequency. A HF J doublet is visible and corresponds to a coupling of ~500 Hz. Spectra are the result of 256 coadded transients collected using a spin echo and the spectral width is 500 kHz. The ^{19}F chemical shift scale is referenced to β-Polyvinylidene fluoride (PVDF) with a chemical shift of –91 ppm.[4] (B) A ^{1}H single-pulse spectrum of $HF@C_{60}$ with a HF doublet visible centered around –3 ppm. 256 transients were coadded, with a MAS frequency of 10 kHz and a spectral width of 50 kHz. The ^{1}H chemical shift scale is referenced to adamantane at 1.8 ppm.[4] (C) A ^{13}C single pulse spectrum of $HF@C_{60}$. 1024 transients were coadded, with a MAS frequency of 10 kHz. The ^{13}C chemical shift scale is referenced with respect to the downfield peak of adamantane at 38.5 ppm.[4] The observed chemical shift is consistent with that for C_{60}.[5]

References

1. Krachmalnicoff, A.; Bounds, R.; Mamone, S.; Levitt, M. H.; Carravetta, M.; Whitby, R. J. *Chem. Commun.* **2015**, *51*, 4993.
2. Hogben, H. J.; Krzystyniak, M.; Charnock, G. T. P.; Hore, P. J.; Kuprov, I. *J. Magn. Reson.* **2011**, *208*, 179.
3. Bak, M.; Rasmussen, J. T.; Nielsen, N. C. *J. Magn. Reson.* **2000**, *147*, 296.
4. Morcombe, C. R.; Zilm, K. W. *J. Magn. Reson.* **2003**, *162*, 479.
5. Pennington, C.; Stenger, V. *Rev. Mod. Phys.* **1996**, *60*, 855.

^{14}N Overtone Transition in Solid-State NMR Double Rotation Technique

Ibraheem M. Haies,[1,2] James A. Jarvis,[3] Philip T.F. Williamson[3] and Marina Carravetta[1]

[1]*School of Chemistry, University of Southampton*

[2]*Department of Chemistry, University of Mosul, Mosul, Iraq*

[3]*School of Biological Sciences, University of Southampton*

Overview

In order to overcome the resolution problems in quadrupolar systems, various techniques have been reported for half-integer quadrupole nuclei. Double rotation (DOR)[1-3] is a mechanical technique that manipulates the spatial part of the quadrupolar Hamiltonian. Specifically, DOR averages out anisotropic broadening that depends on the second- and fourth-rank Legendre polynomials by rotating the sample at two angles, one at the magic angle and the other one at 30.56° or 70.12°. Here we demonstrate that this method can be used to reduce the linewidth of ^{14}N overtone NMR spectra and we provide exact numerical simulation of the data using the Spinach package.[4] All data here were acquired at 20.0 T.

^{14}N Overtone Spectra

Figure 1 presents *Spinach* simulations and experimental results of ^{14}N overtone spectra for deuterated glycine and deuterated N-acetyl-valine (NAV) using the DOR technique.

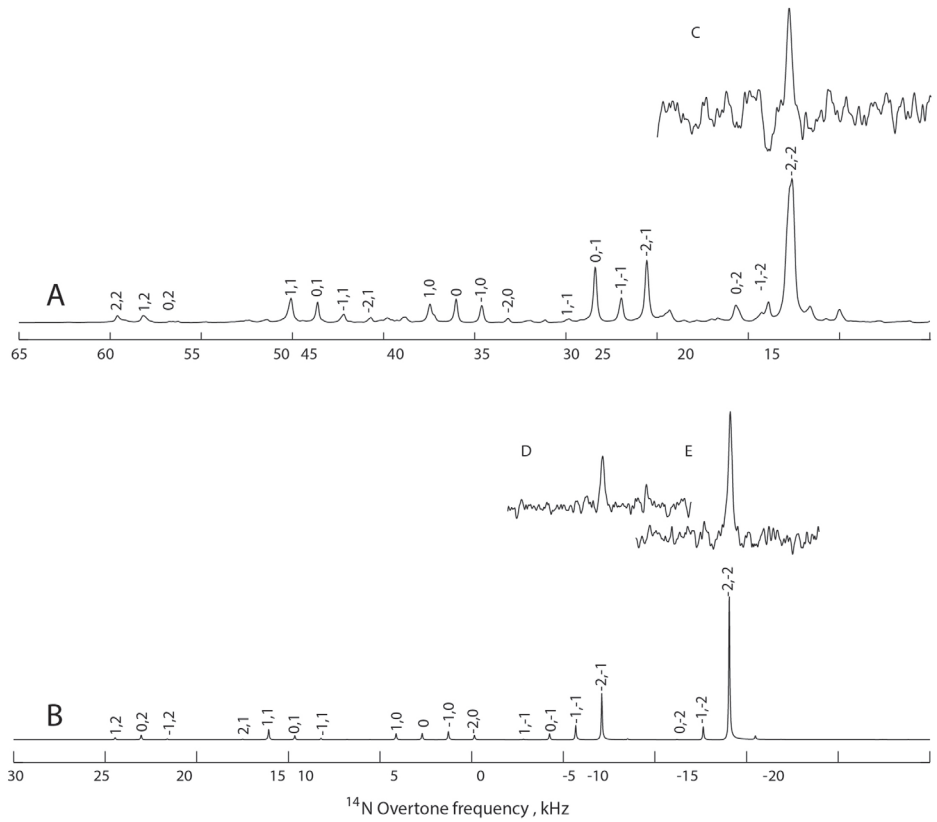

Figure 1. Simulation of ^{14}N overtone transition using 3 MHz rf nutation frequency, 1 μs pulse length. (A) NAV with $\nu_{r\ outer}$ = 1.450 kHz and $\nu_{r\ inner}$ = 7.6 kHz; (B) glycine with $\nu_{r\ outer}$ = 1.425 kHz and $\nu_{r\ inner}$ = 6.95 kHz. The numbers above the peaks are indexes for spinning sidebands of the outer and inner rotors, i.e., 1,2 indicates the first sideband for the outer rotor and second sideband for the inner rotor. (C) Experimental ^{14}N spectrum of the 2,2 spinning sideband of deuterated NAV acquired with 550,000 coadded transients using a 300 μs pulse length and 21 kHz rf nutation frequency. (D-E) Experimental ^{14}N spectra of the 2,2 and 2,1 spinning sidebands of deuterated glycine, acquired with 40,000 coadded transients using a 800 μs pulse length and 21 kHz rf nutation frequency.

Optimization of the pulse length at 21 kHz rf nutation frequency for deuterated glycine has been performed near the most intense signal (2,2 spinning sideband at about 9.1 kHz). The optimal pulse length (strongest signal) is between 600 μs and 1200 μs at this rf nutation frequency. Simulation of the spinning sideband using the same rf nutation frequency and the same spinning frequency shows that the optimal pulse length is about 1200 μs. The most intense signal for NAV is the 2,2 spinning sideband at about 22.7 kHz, and this has a shorter optimal pulse length (about 450 μs).

Simulations show that the 2,2 spinning sideband for glycine is more intense than the 2,1 sideband, in agreement with our experimental results (Figures 2A and 2B). Both signals are much narrower than the ^{14}N overtone signal under MAS (Figure 2C). Other spinning sidebands were acquired by moving the carrier frequency to match the conditions (1,0), (2,0), (0,2) and (1,2), but no signal could be observed with only 8,000 coadded transients and these data are not shown here.

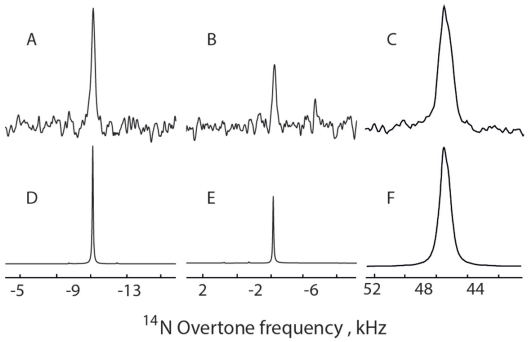

Figure 2. (A-B) Experimental ^{14}N DOR spectra for the 2,2 (at about 9.1 kHz) and 2,1 (at about 2.1 kHz) spinning sidebands respectively of deuterated glycine acquired with 40,000 coadded transients. (C) ^{14}N MAS data for the signal the 2 spinning sideband of natural abundance glycine with 1024 coadded transients, acquired using a 3.2 mm probe. D, E and F are the corresponding simulations of A, B and C, respectively. DOR data were acquired using a nominal RF amplitude of 21 kHz, and a 800 μs pulse length without decoupling during the acquisition, under spinning frequency $\nu_{r\ outer}$ = 1.425 kHz and $\nu_{r\ inner}$ = 6.95 kHz. MAS data were acquired using a nominal rf nutation frequency of 70 kHz, and 275 μs pulse length using SPINAL64 decoupling during acquisition, at ν_r = 19.84 kHz.

Simulations show that NAV gives many spinning sidebands with slightly different intensity. Experimental data at the 2,2 spinning sideband of deuterated NAV were acquired using a 300 μs pulse length (see Figure 3A).

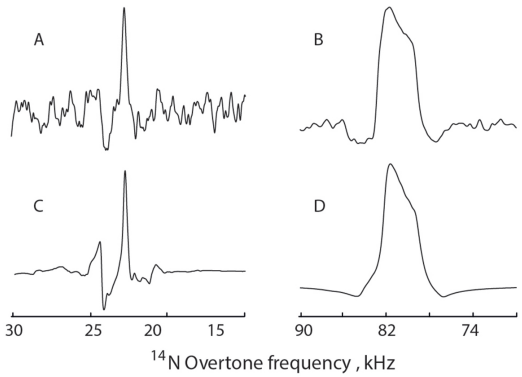

Figure 3. Simulation and experimental data for the ^{14}N overtone transition of deuterated NAV (DOR data) and natural abundance NAV (MAS data). DOR data were acquired using a nominal RF amplitude of 21 kHz, and a 300 μs pulse length without decoupling during the acquisition, under a spinning frequency of $\nu_{r\ outer}$ = 1.45 kHz and $\nu_{r\ inner}$ = 7.6 kHz. MAS data were acquired using a nominal RF amplitude of 70 kHz, and a 275 μs pulse length using SPINAL64 decoupling during acquisition, at ν_r = 19.84 kHz. (A) DOR experimental data for the signal at about 22.7 kHz (2,2 spinning sideband) of deuterated NAV acquired with 550,000 coadded transients. (B) MAS data for the signal at the 2 spinning sideband of NAV acquired with 40,000 coadded transients. (C-D) are the corresponding simulations of A and B, respectively.

References

1. Samoson, A.; Lippmaa, E.; Pines, A. *Mol. Phys.* **1988**, *65*, 1013.
2. Chmelka, B. F.; Mueller, K. T.; Pines, A.; Stebbins, J.; Wu, Y.; Zwanziger, J. W. *Nature* **1989**, *339*, 42.
3. Samoson, A.; Pines, A. *Rev. Sci. Instrum*. **1989**, *60*, 3239.
4. Hogben, H. J.; Krzystyniak, M.; Charnock, G. T.; Hore, P. J.; Kuprov, I. *J. Magn. Reson.* **2011**, *208*, 179.

^{13}C MAS NMR Studies of Dried and Never-Dried Plant Stems

Thomas J. Simmons,[1] Jennifer C. Mortimer,[1] Dharmesh Patel,[1,2] Steven P. Brown,[2] Ray Dupree[2] and Paul Dupree[1]

[1]*Department of Biochemistry, University of Cambridge*

[2]*Department of Physics, University of Warwick*

Overview

A major technological challenge in using plant biomass for renewable energy is to release the sugars from the main polysaccharides – cellulose and xylan – effectively and cheaply. Pilot biofuel production processes involve the use of harsh energy-intensive biomass pretreatments, and also require the addition of high quantities of enzymes to break down the biomass. Progress in improving these steps is restrained by the limited understanding of the molecular basis of plant cell wall 'recalcitrance' – the difficulty in deconstructing lignocellulose into fermentable sugars. Despite being crucial to this recalcitrance, the molecular architecture (the rotational conformation and molecular arrangement) of the different polymers in the cell walls of woody materials is poorly understood. To enable detailed studies of cell wall molecular architecture we have developed methodologies to analyse commercially obtained, lyophilised, mature stems of the model plant *Arabidopsis*, grown in air enriched with $^{13}CO_2$ as the carbon source achieving ~97% ^{13}C incorporation. The stems were inserted into MAS rotors with minimal physical pre-treatment and no chemical treatments. As well as continued work on assignments in the spectra from earlier 2D and 3D ^{13}C NMR experiments, recognition that dehydration of cellulose is known to irreversibly affect its structure has directed us toward the development of a strategy for analysis of never-dried Arabidopsis stems. This mandated the in-house construction of a bespoke growth chamber which has allowed us to analyse freshly harvested, never dried, plants as well as mutants (with differing cell wall compositions and architectures) to be studied.

Results

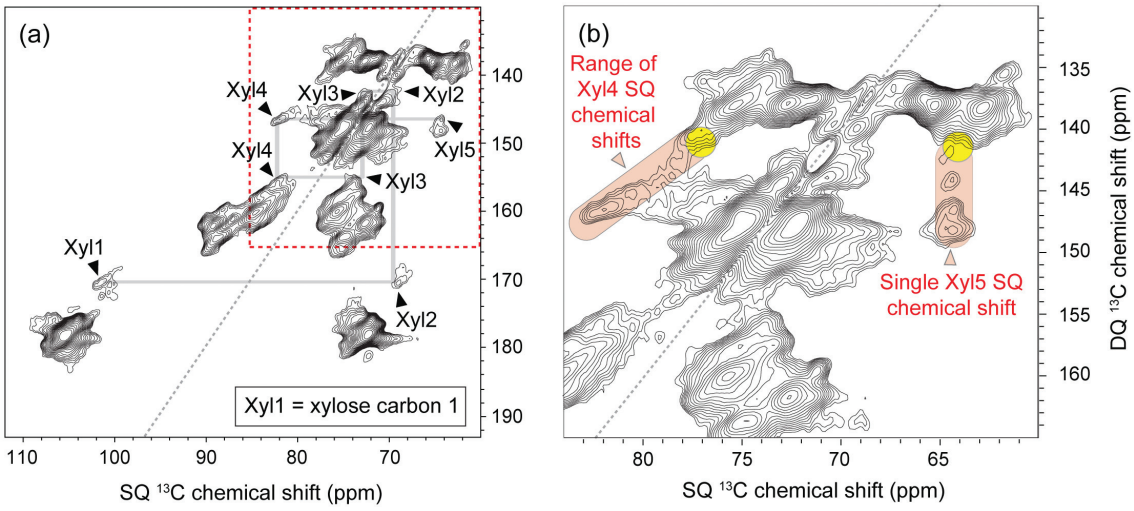

Figure 1. Assignment of xylan xylose in dried mature Arabidopsis stems. (a) refocused ^{13}C INADEQUATE (20 Tesla, 14 kHz MAS) spectrum with arrows showing carbohydrate region peaks assigned to xylose carbons 1–5. (b) zoom-in on (a) (indicated by red dashed square) with lower minimum contour level showing range of xylose carbon 4 chemical shifts all J-coupled to a single carbon 5 chemical shift (pink areas) and chemical shifts of xylan carbon 4 and carbon 5 from solution (yellow areas).

Having previously assigned both domains of cellulose in lyophilised samples, we have now additionally assigned the xylose backbone residues of the major non-cellulose component of the cell wall: xylan[1] (Figure 1a). This assignment is supported by refocused ^{13}C INADEQUATE, ^{13}C RFDR and 3D ^{13}C-^{13}C-^{13}C DARR experiments. Interestingly, while carbons 1, 2, 3 and 5 similar shifts to those reported in the literature for solution state xylan,[2] the major peak for carbon 4 in our assignment from Arabidopsis

mature tissues was roughly 5 ppm higher (~82 ppm compared to ~ 77 ppm). A few other investigations (e.g. Teleman et al.[3]) have also assigned a peak at ~82 ppm to a xylan carbon in wood and wood pulp, though they were unable to assign any more precisely. We suggest that this distinct carbon 4 chemical shift may indicate that xylan in woody materials exists in a distinct conformation relative to its preferred solution conformation. Moreover, there appears to be a range of xylose carbon 4 chemical shifts (SQ values ~79–84 ppm with a range of DQ values from ~143 to 148 ppm) linked to a single xylose carbon 5 chemical shift (64.3 ppm; Figure 1b), suggesting that a range of rotational conformations might be present, perhaps including a very small proportion in the conformation found in solution.

To investigate the molecular architecture in native never-dried material, and to assess the effect of drying on cell wall molecular architecture, we next analysed never-dried stems of home-grown ^{13}C-labelled wild type Arabidopsis stems. A direct polarisation (DP) refocused ^{13}C INADEQUATE experiment, taken with a short relaxation delay to accentuate the faster relaxing more mobile components, showed many peaks most of which could be resolved since their linewidths were often ~ < 0.3 ppm (Figure 2) clearly demonstrating the benefits of using the 850 MHz spectrometer. The cross-polarisation (CP) refocused INADEQUATE spectrum (also shown in Figure 2), which emphasises the less mobile species, shows a distinct carbohydrate profile to the DP experiment including major cellulose peaks, and had significantly broader linewidths. Assignment of these peaks is still in progress, however two sets of arabinose signals (one of which is labelled in Figure 2) are clearly observed in the DP spectrum.[4] None of these arabinose signals are observed in the CP spectrum indicating their high mobility. These results show that use of the 850 MHz spectrometer to study never dried stem materials, ^{13}C labelled with the in-house growth chamber, provides much greater resolution data than achieved on the dried material. These data will provide an insight into the mobility of components of the plant cell wall.

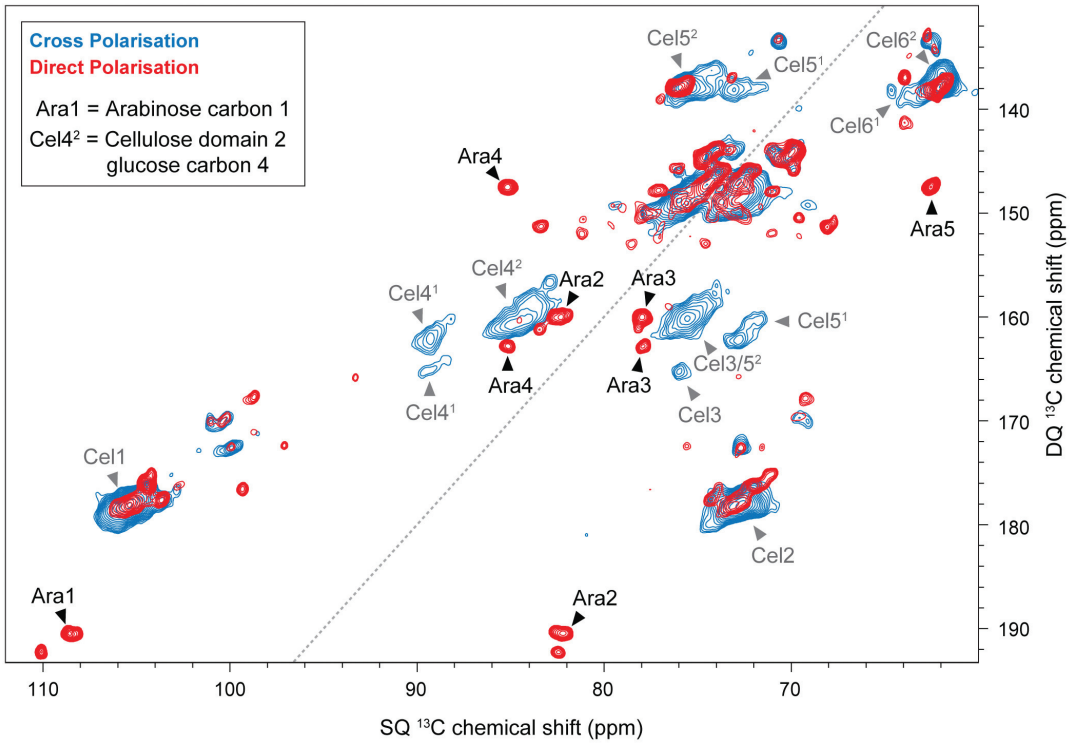

Figure 2. Cross Polarisation and Direct Polarisation refocused ^{13}C INADEQUATE (20 Tesla, 14 kHz MAS) of spectrum of never-dried Arabidopsis stems. Carbon shifts assigned to an arabinose (probably from pectic arabinan) and cellulose are indicated.

References

1. Dupree, R.; Simmons, T. J.; Mortimer, J. C.; Patel, D.; Iuga, D.; Brown, S. P.; Dupree, P. *Biochemistry* **2015**, *54*,2335.
2. Busse-Wicher, M.; Gomes, T. C. F.; Tryfona, T.; Nikolovski, N.; Stott, K.; Grantham, N. J.; Bolam, D. N.; Skaf, M. S.; Dupree, P. *Plant J.* **2014**, *79*, 492.
3. Teleman, A.; Larsson, P. T.; Iversen, T. *Cellulose* **2001**, *8*, 209.
4. Wang, T.; Salazar, A.; Zabotina, O. A.; Hong, M. *Biochemistry* **2014**, *53*, 2840.

^{17}O DOR and MQMAS and Studies on Silico-Oxyphosphate ($Si_5O(PO_4)_6$) and α-Calcium Pyrophosphate (α-$Ca_2P_2O_7$)

Maria C. Vlachou,[1] Christian Bonhomme,[2] Franck Fayon,[3] Zhongjie Lin,[1] Peter R. Slater[4] and John V. Hanna[1]

[1] *Department of Physics, University of Warwick*

[2] *Laboratoire de Chimie de la Matèrie Condensée, UPMC, Paris, France*

[3] *CNRS, UPR3079 CEMHTI, Orleans, France*

[4] *School of Chemistry, University of Birmingham*

Overview

Numerous perovskite, pyrochlore, apatite and other related oxo-based systems have exhibited much potential as electrolyte and electrode materials in fuel cell applications. These systems demonstrate the structural flexibility to incorporate significant amounts of oxyanion doping. Doping in such perovskite-related systems can be achieved through carbonate, phosphate and sulphate incorporation.[1] Whilst carbonate doped perovskites have been shown to stabilise phases that are inaccessible without doping, current research into such systems has shown that they generally possess low thermal stability.[2] The silico-oxyphosphate $Si_5O(PO_4)_6$ structure consists of isolated SiO_6 octahedra and Si_2O_7 moieties connected by PO_4 tetrahedra forming a three dimensional network, without the requirement of cation species to perform charge balancing throughout the overall structure. These networks do exhibit ionic conduction properties and they are being investigated for suitability as solid oxide fuel cell materials. The solid-state NMR characterisation of these structures is incomplete as fundamental measurements characterising the ^{17}O speciation had previously not yet been attempted. An understanding of the increasing structural complexity upon structural alteration will be based on an accurate characterisation of the O speciation defining the base materials. Furthermore, the formation of vacancy and/or interstitial species may be very site-specific to certain parts of the structure, with the modes of O conductivity being highly directional and anisotropic.

Calcium phosphates are biocompatible materials, applicable to the fields of dentistry, orthopaedic implants and bone repair. Recently, it has been shown that bioactivity enhancements are exhibited upon doping of these systems where the apatite structure can incorporate a wide range of ions, changing its anionic and cationic sublattices.[3] Calcium pyrophosphate α-$Ca_2P_2O_7$ consists of P_2O_7 units connected by CaO_6 and CaO_7 units. Recent experimental ^{17}O NMR measurements and first principles calculations suggest that ^{17}O chemical shifts and quadrupolar parameters can easily identify the different O moieties of these systems.[4]

^{17}O DOR NMR Results

Double rotation (DOR) NMR satisfies the dual averaging over two angles for which the quadrupolar interaction is dependent, thus removing the associated broadening. However, the quadrupolar shift resulting from the second order perturbation of the central transition acts to move the apparent centre-of-gravity shift, δ_{CG}, to lower frequency $\delta_{CG} = \delta_{iso} + \delta_Q^{(2)}(I,m)$, with the quadrupolar shift inversely dependent on the square of the B_0 field. Here we present ^{17}O DOR NMR data of ^{17}O enriched α-$Ca_2P_2O_7$ and $Si_5O(PO_4)_6$ systems. A variable field approach facilitates graphical analyses from which the gradient determines the quadrupole frequency ($P_Q = C_Q\sqrt{(1+\eta_Q^2/3)}$) and the x-intercept corresponds to the isotropic chemical shift (δ_{iso}).

^{17}O DOR NMR measurements for α-$Ca_2P_2O_7$ obtained at 20 T complement the data acquired at 14.1 and 11.7 T. As shown in Figure 1a single bond ^{17}O- ^{31}P *J* couplings (J^1_{OP}) for the six non-bridging oxygens (NBOs) present in this structure can be observed ($\langle J^1_{OP}\rangle$ ~90 Hz).

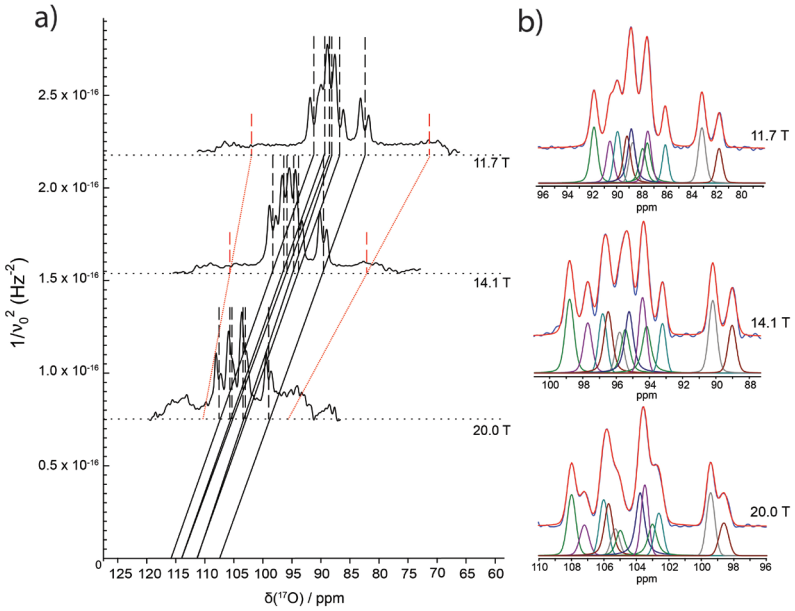

Figure 1: ^{17}O DOR NMR experimental spectra for α-$Ca_2P_2O_7$ (850, 600 and 500 MHz, ν_R(outer-rotor) = 1300 Hz) of (a) the six NBO species sitting above the broad, unaveraged P-O-P moiety, (minimum width shown by the red markers, indicating the field dependence). The gradient is proportional to P_Q and the x intercept corresponds to δ_{iso} and (b) displays spectral simulations (from DMFit) that facilitated the measurement of the δ_{CG} and J^1_{OP} values.

The observed imbalance in the J^1_{OP} coupling patterns are caused by the relative signs and orientations of the J^1_{OP}, ^{17}O-^{31}P dipolar coupling (D_{OP}) and the ^{17}O CSA tensors. All δ_{CG} values were determined by spectral simulation as shown in Figure 1b, thus facilitating the elucidation of P_Q and δ_{iso} values which agree with calculated values derived from GIPAW DFT computation. For the bridging P-O-P oxygen a larger quadrupolar coupling constant of ~7.5 MHz is expected, which is in agreement with previously reported literature values;[5] however, initial estimations from this work suggest a C_Q value of ~15-18 MHz for this species. A number of rationales are possible including the hydration/protonation of the bridging P-O-P linkage; further work is underway to develop these interpretations.

Distinct spectral features corresponding to the five oxygen sites expected from the crystallographic structure of $Si_5O(PO_4)_6$ are observable at the three magnetic fields as shown in Figure 2. Two outer rotor spinning frequencies were used at each field (1300 Hz in red and 1500 Hz in black) in order to identify the sidebands. The extracted experimental quadrupolar parameters are in good agreement with calculations carried out via a DFT approach. Whilst ^{29}Si MAS NMR confirms the presence of amorphous silica (a secondary product), we propose that the bridging oxygen (Si-O-Si) of $Si_5O(PO_4)_6$ with δ_{iso} ~ 40 ppm is unresolved from the oxygen species of amorphous SiO_2. This is further supported by ^{17}O MQMAS data acquired at 16.4 T (not shown).

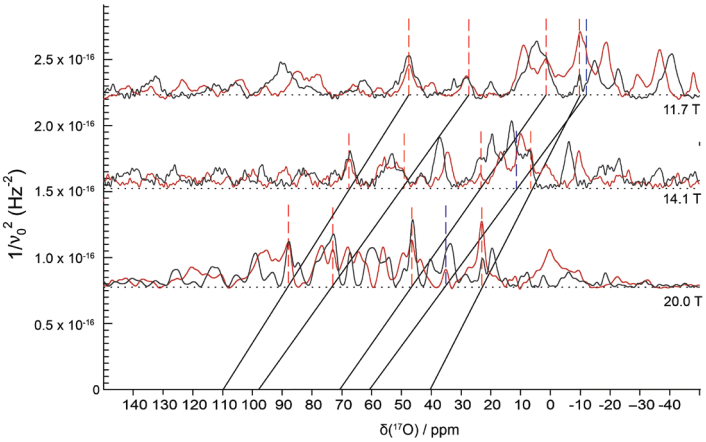

Figure 2: ^{17}O DOR NMR experimental data of $Si_5O(PO_4)_6$ (850, 600 and 500 MHz, ν_R(outer-rotor) = 1300 Hz) where the gradient is proportional to P_Q and the x intercept corresponds to δ_{iso}.

References

1. Porras-Vazquez, J. M.; Slater, P. R. *J. Power Sources*, **2012**, *209*, 180.
2. Slater, P. R.; Greaves, C.; Slaski M.; Muirhead, C.M. *Physica C: Superconductivity*, **1993**, *208*, 193.
3. Vallet-Regi, M. *Dalton Transactions*, **2006,** 5211.
4. Pourpoint, F.; Diogo, C. C.; Gervais, C.; Bonhomme, C.; Fayon, F.; Dalicieux, S. L.; Gennero, I.; Salles, J.-P.; Howes, A. P.; Dupree, R.; Hanna, J. V.; Smith, M. E.; Mauri, F.; Guerrero, G.; Mutin, P. H.; Laurencin, D. *J. Mater. Res.*, **2011**, *26*, 2355.
5. Pourpoint, F.; Gervais, C.; Bonhomme-Coury, L.; Azaïs, T.; Coelho, C.; Mauri, F.; Alonso, B; Babonneau, F.; Bonhomme, C. *Appl. Magn. Reson.*, **2007**, *32*, 435.

CLASSIC NMR Studies of Crystallization Kinetics

Colan E. Hughes, Victoria L. Keast and Kenneth D. M. Harris

School of Chemistry, Cardiff University

Overview

Combined **L**iquid- **A**nd **S**olid-**S**tate ***I**n-situ* **C**rystallization (CLASSIC) NMR (Figure 1) has been developed by our group[1] to allow detailed studies of crystallization processes by monitoring simultaneously the time-evolution of *both* the solution phase *and* the solid phase during crystallization from solution. As the data are recorded *in situ* as a function of time, they can reveal direct insights into the kinetics of crystallization. In particular, the rate of crystallization can be monitored from the time-dependence of the concentration of the solute in solution (from the liquid-state NMR spectra) and from the time-dependence of the amount of solid obtained (from the solid-state NMR spectra). Together, such measurements allow a detailed assessment of the influence of a variety of experimental parameters on the rate of the crystallization process.

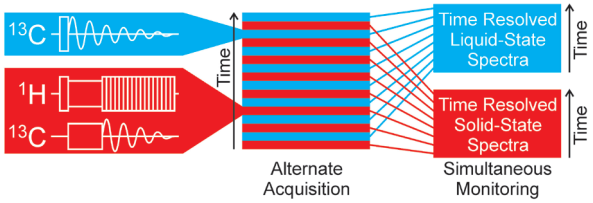

Figure 1. Schematic of the CLASSIC NMR procedure.

Crystallization of Glycine from Water

As a prototypical polymorphic system, glycine has been the focus of many studies of crystallization behaviour, including our own early *in-situ* solid-state NMR studies.[2,3] By exploiting the sensitivity advantage offered by the UK 850 MHz Solid-State NMR Facility, we have studied in detail the kinetics of crystallization of glycine from H_2O, focusing on a sample of glycine ^{13}C labelled in the carboxylate group.

An aqueous solution of 1-^{13}C-glycine was cooled from 65 °C to 20 °C over 13.3 hrs. CLASSIC NMR was carried out during cooling and for another 3 hrs after reaching 20 °C. ^{1}H⟶^{13}C CP MAS NMR spectra (Figure 2a) show growth of the α polymorph throughout the experiment (Figure 3a). The growth is most rapid during the cooling period and continues more slowly after cooling is complete. Direct-excitation ^{13}C NMR spectra (Figure 2b) show a decline in the solution concentration over the same period (Figure 3b). After *ca*. 8 hrs, the intensity of the solution peak decreases significantly and is *not* matched by a rise in the intensity of the peak in the solid-state NMR spectrum. A weak peak due to the α polymorph is also present in the direct-excitation spectra. Surprisingly, the time-dependence of the intensity of this peak does not match that of the peak for the α polymorph in the ^{1}H⟶^{13}C CP NMR spectra and, moreover, shows an abrupt increase in growth rate at the same time that the solution-state peak (i.e., for dissolved glycine) exhibits an abrupt decrease in intensity. Interestingly, in the direct-excitation NMR spectra, the increase in the intensity of the peak for the α polymorph over the duration of the experiment is substantially less than the decrease in the intensity of the peak for dissolved glycine, perhaps due to slow ^{1}H T_1 relaxation for the solid phase.

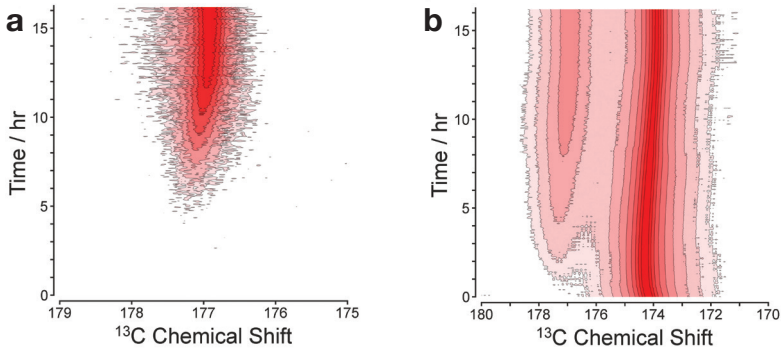

Figure 2. (a) ^{1}H⟶^{13}C CP MAS and (b) direct-excitation ^{13}C NMR spectra (20.0 Tesla) acquired during crystallization of 1-^{13}C-glycine from H_2O.

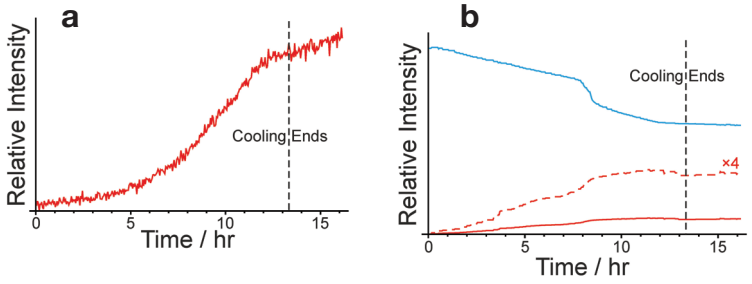

Figure 3. Signal intensities from (a) ^{1}H⟶^{13}C CPMAS and (b) direct-excitation ^{13}C NMR spectra (20.0 Tesla) acquired during crystallization of 1-^{13}C-glycine from H_2O. In (b), the blue line is for the liquid-state peak and the red line for the solid-state peak.

The differing behaviour of the peaks for the α polymorph in the $^{1}H \longrightarrow ^{13}C$ CP and direct-excitation ^{13}C NMR spectra suggests that the different techniques may be detecting different populations of glycine molecules within the solid phase. We estimate[4] that a particle size of *ca*. 4×10^{7} Å^{3} is required for a signal to be observed in such CP experiments. On this basis, we postulate that a significant proportion of the glycine molecules are present in solid particles of the α polymorph that are below this size limit and are therefore only observed by the direct-excitation measurements, whereas the $^{1}H \longrightarrow ^{13}C$ CP measurements only detect solid particles of the α polymorph that are above this size limit.

In a second experiment, with the same solution cooled from 70 °C to 20 °C over 11.7 hrs, the γ polymorph was observed (Figure 4). Integration of peak intensities (Figure 5) shows that a small amount of the γ polymorph was present at the beginning of the experiment, possibly as it has slower dissolution rate than the α polymorph at high temperature (70 °C). After 2 hrs, the amount for the α polymorph increases and soon dominates the solid-state NMR spectrum, although the amount of the γ polymorph also begins to increase (but much more slowly) at this time. The amount of the α polymorph is maximal between 5 and 6 hrs, then falls while the rate of growth of the γ polymorph increases slightly. Between 7.5 and 11.5 hrs, the amount of the α polymorph increases much more rapidly as it once again dominates the $^{1}H \longrightarrow ^{13}C$ CP spectrum. Meanwhile, the amount of the γ polymorph increases slowly but steadily, continuing to grow after completion of the cooling process, whilst the amount of the α polymorph starts to decline at this stage.

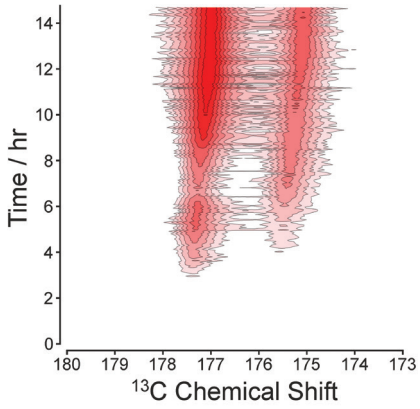

Figure 4. $^{1}H \longrightarrow ^{13}C$ CP MAS NMR spectra (20.0 Tesla) acquired during crystallization of 1-^{13}C-glycine from H_2O.

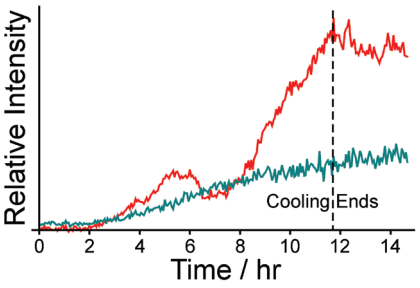

Figure 5. Peak intensities for the α (red) and γ (green) polymorphs of 1-^{13}C-glycine during crystallization from H_2O.

Clearly, crystallization in the presence of a small initial quantity of the γ polymorph (arising from incomplete dissolution) is much more complicated than crystallization in the absence of residual amounts of the polymorph. During the cooling process, the competing rates of growth of the two polymorphs and the rate of conversion from the less stable α polymorph to the more stable γ polymorph result in the complex behaviour observed in these experiments.

Concluding Remarks

By combining the advantages of both high field and isotopic labelling, our studies have revealed details of the evolution of a complex crystallization system, including the first evidence that a portion of the solid phase forms particles below the size limit for detection by $^{1}H \longrightarrow ^{13}C$ CPMAS NMR. This observation allows an improved interpretation of other experimental results and points to the advantages of the CLASSIC NMR approach for studying crystallization systems. Furthermore, our observations for the case in which a small amount of a slow growing, but more stable, polymorph is present from the beginning of the crystallization process further demonstrate the complexity that can be exhibited by crystallization systems for which competing processes occur. The literature on glycine crystallization is replete with reports of *ex situ* studies for which small, undetectable amounts of the γ polymorph could potentially give rise to the effects observed. The results of the present study may provide a possible explanation of such effects.

References

1. Hughes, C. E.; Williams, P. A.; Harris K. D. M. *Angew. Chemie Int. Ed.* **2014**, *53*, 8939.
2. Hughes, C. E.; Harris K. D. M. *J. Phys. Chem. A* **2008**, 112, 6808.
3. Hughes, C. E.; Harris K. D. M. *Chem. Commun.* **2010**, *46*, 4982.
4. Hughes, C. E.; Williams, P. A.; Keast, V. L.; Charalampopoulos, V. G.; Edwards-Gau, G. R.; Harris, K. D. M. *Faraday Discuss.*, published online [DOI: 10.1039/C4FD00215F].

In-Situ NMR Studies of the Crystallization of Solid Solutions

Colan E. Hughes, Victoria L. Keast and Kenneth D. M. Harris

School of Chemistry, Cardiff University

Overview

Solid solutions are a class of materials in which two similar but distinct chemical species form crystals in which each crystallographic site is occupied by either species with a random distribution of occupancies. Examples include many metal alloys as well as several organic co-crystals. An example is the co-crystal formed between benzoic acid (BA) and *p*-fluorobenzoic acid (*p*-FBA). In crystal structures, these molecules (Figure 1) form hydrogen-bonded dimers (involving a cyclic hydrogen-bonding arrangement of the acid groups) with a random distribution of BA and *p*-FBA molecules. We have applied our CLASSIC NMR technique[1] to study crystallization in this system; however, owing to slow ^{1}H T_1 relaxation, solid-state ^{13}C NMR spectra cannot be acquired sufficiently quickly to obtain good time resolution in the *in-situ* study. Instead, we have focused on liquid-state NMR to elucidate the behaviour of the solution phase before, during and after co-crystallization.

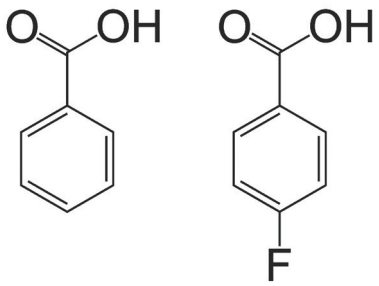

Figure 1. Benzoic acid (left) and p-fluorobenzoic acid (right).

Experimental Results

Figures 2 and 3 show the time-dependence of the liquid-state ^{1}H NMR spectra of solutions containing BA and *p*-FBA in ethanol [with BA:*p*-FBA molar ratios of 30:70 (Figure 2) and 70:30 (Figure 3)] on cooling from 70 °C to 20 °C over 1 hr. In each case, within just a few minutes of completing the cooling process, the peak positions change abruptly, most significantly for the peak (*ca*. 6 ppm) corresponding to OH protons. Although there are three different OH environments (BA, *p*-FBA and ethanol), only one OH peak is observed as a consequence of rapid proton exchange.

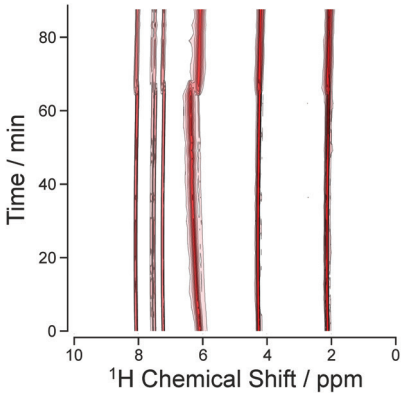

Figure 2. Liquid-state ^{1}H (850 MHz) NMR spectra of BA and p-FBA (30:70) co-crystallizing from ethanol.

Discussion

The two experiments with different BA:*p*-FBA ratios behave in a very similar manner, as may be expected for a system that forms isostructural solid solutions across a wide composition range. For the aromatic protons, the chemical shifts for the different BA:*p*-FBA ratios are very similar and there is very little change in the chemical shifts at the point of crystallization, suggesting that π-π stacking does not play a significant role in the solution state. However, for the OH peak, much more significant differences are observed between the different BA:*p*-FBA ratios (ascribed to the changing ratio of the acids in the exchanging system), as well as a much larger change in the average chemical shift at the moment that crystallization occurs, reflecting the sudden change in the amounts of BA and *p*-FBA present in the solution phase.

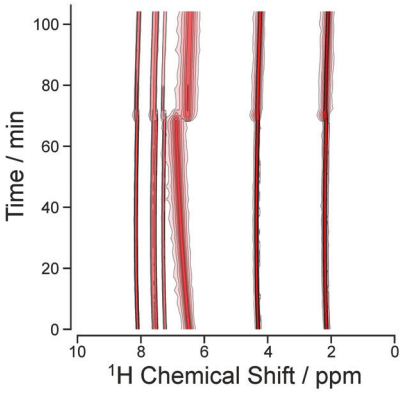

Figure 3. Liquid-state ^{1}H (850 MHz) NMR spectra of BA and p-FBA (70:30) co-crystallizing from ethanol.

Concluding Remarks

While it may seem non-ideal to measure liquid-state NMR spectra on a solid-state NMR spectrometer, such measurements cannot be carried out using a liquid-state instrument as the shimming is badly compromised by the presence of solid material in the NMR tube. Consequently, the type of experiment reported here is the only viable method for probing the behaviour of the solution state during the crystallization process in this system.

References

1. Hughes, C. E.; Williams, P. A.; Harris K. D. M. *Angew. Chemie Int. Ed.* **2014**, *53*, 8939.

In-Situ NMR Studies of a Model Polymorphic System: *p*-ABA

Colan E. Hughes, Victoria L. Keast and Kenneth D. M. Harris

School of Chemistry, Cardiff University

Overview

The wide interest in polymorphism has been one of the driving forces for our *in-situ* studies of crystallization processes. In addition to our work on commercial pharmaceuticals,[1] we have also investigated model systems known to exhibit polymorphism (e.g., *m*-aminobenzoic acid; *m*-ABA).[2] We have recently investigated another isomer of aminobenzoic acid, namely *p*-aminobenzoic acid (*p*-ABA; Figure 1) which has three known polymorphs (note that *m*-ABA has five known polymorphs). As with other amino acids, *p*-ABA has the possibility, in principle, to exist in the zwitterionic or non-zwitterionic form. However, to date, all known polymorphs of *p*-ABA contain only non-zwitterionic molecules.

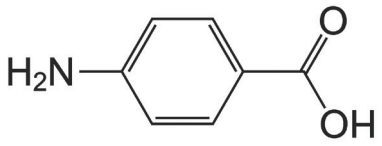

Figure 1. The p-ABA molecule.

Results

Figure 2 shows *in-situ* liquid-state ^{1}H NMR spectra recorded as a function of time for a solution of *p*-ABA in ethanol cooled from 50 °C to 11 °C. The overall drift in peak positions as a function of time arises from the sample cooling and the cooling of the shims (the latter causes all peaks to drift to lower chemical shift with time). Just before the end of the cooling process, a sudden change is observed in the position of the ^{1}H peak for the NH_2 group (*ca*. 5.5 ppm; red). Figure 3 shows the evolution of this peak in more detail. In the early stages of cooling, this peak moves to higher chemical shift with the other peaks, but then abruptly starts to move to lower chemical shift. Significantly, none of the other peaks show this abrupt change in behaviour. Furthermore, the peak for the NH_2 group also broadens significantly during cooling, again unlike any change observed for the other peaks.

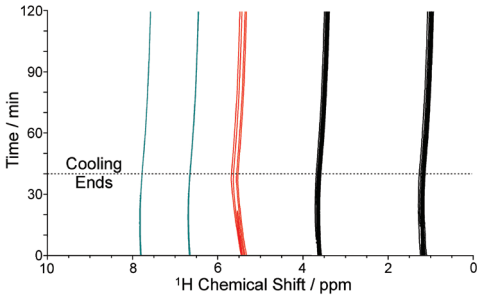

Figure 2. Liquid-state ^{1}H (850 MHz) NMR spectra acquired during crystallization of p-ABA from ethanol.

Discussion

The β polymorph of *p*-ABA is known to be difficult to produce, but the best methods for obtaining it operate in a narrow temperature range (13 °C to 15 °C).[3] Significantly, this range coincides with the temperature at which the abrupt change occurs in the position of the NH_2 peak in our *in-situ* ^{1}H NMR study. Due to slow ^{1}H T_1 relaxation, solid-state ^{13}C NMR spectra cannot be recorded sufficiently quickly for this system to observe polymorphic evolution during crystallization, although we aim to carry out such experiments in the future using ^{13}C labelled *p*-ABA. Nevertheless, our observation at this stage points towards a sudden change in crystallization behaviour at the specific temperature at which the β polymorph is reported to be produced.

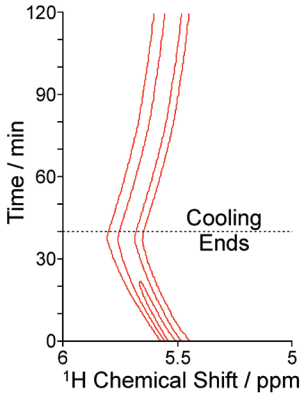

Figure 3. Expanded view of the NH_2 peak in Figure 2.

Concluding Remarks

In addition to acquiring *in-situ* solid-state ^{13}C NMR spectra for the same system using ^{13}C labelled *p*-ABA, we also plan to exploit other experimental methods to probe the behaviour of *p*-ABA in the temperature range at which the β polymorph is reported to be produced.

References

1. Williams, P. A.; Hughes, C. E.; Harris K. D. M. *Cryst. Growth Des.* **2012**, *12*, 5839.
2. Hughes, C. E.; Williams, P. A.; Harris K. D. M. *Angew. Chemie Int. Ed.* **2014**, *53*, 8939.
3. Hao, H.; Barrett, M.; Hu, Y.; Su, W.; Ferguson, S.; Wood, B.; Glennon, B. *Org. Process Res. Dev.* **2012**, *16*, 35.

Solid-State NMR of a Protein in a Precipitated Complex with a Full-Length Antibody

Jonathan M. Lamley,[1] Dinu Iuga,[2] Carl Öster,[1] Hans J. Sass,[3] Marco Rogowski,[3] Stephan Grzesiek[3] and Józef R. Lewandowski[1]

[1]*Department of Chemistry, University of Warwick*

[2]*Department of Physics, University of Warwick*

[3]*Biozentrum, University of Basel, Switzerland*

Overview

Ultimately, a complete understanding of biological processes at the molecular level requires the determination of the structures and dynamics of not only isolated proteins, but biomolecular complexes of interacting proteins. Such complexes are traditionally studied by solution-state NMR spectroscopy[1] or X-ray crystallography.[2] Above a certain limiting molecular weight, however, overall tumbling in solution slows such that NMR lines are severely broadened due to enhanced transverse relaxation. At the same time, crystallisation of protein complexes can often prove challenging or even impossible. In solids, the lack of overall tumbling means that broadening does not occur as a function of increasing molecular weight. On account of this, provided challenges in sensitivity and resolution can be addressed, solid-state NMR can provide an alternative for studying large proteins and protein complexes that are beyond the reach of solution-state NMR. We recently found that, by combining high magnetic fields (e.g. 850 MHz), fast spinning frequencies (60-100 kHz) and proton detection with optional sample deuteration, sufficient sensitivity and resolution could be obtained for very large complexes (>300 kDa) in quantities as small as 2 nanomoles, for quantitative studies of their structures and dynamics.[3] For structural studies, experimental time scales can be shortened further by using paramagnetic relaxation enhancement agents, e.g. Cu^{II}-EDTA. Importantly, these complexes do not have to be special-case, multimeric assemblies of multiple identical subunits (which multiply the achievable sensitivity) for this method to be effective.

In this study, we applied this approach to a complex of a small protein, GB1 (~6 kDa), with the full-length antibody Immunoglobin G (IgG, ~150 kDa), which precipitates upon combination of the two proteins. Protein-antibody interactions are of interest in a hugely diverse array of applications; protein G in particular is widely used in immunoprecipitation studies owing to its ability to specifically bind to a range of antibodies. While the interactions of various protein G domains with isolated fragments of IgG have been studied by solution NMR and X-ray crystallography,[4-6] similar studies of the full construct have not been possible. As we previously found, though, under the solid-state NMR conditions described above, this complex gives spectra with resolution rivalling crystalline preparations, with sensitivity such that 2D and 3D experiments for resonance assignment are practical. As we briefly outline below, this has enabled us to characterise the interactions between the GB1 and IgG proteins. The results of this project were recently published.[3]

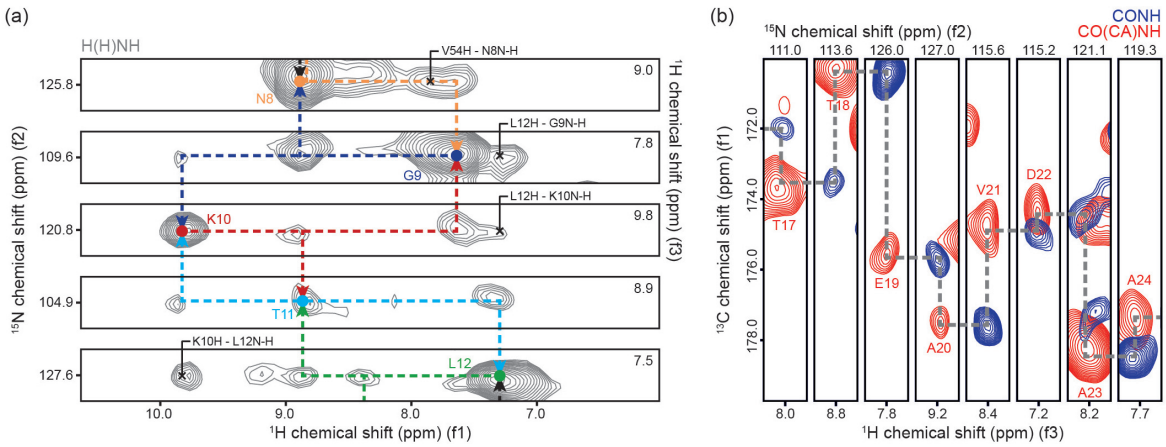

Figure 1. Representative strips from proton-detected (a) H(H)NH and (b) CONH and CO(CA)NH 3D experiments on deuterated [U-^{13}C,^{15}N]GB1 in a precipitated complex with full-length human IgG, performed at 850 MHz and 60 kHz MAS. f3 is the dimension of direct detection. Dashed lines show the assignment pathways. Autopeaks are labelled in colour, while peaks resulting from transfer across more than one residue through space are indicated with black crosses.

Resonance Assignment with Proton-Detected 3D Experiments

Extensive changes in the local nuclear environments are caused by the binding of GB1 to IgG. On account of this, the assignments of GB1 could not simply be taken from other existing forms (e.g. solution, crystal) of the protein. Instead, assignment was performed on the basis of a series of proton-detected 3D experiments performed at the 850 MHz facility, using a Bruker 1.3 mm probe at a MAS frequency of 60 kHz. To enhance resolution, the GB1 was deuterated (fully reprotonated at exchangeable sites), while rapid recycling was enabled by the addition of 50 mM Cu^{II}-EDTA. Initial assignments were made using a H(H)NH 3D experiment (Figure 1a), with RFDR (dipolar) ^{1}H-^{1}H mixing to establish inter-residue contacts between neighbouring H^{N} protons. To eliminate ambiguities, refinement of the assignments was achieved by performing a "backbone walk" using CONH and CO(CA)NH 3D experiments (Figure 1b). A CANH 3D spectrum was also recorded and C^{α} assignments obtained, and comparison of these chemical shifts with solution-state secondary chemical shifts confirmed that the secondary structure of GB1 was maintained in the complex. Each 3D spectrum was obtained in 1-3 days.

Characterisation of GB1-IgG Interactions

In general, changes in chemical shifts will result from changes in local environment caused by intermolecular interactions or conformational changes of the protein when in the complex. Because of this, we found that we were able to effectively map out the interaction interfaces of the GB1 by comparing the chemical shifts of GB1 in solution with those of GB1 in the complex with IgG (Figure 2). GB1 interacts with both the isolated Fab and Fc fragments of IgG, through different regions of the GB1 molecule. In the complex with full-length IgG, we observed chemical shift perturbations (CSPs) in both regions, while observing only a single set of resonances. Further, in both the Fab- and Fc-binding regions of GB1 in the complex with full-length IgG, the "modified" chemical shifts agreed remarkably well with the chemical shifts in the Fab- and Fc-binding regions of GB1 in the GB1-Fab and GB1-Fc complexes in solution,[5,6] respectively. These results are consistent with GB1 interacting with both the Fab and Fc fragments simultaneously, forming a complex of at least 300 kDa.

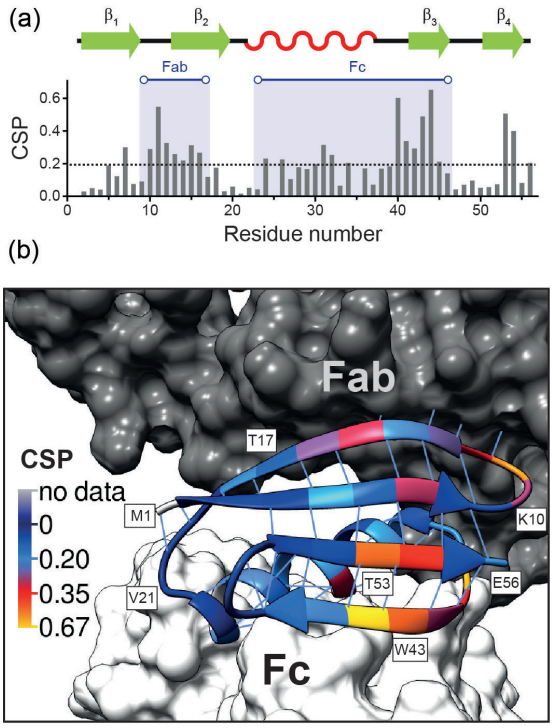

Figure 2. Chemical shift perturbations (CSPs, calculated as $[0.5(\delta_H^2+(\delta_N/5)^2)]^{1/2}$), for GB1 in a precipitated complex with IgG and GB1 free in solution (a) as a function of residue number and (b) projected onto the structure of GB1 in a model of the complex. The two IgG molecules interacting with GB1 are coloured light grey and dark grey. The dotted line in (a) indicates the average value of the CSPs. There are no data for T25 or N35.

References

1. Zuiderweg, E. R. *Biochemistry* **2002**, *41*, 1.
2. Garman, E. F. *Science* **2014**, *343*, 1102.
3. Lamley, J. M.; Iuga, D.; Öster, C; Sass. H. J.; Rogowski, M.; Oss, A.; Reinhold, A.; Grzesiek, S.; Samoson, A.; Lewandowski, J. R. *J. Am. Chem. Soc.* **2014**, *136*, 16800.
4. Derrick, J. P.; Wigley, D. *Nature* **1992**, *359*, 752.
5. Gronenborn, A. M.; Clore, G. M. *J. Mol. Biol.* ***1993***, *233*, 331.
6. Lian, L.-Y.; Barsukov, I. L.; Derrick, J. P.; Roberts, G. C. *Nat. Struct. Mol. Biol.* **1994**, *1*, 355.

Protein Dynamics in Different Molecular Environments: >300 kDa Complex versus Crystal

Jonathan M. Lamley,[1] Hans J. Sass,[2] Marco Rogowski,[2] Stephan Grzesiek[2] and Józef R. Lewandowski[1]

[1]*Department of Chemistry, University of Warwick*

[2]*Biozentrum, University of Basel, Switzerland*

Overview

Protein dynamics are fundamental to a hugely diverse range of biological processes, from enzymatic catalysis to signalling and molecular recognition.[1] The functional mechanisms that underlie these processes rely on the interactions of proteins with other molecules, including other proteins. To understand these processes, therefore, characterisation of the dynamics of proteins interacting within complexes is required. Solid-state NMR is an ideal method for the study of protein dynamics, as in the absence of overall molecular tumbling, relaxation measurements allow quantitative insights into the correlation times and amplitudes of motions across the entire time scale range of protein motions from ps to ms.[2] This is in contrast to solution NMR relaxation measurements, for which motions occurring on the ns-time scale are effectively "masked" by the overall tumbling. Such "slow" motions potentially include large-scale events, such as whole-domain motions or folding. Rotating frame spin-lattice relaxation ($R_{1\rho}$) rates conducted at high MAS rates (>50 kHz) in solids are extremely sensitive to motions on this time scale, and hence provide an extremely useful probe of their amplitudes, correlation times and even directions.[2,3]

Large protein complexes are extremely difficult targets for solution-state NMR, as their slow overall tumbling and correspondingly enhanced transverse relaxation leads to broad resonances. In solids this effect is not present, and hence solid-state NMR represents a promising opportunity for the study of the structures and dynamics of large protein complexes, provided that challenges regarding sensitivity and resolution can be addressed. We recently introduced an approach aimed at overcoming these by combining high field (850 MHz), high MAS rates (60-100 kHz) and proton detection, with optional sample deuteration for maximum resolution.[4] Using this method, the sensitivity and resolution obtained were suitable for performing quantitative measurements of parameters relevant to protein structures and dynamics, even without the addition of paramagnetic agents to reduce the experimental recycle delay. Here we report on the application of this methodology to study the slow motions of GB1 in a >300 kDa complex with full-length human IgG, and compare them to those of the same molecule in a crystal.

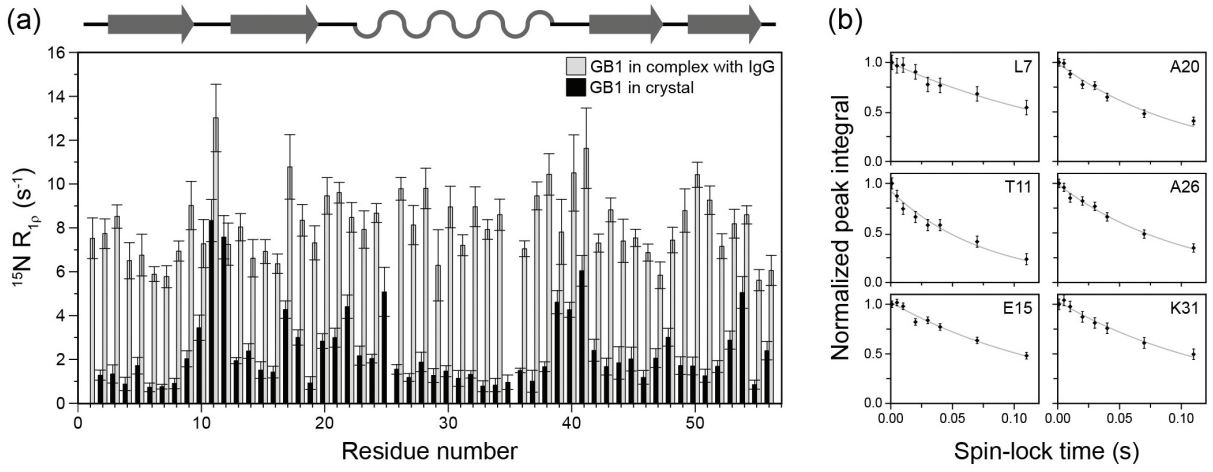

Figure 1. (a) Experimentally measured ^{15}N $R_{1\rho}$ relaxation rates for deuterated (100% proton back-exchanged) GB1 in a complex with IgG (grey) and fully-protonated crystalline GB1 (black) plotted against residue number. Note that if the crystalline sample had also been deuterated, the measured rates would have been even lower, although not significantly as the dominant contribution to the relaxation is still the ^{1}H-^{15}N dipolar interaction. The protonated sample suffices for a qualitative comparison. Relaxation rates were measured at 850 MHz ^{1}H Larmor frequency, 60 kHz MAS and with a 17 kHz spin-lock field. The sample temperature in either case was 27 °C as calculated from the shift of water protons with respect to DSS. (b) Example ^{15}N $R_{1\rho}$ decay curves for GB1 in the complex with IgG.

^{15}N $R_{1\rho}$ measurements

In general, the local molecular environment of a protein has a potentially significant effect on its ability to experience motions and sample different conformations that are relevant to its function. We measured backbone amide ^{15}N $R_{1\rho}$ rates for GB1 in both a crystalline form and, using proton-detected 2D ^{15}N-^{1}H experiments, in a complex with IgG. The measured rates for both are displayed as a function of residue number in Figure 1a. Representative relaxation curves are shown in Figure 1b. For the complex, each 2D spectrum took ~10 h to record. It is immediately obvious that the rates are, on average, ~3.5 times higher in the complex than in the crystal, indicating more prominent slow motions throughout the complex. The range of measured rates in either case, however, is approximately the same, suggesting an overall offset in rates caused by an overall change in GB1 dynamics (e.g. an overall rocking motion). The general pattern of rates also appears somewhat similar in each case. For example, in both sets of data, elevated rates are seen in the flexible loops 1 and 3, with generally lower rates towards the centres of the β-strands, implying that generally similar modes of motion within the molecule are taking place in either molecular environment.

Figure 2 shows the $R_{1\rho}$ rates projected onto the structure of GB1, with the radii and colours scaled such the minimum and maximum radii (coloured blue and yellow, respectively) correspond approximately to the minimum and maximum relaxation rates in either case. Displayed in this manner, more striking similarities are made obvious, for example higher rates around residues T17-T18 and T53-V54, and lower rates at various points in the β-sheet. On the other hand, in the complex, the rates for Y3 and especially T49-T51 appear noticeably enhanced relative to the rest of the protein. Even more obvious is that in the complex, the rates in the helix of GB1 are especially elevated in comparison to the rest of the protein, whereas in the crystal they appear suppressed. This may be a result of either an independent collective motional mode of the helix that is modified by its interaction with the IgG molecule, or due to an overall anisotropic motion of the GB1 molecule with an appropriate direction so as to enhance the rates in the helix preferentially (the ^{1}H-^{15}N vectors within the α-helix lie in a different direction to those within the β-sheet). This latter argument could also go some way to explaining the overall offset in rates. The true cause is most likely a combination of effects, which should become more apparent with further studies (e.g. ^{13}C relaxation measurements).

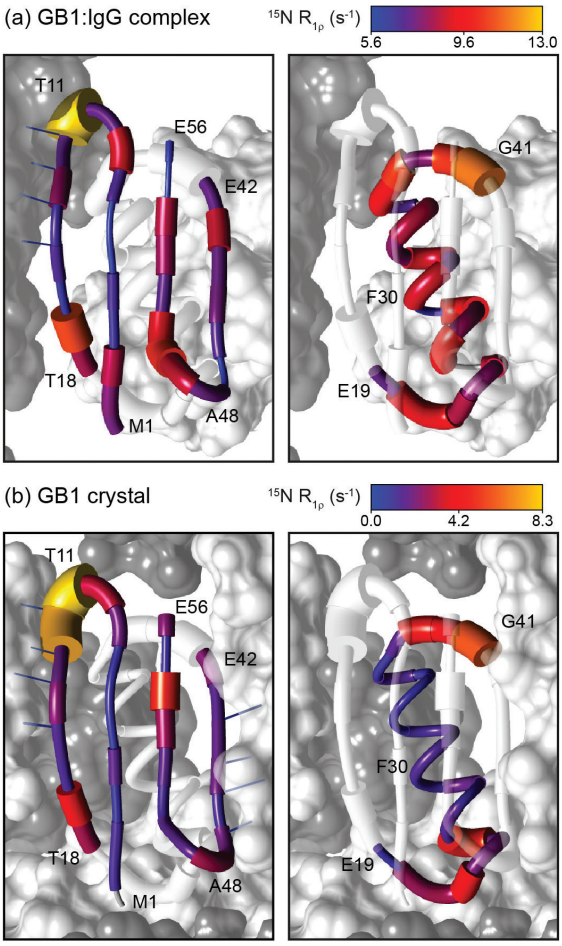

Figure 2. (a) Measured ^{15}N $R_{1\rho}$ relaxation rates for (a) GB1 in a complex with IgG and (b) crystalline GB1, projected onto the structure of GB1. The β-sheet and loops 1 and 4 are shown in the left-hand panels, while the helix and loops 2 and 3 are shown the right-hand panels. The radii and the colouring of the tubes reflect the magnitude of the measured rate. Residues with no data are coloured grey. Intermolecular hydrogen bonds are shown as dark blue lines.

References

1. Henzler-Wildman, K.; Kern, D. *Nature* **2007**, *450*, 964.
2. Lewandowski, J. R. *Acc. Chem. Res.* **2013**, *46,* 2018.
3. Lewandowski, J. R.; Sass. H. J.; Grzesiek, S.; Blackledge, M.; Emsley, L. *J. Am. Chem. Soc.* **2011**, *133*, 16762.
4. Lamley, J. M.; Iuga, D.; Öster, C; Sass. H. J.; Rogowski, M.; Oss, A.; Reinhold, A.; Grzesiek, S.; Samoson, A.; Lewandowski, J. R. *J. Am. Chem. Soc.* **2014**, *136*, 16800.

High-Field ^{13}C Solid-State NMR Reveals the Structural Details of Protein Fibrils Associated with Aortic Medial Amyloidosis

Hannah A. Davies,[1] Jillian Madine[1] and David A. Middleton[2]

[1]*Institute of Integrative Biology, University of Liverpool*

[2]*Department of Chemistry, Lancaster University*

Overview

Over 30 proteins form pathogenic amyloid fibrillar networks associated with human disease. The β-amyloid (Aβ) peptides associated with Alzheimer's disease are the best characterised of the amyloid proteins and detailed structural models of the fibrils have been assembled from solid-state NMR restraints.[1] The models indicate that some Aβ fibril morphologies are stabilised by a salt bridge between aspartic acid 23 (D23) and lysine 28 (K28) (Figure 1a). A less well understood form of amyloid, aortic medial amyloid (AMA), occurs in the aorta in 97 % of Caucasians over the age of fifty and may play a role in thoracic aneurysm. The principal protein component of plaques is medin, a 50-residue cleavage product of the protein lactadherin. Medin and Aβ have a high sequence similarity within an amino acid stretch incorporating the turn region of Aβ from residues 25-29 (Figure 1b). Strikingly, the salt bridge amino acids D23 and K28 of Aβ correspond precisely with aspartic acid D25 and lysine K30 of medin.

We used the UK 850 MHz Solid-State NMR Facility, together with lower field (400 MHz) solid-state NMR and biochemical methods, to investigate the structure of medin fibrils and to determine whether D25 forms a salt bridge with K30 that influences self-assembly.

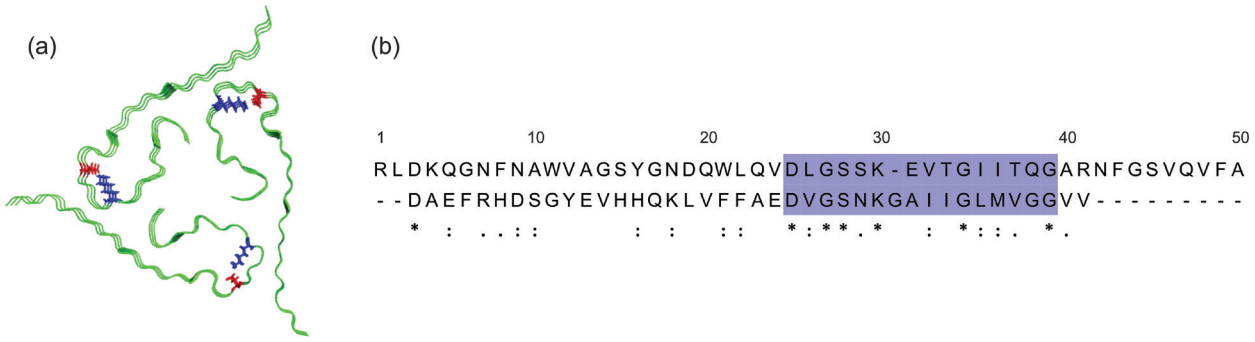

Figure 1. (a) A structural model of $A\beta_{1\text{-}40}$ fibrils (cross section perpendicular to the fibril axis) from solid-state NMR restraints,[1] highlighting the salt bridge between D23 (red) and K30 (blue). (b) Sequence alignment of medin (top) and $A\beta_{1\text{-}40}$ (bottom), highlighting the similarity with the $A\beta_{1\text{-}40}$ salt bridge region.

Preliminary Structural Analysis

To test for the presence of a salt bridge, medin fibrils were prepared with uniformly ^{13}C-labelled D25 and ^{15}N-labelled K30, to enable measurements of distance-dependent ^{15}N-^{13}C dipolar couplings between the two residues by frequency selective REDOR (FSR) solid-state NMR. A D25-K30 salt bridge would require a short (approximately 4.0 Å) separation of the carbon and nitrogen atoms of the amino acid COO^- and NH_3^+ groups. FSR measurements were carried out under conditions that aim to detect a dipolar interaction between the amino ^{15}Nζ of K30 and carboxyl Cγ of D25 by measuring the intensities of the carboxyl ^{13}C resonance at 173 ppm. The ratio of the peak intensities measured with radiofrequency pulses applied at the ^{15}Nζ frequency (S) and the measured intensities in the absence of pulses (S_0), is proportional to the ^{13}C-^{15}N interatomic distance. Figure 2a shows a progressive decrease in S/S_0 as the dephasing time increases, corresponding to a ^{13}C-^{15}N distance of 3.2-3.8 Å that is consistent with a salt bridge that would constrain the sequence from D25 to K30 in a turn. Interestingly, replacement of D25 with asparagine (D25N) prevents the formation of the fibrils observed for wild-type medin and instead directs the peptide along a different assembly pathway resulting in stable spherical oligomers (Figure 2b).

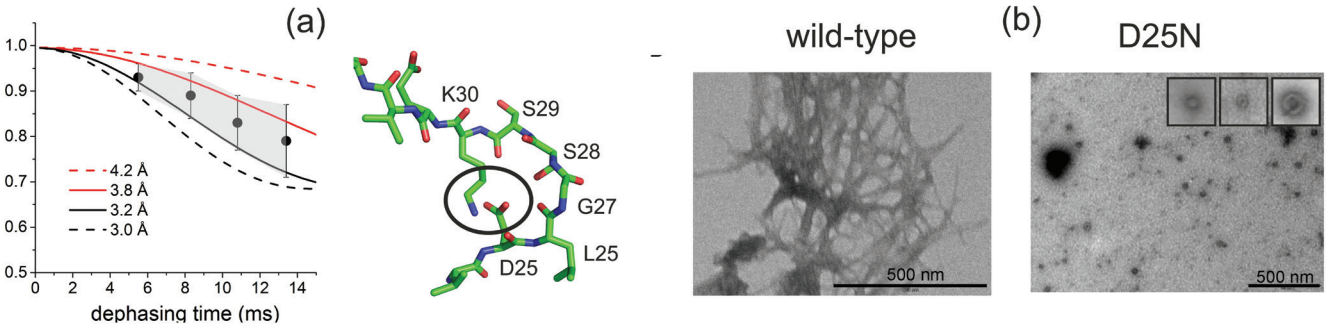

Figure 2. (a) FSR solid-state NMR (9.3 T; 100.1 MHz for ^{13}C) dephasing indicates a close-range interaction between the side-chain carboxyl group of D25 and amino group of K30, consistent with a D25-K30 salt bridge. (b) Transmission electron micrographs of wild-type medin and D25N aggregates.

High-Field Dipolar-Assisted Rotational Resonance

Figure 3a shows a structural model of medin fibrils that was generated using the $A\beta_{1\text{-}40}$ hairpin model as a template. This model favours the D25-K30 salt bridge and has several features that can be tested with NMR measurements. A high-field ^{13}C dipolar-assisted rotational resonance (DARR) solid-state NMR spectrum of uniformly $^{13}C/^{15}N$-labelled medin fibrils exhibits fine detail in the aromatic region, including an inter-residue cross-peak indicative of coupling between tryptophan residues W11 or W21 and isoleucine residues I35 or I36 (Figure 3b). This supports the model in which W21 and I35 form part of a hydrophobic interface between opposing β-sheets. Figure 3c shows the full DARR spectrum compared with a simulated spectrum based on chemical shift values predicted from the medin model using SHIFTX2. The simulated spectrum agrees well with the experimental spectrum, lending further support to the structural model, whereas simulated spectra for medin in purely α-helical, β-sheet or random coil structures were substantially different from the observed spectrum.

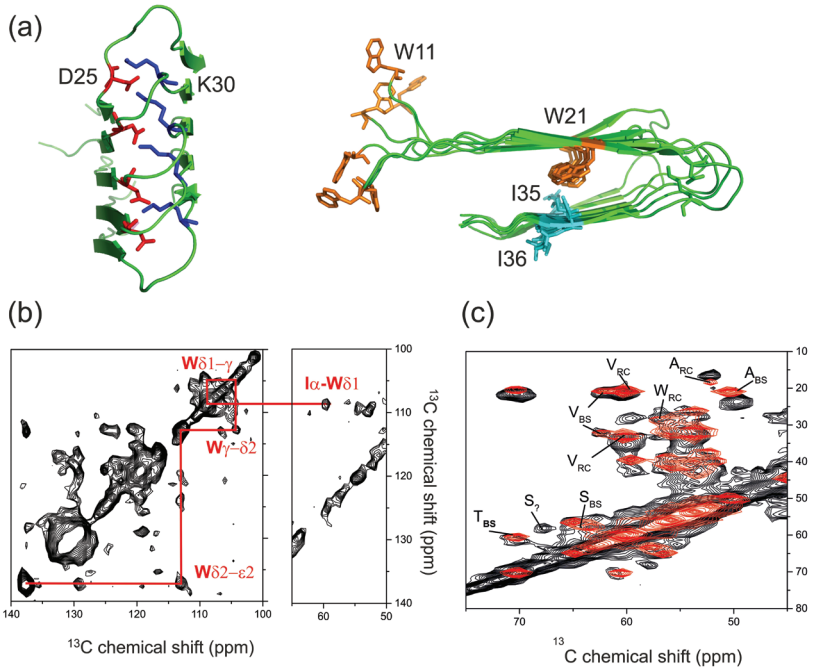

Figure 3. (a) Structural model of medin fibrils (viewed down the long axis of the fibrils), based on the $A\beta_{1\text{-}40}$ hairpin structure. (b) A ^{13}C DARR solid-state NMR spectrum obtained at the UK 850 MHz Facility supports the model, indicating through-space coupling between tryptophan (W21) and isoleucine (I35) residues. (c) A simulated spectrum calculated from the structural model (red) corresponds closely with the experimental spectrum (black).

In summary, solid-state NMR measurements reveal remarkable similarity in the structures of fibrils formed by the unrelated polypeptides medin and Aβ, and provide the first detailed structural insights into the precursor of AMA, a widespread but poorly understood amyloid disease.[2]

References

1. Paravastu, A. K.; Leapman, R. D.; Yau, W. M.; Tycko, R. *Proc. Natl. Acad. Sci. U. S. A.* **2008**, *105*, 18349.
2. Davies, H. A.; Madine J.; Middleton, D. A., *J. Biol. Chem*. **2015** (in press) DOI: 10.1074/jbc.M114.602177.

^{17}O-^{29}Si Correlation Spectra of a ^{29}Si- and ^{17}O-Enriched UTL-Derived Zeolite

Giulia P. M. Bignami, Daniel M. Dawson, Sharon E. Ashbrook and Russell E. Morris

School of Chemistry and EaStCHEM, University of St Andrews

Overview

The great utility and importance of zeolites in industry drives considerable work to develop new structural architectures with novel adsorption and catalytic properties. Hydrothermal synthesis and related solution-mediated techniques have dominated the field for many years. Recently, however, manipulation of zeolites into hierarchical porous structures and ultra-thin layers has also risen to great prominence as a method of introducing new features into zeolite structures.[1-3] The journal Science rated this type of research as one of the ten most important current areas of current science.[4] In preliminary work, we have developed unprecedented routes to new zeolitic materials, which we are calling the assembly-disassembly-organisation-reassembly (ADOR) method.[5,6] Following this synthetic method, solids with targeted structures can be obtained by selectively disassembling a pre-prepared parent zeolite and then reassembling the resulting products into a new topology, as shown in Figure 1. However, the hydrolytic mechanisms underlying the ADOR method are not entirely understood, requiring further investigation of the chemical and structural changes resulting from hydrolysis.

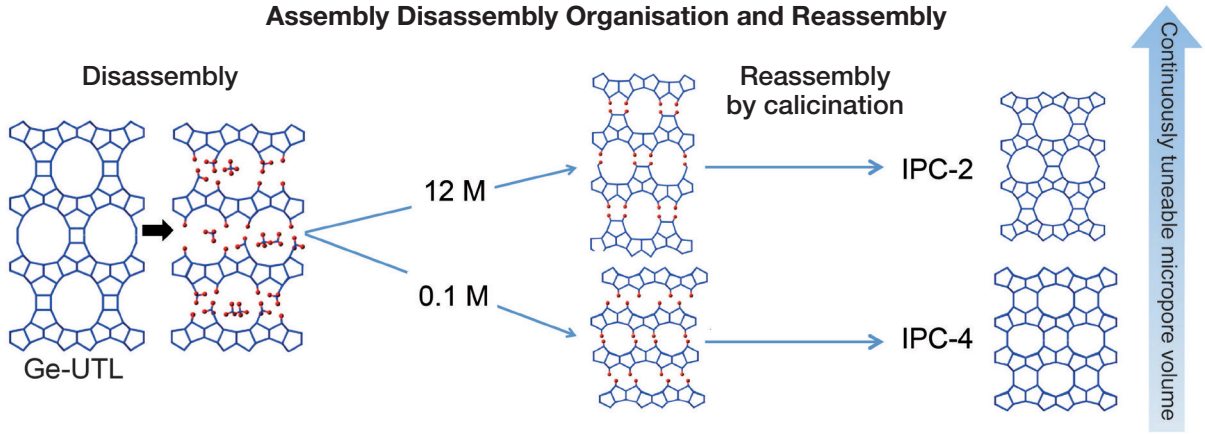

Figure 1. Schematic representation of the ADOR process. The initial disassembly of the materials is independent of the hydrolysis conditions but, upon heating at 95 °C, the concentration of acid makes a significant difference and the final material formed is dependent on two competing reactions, silica re-organisation and de-intercalation, yielding the two new zeolite materials IPC-2 and IPC-4, respectively. Consequently, by controlling the acidity of the solution used to disassemble the parent zeolite, different outcomes can be targeted and the porosity of the final material can be tuned over a wide range.

NMR spectroscopy can be usefully applied to the study of this type of material and, in particular, ^{17}O and ^{29}Si are two nuclei of interest. While ^{29}Si, with a low natural abundance of 4.7%, is routinely employed for the NMR characterisation of zeolites, ^{17}O is less commonly used because of its very low natural abundance (0.037%), moderate gyromagnetic ratio and quadrupolar nature (I = 5/2). For these reasons, to allow a complete and high-resolution spectroscopic investigation of the zeolitic structures, small-scale synthetic processes for double isotopic enrichment, *i.e.,* both in ^{29}Si and ^{17}O, have been optimised and successfully implemented in the ADOR method. Specifically, a ^{29}Si-enriched Ge-UTL has been synthesised (starting from 18% ^{29}Si-enriched $Si(OEt)_4$), used as the parent zeolite and then disassembled in a low-volume hydrolysis using 6 M HCl, freshly prepared from 1.2 ml of 12 M HCl and 1.2 ml of 41% ^{17}O-enriched $H_2{}^{17}O$.

^{17}O-^{29}Si Correlation Spectra

We have studied one sample of hydrolysed ^{17}O- and ^{29}Si-enriched Ge-UTL-derived zeolite, acquiring ^{17}O and ^{29}Si conventional MAS, and, most importantly, ^{17}O-^{29}Si heteronuclear correlation NMR spectra. The latter ^{17}O-^{29}Si correlation experiments (D-HMQC, utilising the $SR4^2_1$ recoupling scheme) were acquired in only 12-16 h with good signal and resolution using various recoupling times, as shown in Figure 2.

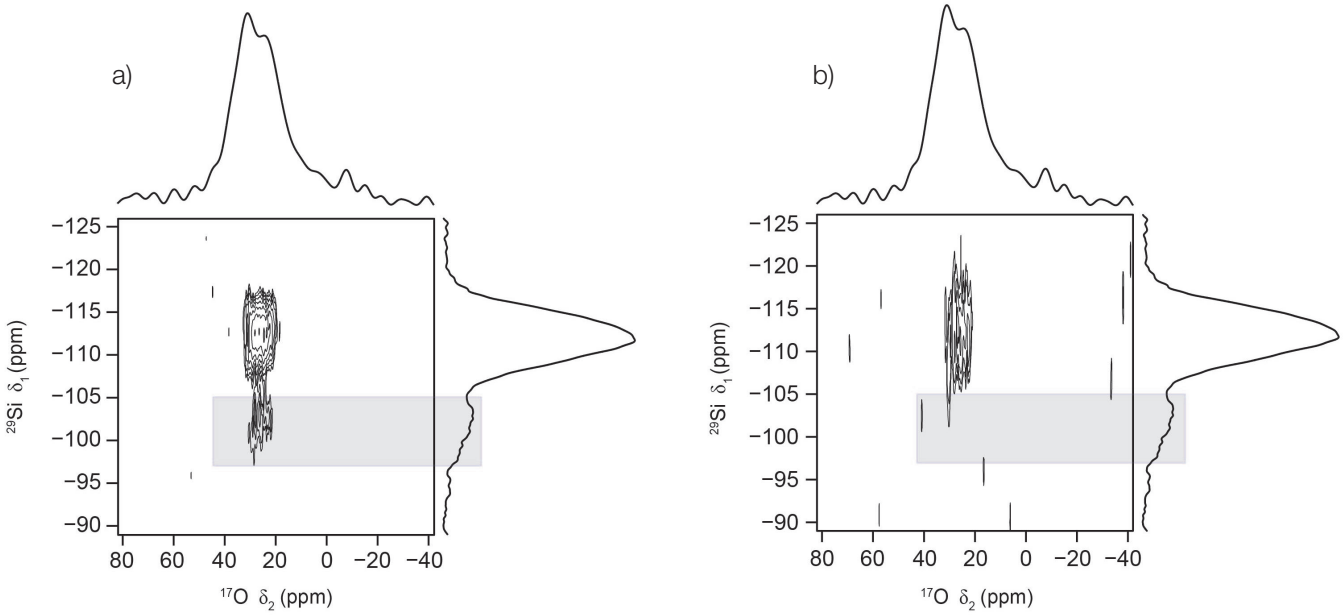

Figure 2. ^{17}O-^{29}Si D-HMQC correlation MAS spectra (20 kHz, 20.0 T) of an ^{17}O- and ^{29}Si-enriched Ge-UTL-derived zeolite (hydrolysed in 6 M HCl) recorded with (a) 4 loops (24 rotor periods, 1200 µs) and (b) 2 loops (12 rotor periods, 600 µs) of $SR4^2_1$ recoupling applied to enhance magnetisation transfer.

Using high field in this type of experiment proved of crucial importance not only for the resulting improvement in sensitivity and resolution, but also because of the intrinsic small frequency difference between ^{29}Si and ^{17}O at lower field, with equipment for these experiments not available in house. In particular, the high-resolution 2D spectrum in Figure 2a highlights the presence of two clearly distinct correlations to the broad oxygen signal of the Q^4 sites, fully coordinated ^{29}Si atoms, and the Q^3 sites, ^{29}Si atoms with one hydroxyl moiety, -OH, in their coordination environment. In a further correlation experiment, carried out with a shorter recoupling time and shown in Figure 2b, the absence of the Q^3 correlation peak was observed. While such evidence could, in principle, indicate that Si-OH bonds are longer than Si-O bonds, practically the Q^3 correlation peak could also be not evident above the noise compared to the more intense Q^4 correlation peak. For this reason, future work will involve a more thorough investigation of recoupling times and also further correlation experiments, exploiting the sensitivity enhancement resulting from the successfully developed double enrichment, to achieve a better understanding of the structural outcomes of the ADOR method.

References

1. Na, K.; Jo, C.; Kim, J.; Cho, K.; Jung, J.; Seo, Y.; Messinger, R. J.; Chmelka, B. F.; Ryoo, R. *Science* **2011**, *333*, 328.
2. Ng, E.-P.; Chateigner, D.; Bein, T.; Valtchev, V.; Mintova, S. *Science* **2012**, *335*, 70.
3. Zhang, X.; Liu, D.; Xu, D.; Asahina, S.; Cychosz, K. A.; Agrawal, K. V.; Wahedi, Y. A.; Bhan, A.; Hashimi, S. A.; Terasaki, O.; Thommes, M.; Tsapatsis, M. *Science* **2012**, *336*, 1684.
4. *Science* **2011**, 334, 1629.
5. Roth, W. J.; Nachtigall, P.; Morris, R. E.; Wheatley, P. S.; Seymour, V. R.; Ashbrook, S. E.; Chlubná, P.; Grajciar, L.; Položij, M.; Zukal, A.; Shvets, O.; Čejka, J. *Nature Chem.* **2013**, *5*, 628.
6. Wheatley, P. S.; Chlubná-Eliášová, P.; Greer, H.; Zhou, W.; Seymour, V. R.; Dawson, D. M.; Ashbrook, S. E.; Pinar, A. B.; McCusker, L. B.; Opanasenko, M.; Čejka, J.; Morris, R. E. *Angew. Chem. Int. Ed*. **2014**, *53*, 13210.

Solid State NMR at 20 T as a Probe of Materials using Less Commonly Studied Quadrupolar Nuclei (^{25}Mg, ^{43}Ca, ^{87}Sr, ^{127}I)

Christian Bonhomme,[1] Christel Gervais,[1] César Leroy,[1] Danielle Laurencin,[2] Gudrun Scholz,[3] Stephen P. Day,[4] John V. Hanna[4] and Mark E. Smith[4,5]

[1]LCMCP University Paris 06, France. [2]Institut Charles Gerhardt de Montpellier, France. [3]Department of Chemistry, Humboldt-Universität zu Berlin, Germany. [4]Department of Physics, University of Warwick. [5]Vice-Chancellor's Office and Department of Chemistry, Lancaster University

Overview

The application of ever higher magnetic fields is opening up and increasing the range of quadrupolar nuclei to study by solid-state NMR. Here, three separate materials systems are targeted using the capability of the 20 T instrument for such quadrupolar nuclei, namely (i) ^{43}Ca and ^{87}Sr in novel boronate ligand based coordination polymers, (ii) ^{25}Mg to follow coordination changes in magnesium acetate hydrates with hydration state, and (iii) some preliminary observations of ^{127}I in inorganic compounds. This new data shows the utility of solid-state NMR of these nuclei applied to a range of materials.

^{43}Ca and ^{87}Sr NMR of Alkylboronate Coordination Polymers

Boronate ligands ($R\text{-}B(OH)_3^-$) have recently started to attract attention for their formation of novel coordination polymer networks. Recently, three new crystalline structures involving butyl and octylboronate ligands were described ($Sr(Bu\text{-}B(OH)_3)_2$, $Ca(Oct\text{-}B(OH)_3)_2$ and $Sr(Oct\text{-}B(OH)_3)_2$) using synchrotron powder X-ray diffraction data of microcrystalline powders.[1] Such boronate ligands have many potential chemical applications, including as building blocks for metal organic framework porous materials. Comprehensive multinuclear NMR helped to solve the structure combining the experimental NMR data with first-principles calculations. The coordination modes of the boronate anions ($R\text{-}B(OH)_3^-$, R = Ph-, Bu-) to cations like Ca^{2+} are important, being complementary to those of other anionic ligands like phosphonates. Characterisation of the local environments of calcium and strontium was also performed on $Sr(Bu\text{-}B(OH)_3)_2$ and $Ca(Oct\text{-}B(OH)_3)_2$ using natural abundance ^{43}Ca and ^{87}Sr NMR. For $Sr(Bu\text{-}B(OH)_3)_2$, the ^{87}Sr NMR spectrum is consistent with the presence of one Sr site, and could be simulated using the NMR parameters δ_{iso} = 40 ± 100 ppm, C_Q = 20.5 ± 0.8 MHz and η_Q = 0.55 ± 0.10 (Figure 1a). It is worth noting that the quadrupolar coupling constant is consistent with what had been previously observed for $Sr(Ph\text{-}B(OH)_3)_2.H_2O$.[2] For $Ca(Oct\text{-}B(OH)_3)_2$ three different magnetic fields (Figure 1b) were used to ensure that the NMR parameters were well constrained, giving δ_{iso} = 14.9 ± 1.0ppm, C_Q = 1.44±0.15 MHz and η_Q = 0.67 ± 0.10.

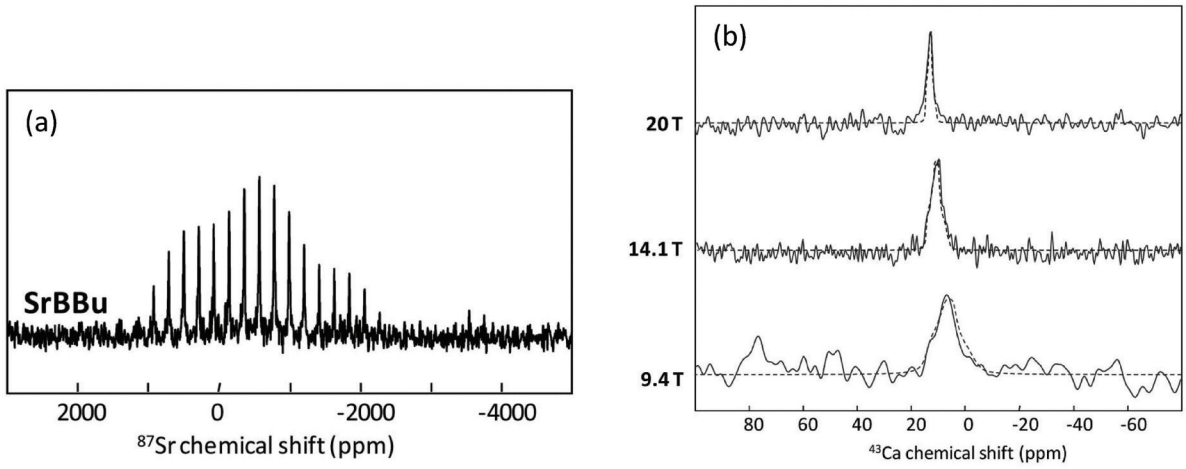

Figure 1. (a) ^{87}Sr static NMR of $(Sr(Bu\text{-}B(OH)_3)_2$ at 20 T using a 7 mm low-γ probe and a VOCS-WURST-QCPMG sequence and (b) ^{43}Ca MAS at 5 kHz of $Ca(Oct\text{-}B(OH)_3)_2$ recorded at three different applied magnetic fields (at 20 T, a 7 mm low-γ probe was used with a RAPT pulse sequence).

^{25}Mg NMR Spectroscopy of Magnesium Acetate Hydrates

Magnesium acetate solvates form a chemically intriguing set of compounds that provide insight into the structural chemistry of magnesium, as well as providing several potential practical applications. Using water as solvent, $Mg(OAc)_2.4H_2O$ is accessible simply by evaporation of water from a saturated aqueous solution of magnesium acetate. $Mg(OAc)_2 H_2O$ and water-free $Mg(OAc)_2$, respectively, can be obtained by partial or complete dehydration.[3] This magnesium acetate system opens a variety of new crystal structures with different, crystallographically distinguishable lattice positions of the Mg^{2+} cations. According to the X-ray structure data, the monohydrate has two distinguishable MgO_6 units, while the completely dehydrated magnesium acetate contains two MgO_6 units, as well as a further unusual MgO_7 coordination. Our preliminary ^{25}Mg NMR data at 20 T confirmed the parameters for the single site in $Mg(OAc)_2{\cdot}4H_2O$[4] and showed the more complex patterns from the samples with multiple magnesium sites (Figure 2).

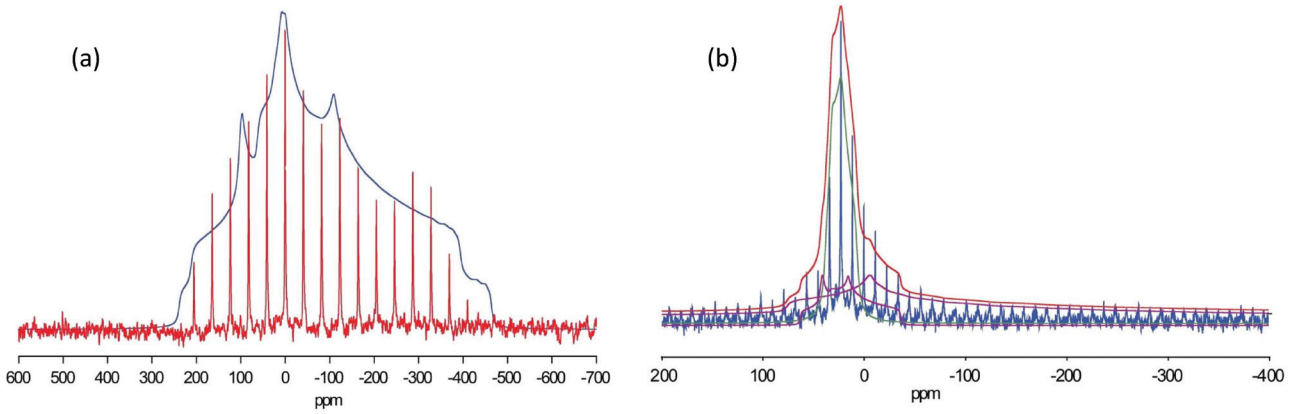

Figure 2. ^{25}Mg static spectra at 20 T using a 4 mm probe and the QCPMG sequence along with preliminary simulations for (a) $Mg(OAc)_2 H_2O$ and (b) water-free $Mg(OAc)_2$.

Initial Investigations of ^{127}I Solid State NMR Spectroscopy

Iodine-127 is a spin 5/2 nucleus with a large nuclear electric quadrupole moment (Q = –696 mb, producing a second-order broadening factor of ~25 relative to ^{27}Al), which is particularly challenging for solid-state NMR.[5] A series of crystalline model phases containing I^- ions was characterised at 20 T (Figure 3). The largest linewidth (~2 MHz) observed here was for CdI_2. Its spectrum could be fully acquired in less than 45 minutes, using the VOCS-WURST-QCPMG pulse sequence. Preliminary tests were then carried out on iodide substituted apatites, showing that subtle differences in ^{127}I NMR spectra can be detected depending on the synthetic procedure used, confirming that ^{127}I NMR has a role to play in the analysis of iodide environments in materials.

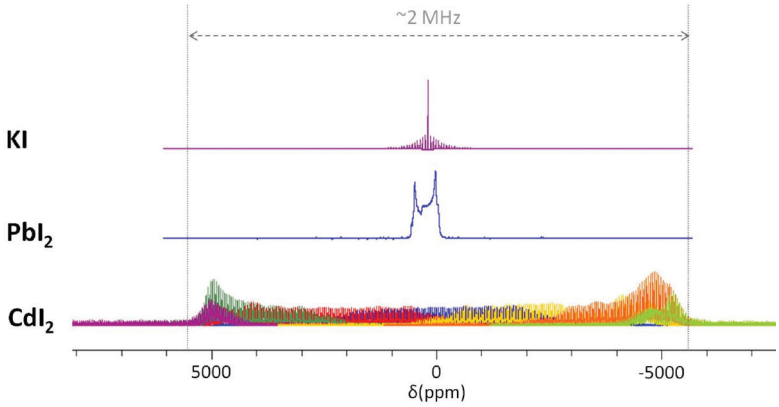

Figure 3. ^{127}I solid state NMR spectra at 20 T of KI (10 kHz MAS, single pulse acquisition, experimental time ~ 2s); PbI_2 (static, solid echo, experimental time ~3 min.), and CdI_2 (static, WURST-QCPMG, 7 offsets, total experimental time ~40 min.).

References

1. Berthomieu, D.; Gervais, C.; Renaudin, G.; Reinholdt, M.; Sene, S.; Smith, M. E.; Bonhomme, C.; Laurencin, D. *EurJIC,* **2014**, 1.
2. Bonhomme, C.; Gervais, C.; Folliet, N.; Pourpoint, F.; Coelho Diogo, C.; Lao, J.; Jallot, E.; Lacroix, J.; Nedelec, J. M.; Iuga, D.; Hanna, J. V.; Smith, M. E.; Xiang, Y. Du, J.; Laurencin, D. *J. Am. Chem. Soc.* **2012**, *134*, 12611.
3. Scholz, G.; Heidemann, D.; Kemnitz, D. *Z. Anorg. Allg. Chem.* **2013**, *639*, 694.
4. Freitas, J, C. C., Smith, M. E. *Ann. Rep. NMR Spectrosc*. **2012**, *75*, 25.
5. Bryce, D. L.; Widdifield, C. M.; Chapman R. P.; Attrell, R.J.in *NMR of Quadrupolar Nuclei in Solids*, eds. Wasylishen, R. E.; Ashbrook, S. E.; Wimperis, S., Wiley, Chichester, **2012**, Chapter 19.

High-Field Solid-State ^{39}K Study of Mixed-Metal Polyoxometalates

Andrew G. M. Rankin,[1] Daniel M. Dawson,[1] Sharon E. Ashbrook[1] and Richard I. Walton[2]

[1]*School of Chemistry and EaStCHEM, University of St Andrews*

[2]*Department of Chemistry, University of Warwick*

Overview

Polyoxometalates (POMs) are inorganic metal-oxo clusters with corner- or edge-sharing octahedra. These materials have diverse cluster geometries, chemical behaviour and electrochemical properties. The Lindqvist hexaniobate ion, $[Nb_6O_{19}]^{8-}$, plays an important role in the field of POM chemistry, being one of the first reported polyoxoniobate structures.[1] Solids containing the Lindqvist ion have been seen as transient phases in the hydrothermal crystallisation of niobium oxides, such as perovskites, which possess ferroelectric or piezoelectric properties of use in important industrial applications such as sensors, actuators and attenuators.[2-4] This has led us to consider whether the Lindqvist ion itself could be used as precursor for oxide formation and whether, by making mixed-metal variants of the POM (*e.g.*, Nb/Ta or Nb/W in the POM and Na/K as the counter-ion), we would have a new way of controlling the composition, and, potentially, local structure, of the oxide formed. Such atomic-scale control of the distribution of dopants could then allow tailoring of the properties of the oxide for different applications.

^{39}K (I = 3/2) has the potential to be used as a tool to investigate the local structures of POMs, but its low receptivity (Larmor frequency = 39.7 MHz at 20.0 T) means that this nucleus can also be quite challenging to study.

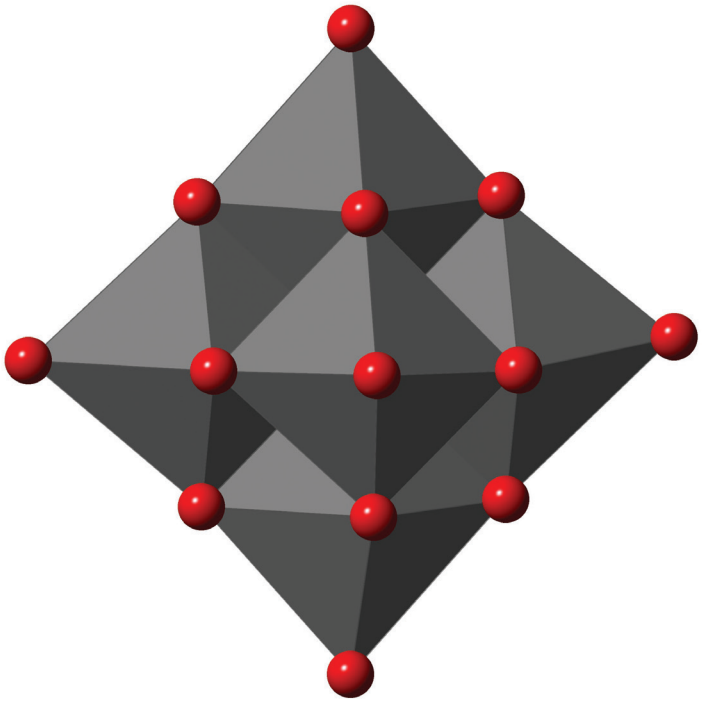

Figure 1. The Lindqvist hexaniobate ion, $[Nb_6O_{19}]^{8-}$

Results

Two POMs were prepared: the $K_8[Nb_6O_{19}]\cdot xH_2O$ end member and the mixed-metal $K_7Na[Nb_2Ta_4O_{19}]\cdot xH_2O$. The end-member perovskite $KTaO_3$ was also prepared from the $K_8[Ta_6O_{19}]\cdot xH_2O$ POM. The ^{39}K MAS NMR spectra of the three samples, recorded at 20.0 T are shown in Figure 1.

These spectra reveal that mixed-metal addition into the POM results in increased structural disorder. This is indicated by the increased linewidth for $K_7Na[Nb_2Ta_4O_{19}]$ compared to that of $K_8[Nb_6O_{19}]$. This is in marked contrast to the resonance of the $KTaO_3$ perovskite, which possesses a well-ordered, cubic structure. The average ^{39}K isotropic chemical shift (and its distribution) appears sensitive to the presence and amount of Na/Ta substitution, while the ^{39}K linewidth appears to be sensitive to the degree of disorder present, as evidenced by the spectra in Figure 2. Experiments at 20.0 T have allowed for the observation of resonances that in several cases are too broad to be observed at lower magnetic fields.

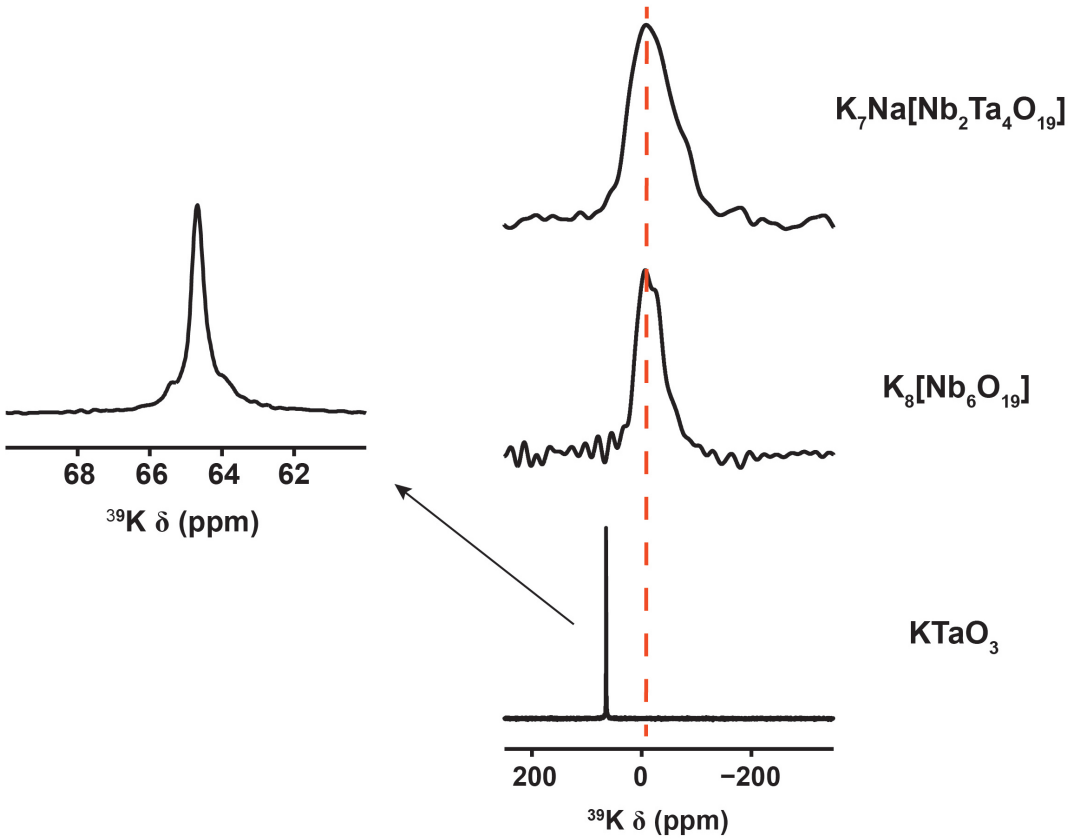

Figure 2. ^{39}K (20.0 T, 25 kHz MAS) single pulse spectra of two prepared POMs and the perovskite $KTaO_3$. An expansion is also shown for the spectrum of $KTaO_3$.

Future work will focus on a series of polyoxometalates with different Nb/Ta ratios and combine the information gained from high-field studies with other NMR experiments to build up a detailed picture of these interesting structures.

References

1. Alam, T. M; Nyman, M.; Cherry, B. R.;Segall, J. M.; Lybarger, L. E. *J. Am. Chem. Soc.,* **2004**, 126, 5610.
2. Dias, A. *J. Solution Chem*., **2009**, 38, 843.
3. Zhu, H. Y.; Zheng, Z. F.; Gao, X. P.; Huang, Y. N.; Yan, Z. M.; Zou, J.; Yin, H. M.; Zou, Q. D.; Kable, S. H.; Zhao, J. C.; Xi, Y. F.; Martens, W. N.; Frost, R. L. *J. Am. Chem. Soc.*, **2006**, 128, 2373.
4. Modeshia, D. R; Darton, R. J.; Ashbrook, S. E.; Walton, R. I. *Chem. Commun.*, **2009**, 68.

Indirect Detection of ^{14}N Spectra in Biological Systems

James Jarvis,[1] Ibraheem Haies,[2] Marina Carravetta[2] and Philip T.F. Williamson[1]

[1]*Centre for Biological Sciences, University of Southampton*

[2]*School of Chemistry, University of Southampton*

Overview

Nitrogen is a nucleus of great importance in the study of biological solids; accordingly, methods for the analysis of the naturally abundant isotope, ^{14}N, by NMR are clearly desirable. Despite its high natural abundance and relatively large gyromagnetic ratio, ^{14}N is rarely exploited in NMR investigations. This stems largely from the fact that it is a spin I = 1 nucleus exhibiting a relatively large, MHz in size, quadrupolar interaction that makes its direct detection challenging. The presence of the large quadrupolar interaction does however provide a wealth of structural and dynamic data that could potentially be exploited for the characterisation of biomolecular systems.

In recent years a number of solid-state magic-angle spinning (MAS) methods have been developed based on liquid-state style HMQC/HMBC experiments which correlate the ^{14}N to neighbouring 'spy' nuclei via the second-order quadrupolar-dipolar interactions, frequently referred to as residual dipolar splittings, which are not averaged under MAS.[1] Such indirect methods permit the site-specific analysis of the ^{14}N sites within the sample providing quantitative information about the quadrupolar interaction at each site.

Efficient Methods for ^{14}N Correlation Spectroscopy

Despite progress in this field, the application of these methods has proved challenging due to the low efficiencies typically observed in these experiments. Recently, we have developed a family of experiments, which replaced the periods of evolution under the second-order quadrupolar-dipolar interactions with an extended rf pulses which significantly enhance the efficiency of these experiments; in favourable cases resulting in efficiencies of over 25% when detected using a ^{13}C 'spy' nuclei.[2] When combined with other signal enhancement methods such as dynamic nuclei polarization (DNP), this now enables the detection and characterisation of ^{14}N labelled biomolecules.

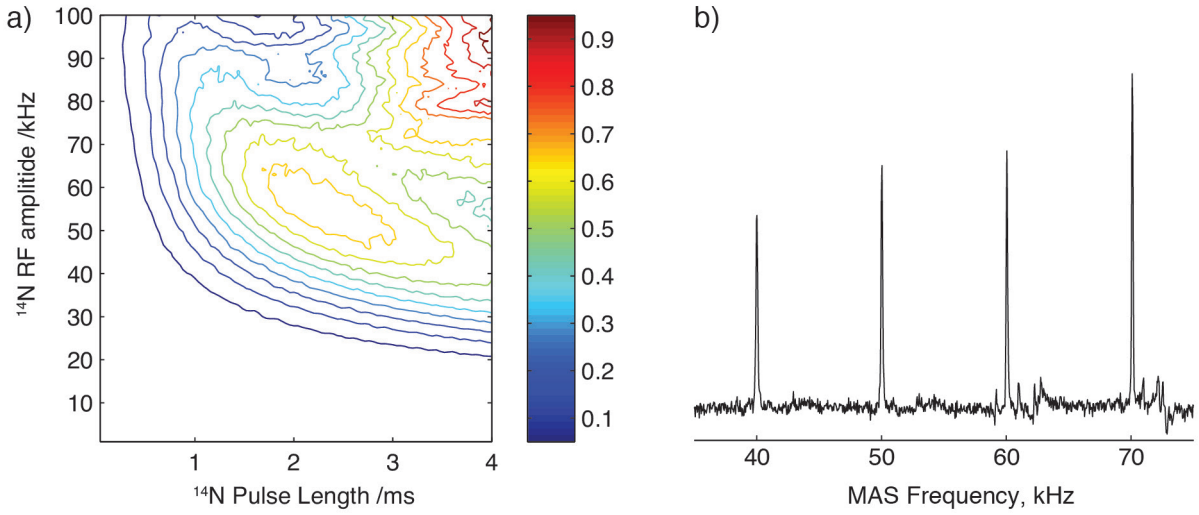

Figure 1. (a) Faster MAS frequencies and higher rf fields available on the fast spinning probes on the 850 MHz spectrometer permit the efficient detection of ^{14}N sites. Simulations conducted in SpinEvolution[3] of signal intensity observed for ^{14}N amide sites such as those found in the protein backbone (assuming a quadrupolar interaction of 3 MHz) highlights the need for higher ^{14}N rf fields. (b) Proton detected ^{14}N filtered experiments conducted on N-acetyl-valine demonstrate the enhanced sensitivity afforded through the application of higher MAS frequencies.

Indirect ^{1}H Detection of ^{14}N Lineshapes

Numerical simulations predict that these methods will benefit from the availability of both higher MAS frequencies and rf fields (Figure 1a). The installation of smaller diameter MAS probes on the 850 MHz spectrometer has provided us with a unique opportunity to exploit the experimental regime allowing us to realise these predicted advantages, giving significant enhancements in experimental efficiency compared to other contemporary experiments (Figure 2a). Coupling these experimental improvements with the well-resolved ^{1}H spectra that can be obtained at these high MAS frequencies and magnetic fields, the inherent gains in sensitivity permit the acquisition of ^{1}H-^{14}N correlation spectra in a matter of minutes/hours in favourable cases (Figure 2b). Studies are currently underway to study a range of unlabelled small molecules and biomolecular systems with significantly enhanced sensitivity. These are providing us with a unique opportunity to study ^{14}N sites within biomolecules and the extraction of highly sensitive structural and dynamic data that is encoded within the quadrupolar interaction present.

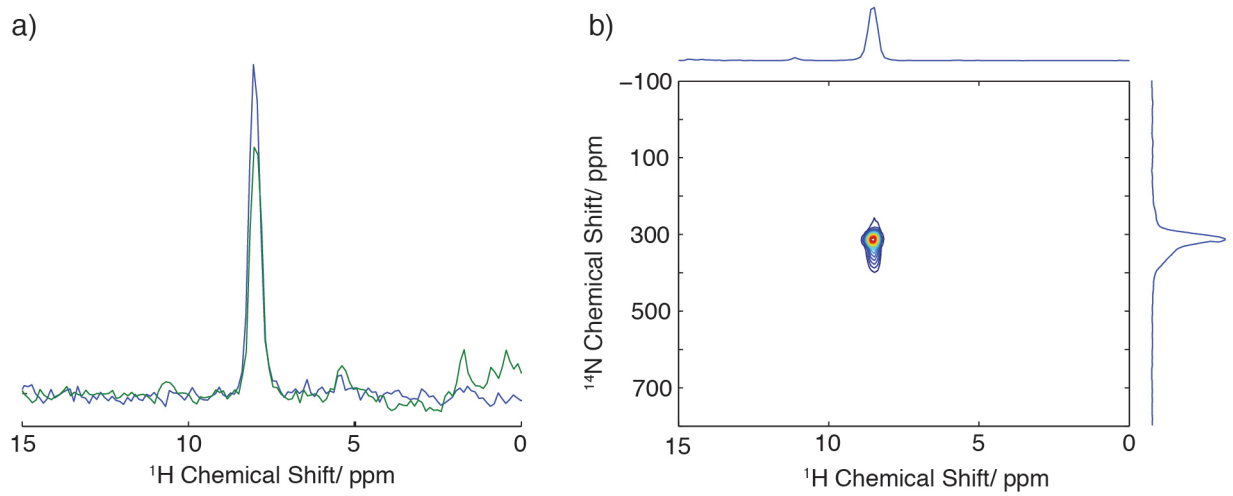

Figure 2. (a) Using rf pulses to generate coherence between the ^{14}N and the spy nucleus, in this instance protons (blue) provides enhanced sensitivity compared to dipolar mediated experiments such as R3-HSQC[4] (green). (b) The enhanced sensitivity afforded by these techniques permits the rapid acquisition of ^{1}H-^{14}N correlation spectra in molecules where the ^{14}N site exhibits a large quadrupolar interaction such as N-acetyl-valine (quadrupolar interaction ~3 MHz).

References

1. Cavadini, S. *Prog. Nucl. Mag. Res. Spectrosc.* **2010**, *56*, 46.
2. Jarvis, J. A.; Haies, I. M.; Williamson, P. T. F.; Carravetta, M. *Phys. Chem. Chem. Phys*. **2013,** *15*, 7613.
3. Griffin, R. G.; Veshtort, M. *J. Magn. Reson.* **2006**, *178*, 248.
4. Gan, Z. H.; Amoureux, J. P.; Trebosc, J. *Chem. Phys. Lett.* **2007**, *435*, 163.

A Natural Abundance ^{33}S STMAS NMR Study of Ettringite

Akiko Sasaki and Stephen Wimperis

School of Chemistry, University of Glasgow

Overview

Despite the prevalence of sulphur in nature and materials science, there have been very few ^{33}S (spin I = 3/2) solid-state NMR studies in the literature, owing to the low natural abundance (0.76%) and low gyromagnetic ratio of ^{33}S (ν_0 = 30.7 MHz at B_0 = 9.4 T), and the high expense of isotopic enrichment. ^{33}S solid-state NMR performed at natural abundance has been dominated by the studies of simple inorganic compounds with S nuclei at high symmetry sites with small quadrupolar interactions.[1] Recently, high-field spectrometers have become accessible to overcome the limitations associated with low-γ nuclei such as ^{33}S.[2] In addition to the intrinsic sensitivity increase at high magnetic field strength, the inverse dependence of the second-order quadrupolar interaction upon magnetic field strength makes the use of high-field NMR highly advantageous for quadrupolar nuclei. Furthermore, sensitivity enhancement techniques for central transitions (CT) of half-integer quadrupolar nuclei have been applied to ^{33}S solid-state NMR,[3] and first-principles calculations of ^{33}S NMR parameters have also emerged in the literature.[4] Natural abundance ^{33}S solid-state NMR, therefore, has great potential for future applications.

The aim of this project is to demonstrate the feasibility of high-resolution natural abundance ^{33}S NMR at the high fields now available. The MQMAS and STMAS NMR experiments yield high-resolution NMR spectra of half-integer quadrupolar nuclei such as ^{33}S. Although STMAS is the more difficult technique to implement, its increased sensitivity, owing to effective excitation of the single-quantum satellite transitions, makes it advantageous for the study of low-γ nuclei.[5]

Ettringite ($Ca_6Al_2(SO_4)_3(OH)_{12}\cdot 26H_2O$) is a hydrous sulfate that occurs naturally as a mineral and synthetically during the production of cements. The crystal structure is known[6] (Figure 1a) and there has been an early ^{27}Al MAS NMR study.[7] There have been two ^{33}S MAS NMR studies of ettringite at high field.[2,3] These two studies disagree, with one simulating the ^{33}S MAS NMR spectrum with a single S site[2] and the other simulating it with three S sites[3] (in accordance with the XRD structure), leaving uncertainty in the number of crystallographically different S sites observed by ^{33}S solid-state NMR. Here, we aim to characterise the distinct S sites in ettringite using ^{33}S STMAS and resolve the ambiguity present in the current literature. In addition, we expect to be able to address questions relating to disorder and dynamics of the intercolumn SO_4^{2-} species in ettringite.

Technical Considerations of ^{33}S STMAS Experiments at B_0 = 20.0 T

Owing to the combination of unfavourable ^{33}S NMR parameters and the stringent technical requirements associated with STMAS experiments, care must be taken to ensure a successful demonstration of ^{33}S STMAS experiments at natural abundance. This project consists of three phases: (i) The first stage of the project was the implementation of ^{33}S STMAS experiments at B_0 = 20.0 T. We established a protocol for accurate spinning angle setting using ^{85}Rb STMAS spectra of $RbNO_3$ using 4 mm and 7 mm rotors (see (iii) below). We also demonstrated how to extrapolate optimum pulse lengths for ^{33}S STMAS experiments,[5] where the sensitivity is too low to optimise the pulse length on the sample of interest. (ii) The second stage was to demonstrate the feasibility of natural abundance ^{33}S STMAS experiments using a model system with known NMR parameters. Our model system is a 1:1 molar mixture of sodium sulfate (Na_2SO_4) and potassium sulfate (K_2SO_4). We recorded a spin-echo ^{33}S MAS spectrum and the fitting parameters agreed with the reported values in the literature. A natural abundance ^{33}S STMAS spectrum of the sulfate mixture was successfully obtained, and the signal-to-noise ratio was sufficient to yield the NMR parameters δ_{CS} = 340.7, 336.3 ppm and P_Q = 646, 966 kHz in good agreement with the ^{33}S MAS spectrum. (iii) The third stage is the application of natural abundance ^{33}S STMAS experiments to our compound of interest, ettringite. Our natural sample, obtained from a mineralogical collection, was packed into a 4 mm rotor owing to the limited amount of samples available, while a 7 mm rotor was used for a synthetic sample. Another 4 mm rotor was required for $RbNO_3$ and, following pneumatic ejection of the $RbNO_3$ rotor after accurate spinning axis calibration, a small amount of bearing gas was applied to retain the magic angle upon insertion of the 4 mm rotor containing ettringite. The synthetic ettringite sample in the 7 mm rotor was layered with $RbNO_3$, avoiding the pneumatic insertion/ejection procedure prior to STMAS experiments.

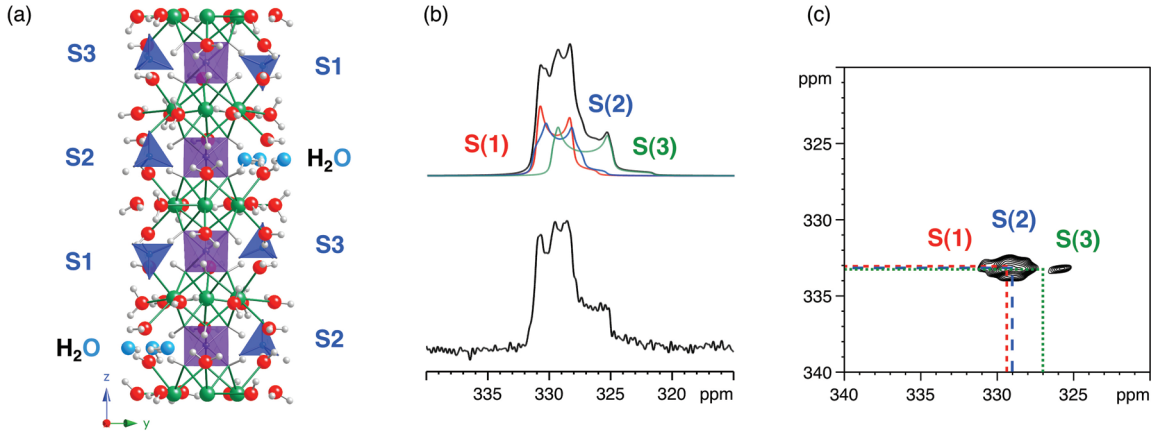

Figure 1. (a) Crystal structure of ettringite showing a column of Al^{3+} (purple) and Ca^{2+} (green) ions linked through O (red) atoms of OH^- ions and H_2O groups. The vertical column of SO_4^{2-} tetrahedra (blue) contains further H_2O molecules located between SO_4^{2-} groups. (b) Natural abundance ^{33}S MAS NMR spectrum of synthetic ettringite at B_0 = 20.0 T (bottom) and corresponding lineshape fit (top). The sample was packed into a 7 mm rotor and spun at 6.4 kHz. A spin-echo pulse sequence was employed. 92160 transients were averaged with a relaxation interval of 0.4 s. Total experiment time: 15 hours. The fitting parameters are δ_{iso} = 331.8, 331.9, 331.0 ppm, C_Q = 620, 660, 800 kHz, η = 0.1, 0.3, 0.1, with relative integral of 1:1:1. (c) Natural abundance ^{33}S STMAS NMR spectrum of synthetic ettringite recorded at B_0 = 20.0 T. The sample was packed into a 7 mm rotor layered with $RbNO_3$ and spun at 5 kHz. 11040 transients were averaged for each of 64 t_1 increments, with a relaxation interval of 0.4 s. Total experiment time: 92 hours.

Natural Abundance ^{33}S STMAS of Ettringite

Our natural abundance ^{33}S MAS and STMAS spectra of a natural sample (not shown) and a synthetic sample (Figure 1b,c) recorded at B_0 = 20.0 T clearly indicate the presence of multiple S sites. We have recently confirmed the presence of three distinct sites by performing ^{33}S STMAS experiments at B_0 = 9.4 T using a 7 mm rotor for a synthetic sample, exploiting the dependence of second-order quadrupolar interaction upon magnetic field strength. Our fitting parameters are consistent within the experimental data sets obtained at different B_0 field strengths (three S sites are expected to overlap at B_0 = 20.0 T). Since STMAS is the high-resolution method sensitive to μs dynamics (results in considerable broadening in isotropic dimension), we conclude that there is no μs dynamics or disorder present at the ^{33}S sites in ettringite at room temperature. We also performed first-principles calculations of ^{33}S NMR parameters of ettringite using the GIPAW method as implemented in the CASTEP code (results not shown). Calculated quadrupolar coupling constants are known to overestimate the observed C_Q values if there is a presence of dynamics at finite temperature. Here we suspect the presence of motional averaging of second-order broadened ^{33}S CT lineshapes occurring at room temperature. We also note that the ^{33}S T_1 relaxation time of ettringite is significantly short (< 0.4 s). These observations indicate the presence of dynamics on a very short time scale, *i.e.*, very fast motion that gives rise to the modulation of the local field comparable to the Larmor frequency. Since anhydrous sulfates are known to show much longer ^{33}S T_1 values,[1] the efficient ^{33}S T_1 relaxation in ettringite possibly originates from the motion of water molecules. Unlike other hydrous sulfates, however, the ^1H T_1 relaxation time of ettringite was unusually fast. The presence of complicated dynamics in ettringite could not have been realised unless the combination of experiments and calculations was employed.

References

1. Wagler, T. A.; Daunch, W. A.; Panzner, M.; Youngs, W. J.; Rinaldi, P. L. *J. Magn. Reson.* **2004**, *170*, 336.
2. d'Espinose de Lacaillerie, J.-B.; Barberon, F.; Bresson, B.; Fonollosa, P.; Zanni, H.; Fedorov, V. E.; Naumov, N. G.; Gan, Z. *Cem. Concr. Res.* **2006**, *36*, 1781.
3. Hansen, M. R.; Brorson, M.; Bildsøe, H.; Skibsted, J.; Jakobsen, H. J. *J. Magn. Reson.* **2008**, *190*, 316.
4. Pallister, P. J.; Moudrakovski, I. L.; Enright, G. D.; Ripmeester, J. A. *CrystEngComm* **2013**, *15*, 8808.
5. Dowell, N. G.; Ashbrook, S. E.; Wimperis, S. *J. Phys. Chem. B* **2004**, *108*, 13292.
6. Goetz-Neunhoeffer, F.; Neubauer, J. *Powder Diffr.* **2006**, *21*, 4.
7. Skibsted, J.; Henderson, E.; Jakobsen, H. J. *Inorg. Chem.* **1993**, *32*, 1013.

Using ^{77}Se Solid-State NMR and J Coupling to Study Novel Organoselenium Compounds

Paula Sanz Camacho,[1] Kasun S. A. Arachchige,[1] Daniel M. Dawson,[1] Alexandra M. Z. Slawin,[1] Jonathan R. Yates,[2] J. Derek Woollins[1] and Sharon E. Ashbrook[1]

[1]*School of Chemistry and EaStCHEM, University of St Andrews*

[2]*Department of Materials, University of Oxford*

Overview

NMR studies of heavier nuclei, such as ^{77}Se, present challenges both experimentally and theoretically, firstly, due to long T_1 relaxation times and large chemical shift anisotropies (CSAs), and additionally due to relativistic effects, which can complicate theoretical analysis. However, solid-state NMR presents an ideal technique for studying chalcogen-containing materials, owing to the sensitivity of the chemical shift (ranging over 3000 ppm for ^{77}Se) to changes in molecular structure. Whilst there are many materials that could benefit from such characterization, ^{77}Se solid-state NMR remains underutilised in comparison to ^{77}Se solution-state NMR, and only a few examples are known in the literature.[1]

We have synthesized a series of novel P-Se and P-S heterocycles with potential applications in spintronics, differing only in the nature of the R group attached to P, for which structures have been determined by single crystal X-ray diffraction and confirmed by ^{77}Se, ^{31}P and ^{13}C solution-state NMR. Although these molecules are structurally very similar, they present very different NMR spectra, with multiplet fine structure that is difficult to understand from measurement at a single field strength. Here, we consider two of the P-Se materials, with R = *iso*-propyl and *tert*-butyl.

Results

^{77}Se solid-state MAS NMR spectra of two P-Se heterocycles (**1** and **2**, with R = ^{t}Bu and ^{i}Pr, respectively), recorded at B_0 field strengths of 9.4 and 20.0 T, are shown in Figure 1.

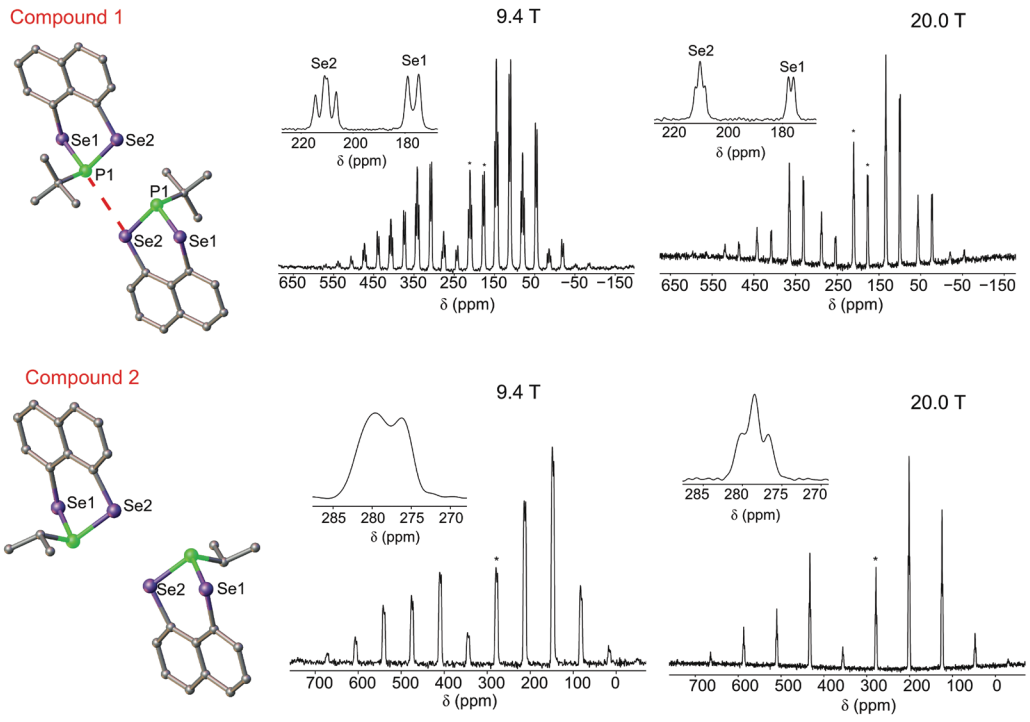

*Figure 1. Portions of the crystal structure and ^{77}Se MAS NMR spectra, acquired at B_0 fields of 9.4 and 20.0 T, of compounds **1** (top) and **2** (bottom). The MAS rates are 5 kHz (9.4 T) and 12.5 kHz (20.0 T).*

In both materials, two crystallographically-distinct Se sites are expected to be present, both bonded to the same P species, with two doublets therefore expected in each of the MAS spectra. For **1**, two distinct signals are observed (centred at ~211 and ~178 ppm), while for **2**, only one composite resonance, at ~278 ppm, is present. Note that the exact shifts observed vary with MAS rate, most likely as a result of the dynamics of the alkyl chains (caused by increased fractional heating at faster MAS rates). In each case, the significant ^{77}Se CSA produces a variety of spinning sidebands. As shown in the expansions (inset), multiplet structures are obseved for all resonances. At both fields the centrebands for **1** show a clear doublet for the upfield Se, but what appears to be a "doublet of doublets" for the Se at higher shift. The doublet splitting for the Se at 178 ppm is ~320 Hz, in relatively good agreement with the ^{1}J ^{31}P-^{77}Se couplings observed in solution. Two couplings of ~ 340 and 270 Hz can be extracted from the multiple field measurements for the signal at ~211 ppm. A significant ^{1}J coupling to ^{31}P would be expected for this Se but, while nominal "through-space" J couplings between *peri*-substituted Se species have been observed in solution, the low natural abundance of ^{77}Se would not produce the multiplet patterns observed in this case. The crystal structure offers some insight, with Se and P of neighbouring molecules separated by only ~3.5 Å, *i.e.*, less than the sum of the van der Waals radii. This raises the possibility of an extremely unusual intermolecular interaction that takes place *via* an intermolecular "through-space" *J* coupling between the P and Se of two different molecules – a phenomenon that has subsequently been confirmed by periodic density functional theory calculations.[2]

For compound **2**, where P and Se species in different molecules are separated by a greater distance, the ^{77}Se spectrum obtained at 9.4 T revealed, unexpectedly, the presence of just one broader resonance, rather than a resolved multiplet. The increased resolution at higher field reveals a more complicated multiplicity, believed to arise from the two crystallographically-distinct Se sites having very similar isotropic chemical shifts and similar ^{77}Se-^{31}P *J* couplings.

Further work is in progress to study in detail the nature and origin of these unusual couplings and to expand the range of novel heterocycles considered.

References

1. Demko, B. A.; Wasylishen, R. E. *Prog. in Nucl. Magn. Reson. Spectrosc.* **2009**, *54*, 208.

2. Sanz Camacho P.; Athukorala Arachchige, K. S.; Slawin, A. M. Z.; Green, T. F.; Yates, J. R.; Dawson, D. M.; Woollins, J. D.; Ashbrook, S. E. *J. Am. Chem. Soc*. **2015**, *137*, 6172.

Development and Application of ^{14}N Overtone NMR Spectroscopy to Biological Solids Under Ultra-Fast MAS

Ibraheem M. Haies,[1,2] James A. Jarvis,[3] Philip T.F. Williamson[3] and Marina Carravetta[1]

[1]*School of Chemistry, University of Southampton*

[2]*Department of Chemistry, University of Mosul, Mosul, Iraq*

[3]*School of Biological Sciences, University of Southampton*

Overview

The PRESTO-II sequence has already been used to transfer polarization from high-gamma species to other spin I = 1/2 nuclei as well as to half-integer quadrupolar spins.[1,2] Recently we reported polarization transfer using PRESTO from ^{1}H to the ^{14}N overtone transition under moderate spinning frequency conditions (10-20 kHz).[3] In this work, we explore a different experimental regime by comparing direct excitation ^{14}N overtone spectra at different spinning frequencies.

^{14}N Overtone Direct Excitation and Polarization Transfer

Figure 1 shows experimental results for ^{14}N overtone direct excitation for glycine at different spinning frequencies using the JEOL 1 mm probe. All spectra are recorded near the 2 overtone spinning sideband, hence each spectrum appears at a different position. For the sake of convenience, the spectra are plotted on an arbitrary scale where the 0 is set at the position for the 2 sideband for each spinning frequency.

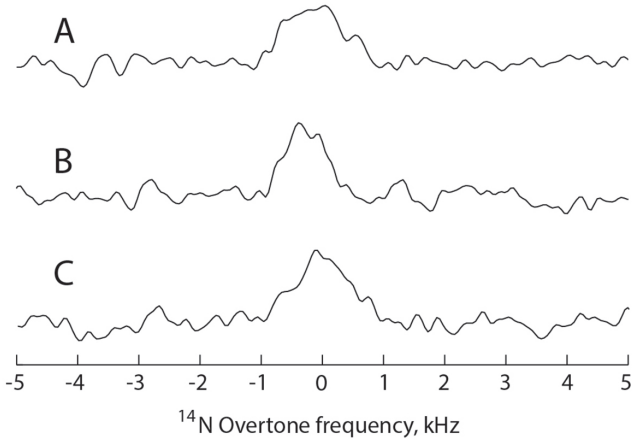

Figure 1. ^{14}N overtone direct excitation spectra of glycine, acquired at 20.0 T with 45,000 coadded transients, using a 130 kHz rf nutation frequency and a 200 μs pulse length, recorded at different spinning frequencies of (A) 80 kHz, (B) 60 kHz and (C) 40 kHz.

References

1. Zhao, X.; Hoffbauer, W.; Gunne, J. S. A. D.; Levitt, M. H. *Solid State Nucl. Magn. Reson.* **2004**, *26*, 57.
2. van Beek, J. D.; Dupree, R.; Levitt, M. H. *J. Magn. Reson*. **2006**, *179*, 38.
3. Haies, I.; Jarvis, J.; Bentley, H.; Heinmaa, I.; Kuprov, I.; Williamson, P.; Carravetta, M. *Phys. Chem. Chem. Phys.* **2015**. *17*, 6577.

Scientific excellence

Excellent Science (2014-2015) at the UK 850 MHz Solid-State NMR Facility

The UK 850 MHz Solid-State NMR Facility offers its users access to high magnetic field, as well as specialist equipment, including ultrafast magic angle spinning (MAS) and double rotation (DOR) probes. The instrumentation available provides substantial gains in both sensitivity and resolution, allowing NMR experiments on isotopes with low receptivity or large quadrupolar couplings. The Facility supports a broad range of excellent science in the UK, from the development of novel NMR methods, through atomic-level studies of materials, pharmaceuticals and catalysts, to fundamental investigations of biological systems.

Materials and catalysts

Materials research at the Facility primarily focuses on the use of quadrupolar nuclei with low magnetogyric ratio or low natural abundance, such as ^{17}O, ^{71}Ga, ^{43}Ca, and ^{87}Sr, as probes of disordered, heterogeneous or defect structures with applications as fast ion conductors for batteries and fuel cells, biocompatible materials for orthopaedic implants and bone repair, and porous media, such as zeolites and metal organic frameworks. For example, ^{17}O and ^{71}Ga experiments carried out by Blanc and co-workers at the Facility in 2014 (pages 18-19) underpin the recent development of Ga-based langasite fast ion conductors (see for example: Rosseinsky *et al.*, *Nat. Mater.*, 2008, **7**, 498–504), providing understanding of the structural flexibility which allows the incorporation of the excess interstitial oxygen responsible for the high conductivity. A similar ^{43}Ca and ^{87}Sr multinuclear study by Laurencin and co-workers[1] gave new structural insight into strontium and calcium co-ordination polymer networks with boronate ligands used as building blocks for metal organic framework porous materials. Taking advantage of the combination of ultrafast MAS and high magnetic field, Walton and co-workers[2] used ^{71}Ga NMR spectroscopy to probe the structural disorder in γ-Ga_2O_3 which results in interesting catalytic properties. Finally, Wimperis and co-workers[3] used natural abundance ^{13}C NMR to characterize a model biocatalyst, demonstrating the potential of high-field solid-state NMR for improving molecular-level understanding of complex systems.

Case Study: New zeolite architectures

*Recent materials research, highlighted in Science as a major breakthrough of 2011 (Science **334**, 1629), involves the design of new zeolite topologies with novel adsorption and catalytic properties. Morris and co-workers have recently introduced a ground-breaking new route to targeted zeolites, but the mechanisms underlying the new synthetic methodology are not understood. Research carried out at the Facility in 2014 shows how solid-state ^{17}O and ^{29}Si NMR of enriched materials can be used to solve this problem (pages 42-43).[4] The use of high magnetic field proved to be of crucial importance for this work both for the improved sensitivity and resolution and because of the small frequency difference between ^{17}O and ^{29}Si at lower field that is increased at 850 MHz.*

Crystallization and self assembly

The combination of high magnetic field and ultrafast sample spinning offers new possibilities for solid-state ^{1}H NMR studies of the intermolecular interactions which drive self assembly, such as hydrogen bonding and π-π interactions. For example, in a NMR crystallography special issue,[5] Brown and co-workers have presented ^{1}H double-quantum and ^{14}N-^{1}H 2D spectra recorded at the Facility for a guanosine derivative. They have also shown how ^{1}H-decoupled ^{11}B spectra identify distinct monomer and dimer components in guanosine-based supramolecular hydrogels (pages 22-23).[6] In related research, Whitby and coworkers[7] reported the preparation of the first open-cage fullerene to encapsulate HF, and recorded high-field solid-state ^{19}F NMR spectra at the Facility to prove that the HF molecule rotates rapidly and almost isotropically in the supramolecular complex (pages 24-25).

Case Study: Following crystallization in pharmaceuticals

The sensitivity gained at high field allows time-resolved measurements of dynamic processes such as crystallization. Harris and co-workers[8] have developed an in-situ high-field NMR strategy for following the time evolution of crystallizing systems via a combination of solution- and solid-state NMR which allows complementary information to be obtained about changes in both phases during crystallization. This has provided important insight into pre-nucleation behaviour in solution, transformations between solid phases during crystallization and the discovery of new polymorphs (pages 32-35).

"The state-of-the-art instrumentation available at the Facility allows researchers to develop new NMR methods which take advantage of specialist hardware."

New NMR phenomena and methodologies

The state-of-the-art instrumentation available at the Facility allows researchers to develop new NMR methods which take advantage of specialist hardware. For example, during 2014 Hanna and co-workers demonstrated how ^{17}O DOR can be used to identify oxygen species in silico-oxyphosphate used for solid oxide fuel cell applications and biocompatible α-calcium pyrophosphate (pages 30-31). Similar developments have seen Carravetta, Williamson and co-workers design efficient methods for observing ^{14}N spectra based on overtone spectroscopy (pages 26-27 & 54), while Ashbrook and co-workers have invented new methods for signal enhancement in quadrupolar nuclei and demonstrated these on the low receptivity ^{25}Mg nucleus (pages 16-17). A major focus of research at the Facility involves optimization of the acquisition of challenging nuclei with low receptivity and large quadrupolar broadening, often demonstrating the feasibility of such measurements for the first time using the high magnetic field available. During 2014, measurements at the Facility included ^{127}I NMR of model crystalline phases (pages 44-45), ^{33}S NMR of natural and synthetic forms of the sulphate mineral ettringite (pages 50-51) and ^{39}K studies of polyoxometalates (pages 46-47).

Case study: Intermolecular scalar couplings

The observation of a scalar coupling in NMR is generally taken as evidence of the presence of a chemical bond between the two coupled sites. Recently, scalar couplings have been measured between nuclei that are not formally bonded in both solution- and solid-state NMR. In research carried out at the Facility, Woollins and co-workers[9] observed intermolecular scalar couplings between ^{77}Se and ^{31}P in new peri-substituted naphthalene-based heterocycles (pages 52-53). Their measurements were supported by relativistic DFT calculations which verified the presence of the couplings between non-bonded atoms and provided insight into the coupling mechanism. The research adds to the range of weak interactions that can be utilized to direct crystal packing in solids for future synthetic exploitation.

Biomaterials in bone and plant cell walls

Understanding complex biological structures requires detailed information about the molecular assembly of the component materials. Solid-state NMR, especially at the high magnetic field available at the Facility, is proving to be a powerful technique for unravelling the molecular interactions which are essential to the biological function of, for example, bone or plant cell walls. For example, Dupree and co-workers[10] made use of the high resolution obtained in ^{13}C solid-state NMR measurements at high field to study the spatial proximities between the molecular constituents of intact ^{13}C-labeled stems from the model plant (pages 28-29) *Arabidopsis thaliana*.

Case Study: Structure of bone

Duer and co-workers[11] have demonstrated that citrate anions play an important role in bone by providing bridges between mineral platelets. Their research used a combination of powder X-ray diffraction, first-principles calculations and multinuclear solid-state NMR, including ^{17}O measurements at the Facility. The resulting model for bone is a layered structure with thin platelets of a hydroxyapatite mineral phase sandwiched between hydrated layers incorporating citrate anions that prevent the formation of large crystals of bone mineral with serious consequences for the mechanical properties. The model can explain many of the known structural features of bone mineral, and the extent to which citrate is incorporated will aid future understanding of the role of bone mineral crystallinity in metabolic diseases and of the molecular basis for the mechanical properties of bone.

Protein Structure and Dynamics

In addition to the above and outside of the EPSRC remit, experiments performed at the Facility have probed protein structure and dynamics (pages 14-15, 36-41).[12-14]

References

(1) Berthomieu, D.; Gervais, C.; Renaudin, G.; Reinholdt, M.; Sene, S.; Smith, M. E.; Bonhomme, C.; Laurencin, D. *Eur. J. Inorg. Chem.* **2014**, *2015*, 1182–1191.

(2) Playford, H. Y.; Hannon, A. C.; Tucker, M. G.; Dawson, D. M.; Ashbrook, S. E.; Kastiban, R. J.; Sloan, J.; Walton, R. I. *J. Phys. Chem. C* **2014**, *118*, 16188–16198.

(3) Fauré, N. E.; Halling, P. J.; Wimperis, S. *J. Phys. Chem. C* **2014**, *118*, 1042–1048.

(4) Wheatley, P. S.; Chlubná-Eliášová, P.; Greer, H.; Zhou, W.; Seymour, V. R.; Dawson, D. M.; Ashbrook, S. E.; Pinar, A. B.; McCusker, L. B.; Opanasenko, M.; Čejka, J.; Morris, R. E. *Angew. Chem. Int. Ed.* **2014**, *53*, 13210–13214.

(5) Reddy, G. N. M.; Cook, D. S.; Iuga, D.; Walton, R. I.; Marsh, A.; Brown, S. P. *Solid State Nucl. Magn. Reson.* **2015**, *65*, 41–48.

(6) Peters, G. M.; Skala, L. P.; Plank, T. N.; Hyman, B. J.; Reddy, G. N. M.; Marsh, A.; Brown, S. P.; Davis, J. T. *J. Am. Chem. Soc.* **2014**, *136*, 12596–12599.

(7) Krachmalnicoff, A.; Bounds, R.; Mamone, S.; Levitt, M. H.; Carravetta, M.; Whitby, R. J. *Chem. Commun.* **2015**, *51*, 4993–4996.

(8) Hughes, C. E.; Williams, P. A.; Harris, K. D. M. *Angew. Chem. Int. Ed.* **2014**, *53*, 8939–8943.

(9) Sanz Camacho, P.; Athukorala Arachchige, K. S.; Slawin, A. M. Z.; Green, T. F. G.; Yates, J. R.; Dawson, D. M.; Woollins, J. D.; Ashbrook, S. E. *J. Am. Chem. Soc.* **2015**, *137*, 6172–6175.

(10) Dupree, R.; Simmons, T. J.; Mortimer, J. C.; Patel, D.; Iuga, D.; Brown, S. P.; Dupree, P. *Biochemistry* **2015**, *54*, 2335–2345.

(11) Davies, E.; Muller, K. H.; Wong, W. C.; Pickard, C. J.; Reid, D. G.; Skepper, J. N.; Duer, M. J. *Proc. Natl. Acad. Sci. USA* **2014**, *111*, E1354–E1363.

(12) Lendel, C.; Bjerring, M.; Dubnovitsky, A.; Kelly, R. T.; Filippov, A.; Antzutkin, O. N.; Nielsen, N. C.; Härd, T. *Angew. Chem. Int. Ed.* **2014**, *53*, 12756–12760.

(13) Lamley, J. M.; Iuga, D.; Öster, C.; Sass, H. J.; Rogowski, M.; Oss, A.; Past, J.; Reinhold, A.; Grzesiek, S.; Samoson, A.; Lewandowski, J. R. *J. Am. Chem. Soc.* **2014**, *136*, 16800–16806.

(14) Davies, H. A.; Madine, J.; Middleton, D. A. *J. Biol. Chem.* **2015**, *290*, 7791–7803.

"Solid-state NMR, especially at the high magnetic field available at the Facility, is proving to be a powerful technique for unravelling the molecular interactions which are essential to the biological function of, for example, bone or plant cell walls."

"The broad spectrum of research now supported by the Facility is beginning to address some of the major challenges faced by society."

Impact

Broader Impact of the UK 850 MHz Solid-State NMR Facility on the Research Landscape in the UK.

Since starting operation in February 2010, the UK 850 MHz Solid-State NMR Facility has hosted research projects from more than 40 Principal Investigators originating from 20 UK institutions. One anonymous EPSRC reviewer on the recent 2014 funding extension noted that the Facility "*has now become an essential part of the NMR landscape in the UK.*"

Despite providing a bedrock for the NMR community, the use of the Facility is not limited to the NMR community within the UK. Increasingly, PIs from a broad spectrum of disciplines including the materials and biological sciences community are frequently non-NMR specialists; this is strong evidence for the wider impact of both the Facility and NMR more generally on the scientific community within the UK. Examples from 2014 include the groups of Walton (Warwick), Dupree (Cambridge), Halling (Strathclyde), and Woollins and Morris (St Andrews) – see the Scientific Excellence section.

The broad spectrum of research now supported by the Facility is beginning to address some of the major challenges faced by society. In the biological sciences, two quite separate studies published in 2014 from the groups of Antzutkin and Middleton have used the 850 MHz Facility to study mechanisms associated with the formation of amyloid fibrils, an important process underpinning a range of protein-misfolding diseases such as Alzheimer's. Other research by Duer and coworkers has used 850 MHz NMR data from the Facility to propose a new structural model for bone. The insights that these studies provides into diseases such as osteoporosis and brittle bone disease was reported in a variety of news outlets, including *The Times*, *The Independent* and *Scientific American* (see, for example, **http://www.independent.co.uk/news/science/scientists-discover-a-natural-goo-in-bones-that-stops-them-from-shattering-9217008.html** and **http://www.scientificamerican.com/podcast/episode/goo-keeps-bones-strong-but-supple**). As featured in, for example, Science Newsline, the Facility is also contributing to the development of new biofuels, supporting research by Dupree and co-workers who are investigating the development of plant cell walls.

The Facility plays a major role in the training of PhD students from NMR research groups across the UK. A total of 25 visited the Facility during 2014, gaining valuable experience in the use of specialist equipment (some not available elsewhere in the UK) such as the ultrafast-MAS probes (1.0- and 1.3-mm rotor diameter) and the double-rotation (DOR) probe, as well as the general protocols involved in working at an away-from-home laboratory.

The 4th Annual Symposium was held in April 2014 and attracted more than 60 attendees from academia and industry. This meeting has become a fixture in the UK solid-state NMR calendar, providing a showcase for the best research to come out of the Facility and a forum for discussions about the future direction of NMR in the UK. Indeed, the role of this meeting in creating a community "feel" for the UK's solid-state NMR spectroscopists cannot be overstated.

"The Facility plays a major role in the training of PhD students from NMR research groups across the UK."

"The evaluation questionnaires speak to the high degree of satisfaction associated with the use of the Facility..."

Improvements

The Facility continues to endeavour to provide the best possible experimental set-up so as to allow users to obtain very high quality data at the 850 MHz solid-state NMR spectrometer. Specific recent improvements include: the anti-vibration legs for enhancing stability when studying gel and liquid-like samples have been activated; new disposable inserts have been purchased to better enable the recording of high resolution NMR spectra for liquid/solid samples; the sample packing area has been re-organised and new procedures implemented to provide an enhanced environment for users; users who do not have access to Bruker software at their home institutions are now provided with TOPSPIN 3.2 to allow data recorded at the Facility to be processed. The evaluation questionnaires (see page 8) speak to the high degree of satisfaction associated with the use of the Facility – nevertheless, users are encouraged to make suggestions for improvements, either directly to the Facility Manager, or via the questionnaires.

As described in the user reports, a significant number of new pulse programs have been implemented by the Facility Manager and/or by users including a VOCS WURST QCPMG sequence (applied to ^{127}I) for recording very wide lines, a FAM-N sequence for improved MQMAS performance, experiments for overtone ^{14}N spectroscopy and 3D experiments providing enhanced resolution for double-quantum homonuclear correlation spectra of half-integer quadrupolar nuclei.

For the operation of the Facility as an EPSRC-funded (with partial support from BBSRC) mid-range facility under contract funding from January 2015, there have been changes to the management structure, notably the creation of an Oversight Committee whose membership comprises the three members of the external advisory board, two user representatives (at least one of whom is an early career researcher) as well as the director and deputy director who represent the Facility Executive (previously called the National Management Committee under grant funding). The Oversight Committee is chaired by the chair of the External Advisory Board, who is a NMR spectroscopist working in UK industry, Dr Stephen Byard from Covance. The new three plus two years funding also includes provision for hardware purchases, notably new magic-angle spinning probes that will, for example, provide better high-temperature capability and enable higher MAS frequencies (100+ kHz).

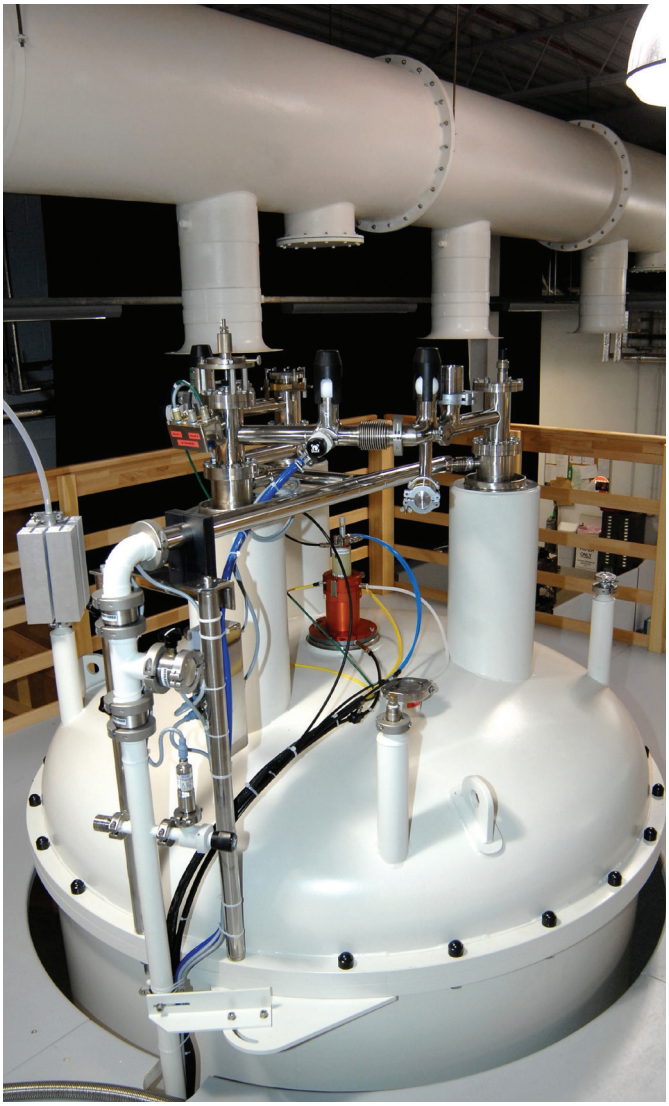

"As a solid-state NMR Facility, it stands comparison with other leading facilities throughout the World."

Strategic fit

In looking at the engineering and physical sciences (EPS) landscape where the high-level strategy has recently been updated, the refreshed strategy clearly builds on the concepts enunciated in EPSRC's shaping capability exercise. The 850 MHz Solid-State NMR Facility can readily demonstrate how it plays to key parts of the shaping capability strategy, namely of quality, importance and capacity. The underpinning quality of any work has to be of really top rank international standing. Much of physical science is underpinned by the quality of the infrastructure available; for a technique such as NMR, that plays a characterisation role, this is of primary importance to the health of a wide range of its sub-disciplines. For techniques such as this to be most effective, the community needs to have access to genuinely leading-edge instrumentation backed up by a first class environment that includes academic and technical expertise. The 850 MHz Facility demonstrably fulfils this role providing unique capability for solid-state NMR within the UK, both in the strength of the magnetic field, as well as the range of probes and experiments that the Facility can provide. As a solid-state NMR Facility, it stands comparison with other leading facilities throughout the World, hence clearly playing into this element of the EPS strategy. The importance to the user community and hence the user need, can be seen by the consistent significant oversubscription rate for time requested on the spectrometer. The quality of the research that has been carried out is indicated by the quality of the publications that have been produced, which has also been highlighted in the reports from the independent International Advisory Board.

In the context of the eight great technologies areas, commercial and wider societal challenges have been highlighted: Research carried out at the Facility has played into at least four of these eight, namely energy storage, advanced materials, regenerative medicine and synthetic biology. Looking at a more fine grained level with the research fields identified in the EPSRC portfolio, several of the areas designated as 'grow', such as catalysis, require NMR as a key characterisation approach. Investigations using the 850 MHz Facility to tackle societal challenges have included, in the wide range of materials investigated, studies of biomaterials for bone replacement, novel battery materials and pharmaceutical products which underpin some key areas of several high priority challenges.

A number of projects have been undertaken directly with industrial partners, including CASE awards. EPSRC's recently launched refreshed strategy identified the importance of providing the vital foundations that stimulate further investigation in bioscience, medicine and environmental sciences; several of the NMR approaches developed using the Facility play directly into this role.

Beyond the core scientific elements of the EPSRC strategy, other areas identified include reforming the provision of equipment with a national prioritisation of needs. Operation of the 850 MHz Facility commenced prior to these concepts becoming fully developed. However, the subsequent detailed consultation and prioritisation exercise around NMR in 2013 very clearly identified the 'pyramidal' model of access to NMR for the physical sciences community. The 850 MHz instrument remains at the apex of national infrastructure and is run very much as a shared capital item, 365/24/7. This approach and philosophy has found more resonance as work on the equipment sharing agenda has gathered pace over the last few years, in particular as new approaches have been developed for capital investment and equipment sharing following the 2010 comprehensive spending review. Through asset sharing, more efficient use of high value capital investments needs to be ensured, and the oversubscription of requests for time at the 850 MHz amply demonstrate how the Facility plays into this agenda. The time allocation mechanism and the highly skilled and experienced Facility Manager have added to the efficient use of the Facility. Under the new contract, the Facility has committed to investigating its sustainability, particularly of the recurrent funding, through targeting a mixture of funding streams to achieve this. In the spirit of equipment sharing, the contribution to the costs by BBSRC is a good example of cross Research Council sharing of assets. The learning in developing the 850 MHz Facility should provide a basis for future cross-Council thinking in developing the 1.2 GHz Facility announced in the Capital Investment Roadmap in December 2014.

User comments

"The 850 MHz National Facility is absolutely indispensable for our work on challenging biomolecular systems including protein aggregates and large protein complexes. Access to high field, the wide range of cutting edge probes and help from a highly experienced manager at the Facility ensures that we can perform our experiments to the highest scientific standards."

Józef Lewandowski, University of Warwick

"The UK is extremely lucky to have a facility like the UK 850 MHz NMR at Warwick. It is great news that it will continue for at least the next five years. The advanced experiments which it enables has certainly helped us get great insight into our chemistry."

Russell E. Morris, University of St Andrews

"The Facility provides unique access to a range of specialist probes and fields that are not otherwise available to the scientific community within the UK. This is enabling us to make significant progress in developing NMR methodologies which will enable us to study biomolecular systems at the atomic level, aiding our understanding of diseases such as amyloid disease and coronary heart disease."

Philip T. F. Williamson, University of Southampton

"The 850 MHz spectrometer has proved absolutely essential to our ^{33}S NMR research work on cementitious minerals. The high magnetic field has allowed us to record spectra of this very insensitive nucleus that we can analyse and interpret."

Stephen Wimperis, University of Glasgow

Yeast ^{15}N labeled autolyzate for insect Cell Protein Expression.

- Many eukaryotic proteins cannot be correctly produced in *E. coli*.
- Existing insect and mammalian cell growth media are highly expensive.

CortecNet is pleased to propose a ^{15}N-Kit for the expression of protein in insect cells. The kits contain 5 or 10 g of ^{15}N labeled Yeast autolyzate as well as 1 L of insect cell media depleted in amino acids (code #CN1001P5 or CN1001P10).

Expression of eukaryotic proteins in insect cells. Many proteins cannot be properly produced in *E. coli* because they need specific chaperones and/or post translational modifications in order to be correctly folded and functional. An alternative way is to express them in insect cells, easier to work with than mammalian cells. However, if commercial insect cell media are available for stable isotope labeling, their prohibitive prices are making the production of labeled samples nearly impossible for most NMR laboratories.

^{15}N labeled yeast autolyzate. An easy, inexpensive and robust method has been developed in collaboration with Bio Springer. The method allows the expression of eukaryotic proteins with **expression yields comparable to commercial media at a cost 5 to 10 times lower** than the already existing uniform insect cells labeling methods. The method has been successfully tested for both Drosophila Schneider 2 and Spodoptera frugiperda cells.

	Cell	Yield with commercial unlabeled media (mg/L)	Yield with our ^{15}N media (mg/L)
15 kDa fragment of viral protein 1	S2	15	17 (13 - 19)
15 kDa fragment of viral protein 2	S2	4	4
42 kDa fragment of cytoskeleton protein 1	Sf9	6	10 (9 - 10)

Comparison of protein expression yields obtained with S2 and Sf9 cells with a commercial unlabeled medium and with our insect cell media containing 10 g.L^{-1} of ^{15}N labeled yeast extract.

Since 20 years, CortecNet is known as one of the most reliable supplier of NMR consumables and stable isotope enriched products. CortecNet is composed of a team of analytical engineers capable to understand and fulfill all your needs. Over the years, CortecNet has developed a strong professional network including thousands of academic labs and industrial companies all around the world.

CortecNet S.A.S
15/17, rue des Tilleuls
78960 Voisins-Le-Bretonneux, France
Tél : 33 (0)1 30 12 11 31 - 33 (0)1 30 43 86 54
Email : pcorcos@cortecnet.com
www.cortecnet.com

cortecnet
INNOVATION ACCELERATOR IN LIFE SCIENCE

CortecNet Corp.
411 Ash Street, Mill Valley
CA 94941, USA
Tel: (415) 380-8700 - Fax: (415) 230-5796
Email : pcorcos@cortecnet.com
www.cortecnet.com/us

JEOL
Solutions for Innovation

NMR Spectrometer Z

JNM-ECZS Series - Next Generation NMR Spectrometer

- ***STS (Smart Transceiver System)***
  High performance in a compact size using digital circuit technology and the latest high frequency technology
- ***High stability measurements from lock feedback circuitry***
  Providing digital control of the interlock between lock frequency and the shim controller
- ***High order shim control yields high magnetic field homogeneity***
- ***Enhanced S/N without the helium - new nitrogen SuperCool cryogenic probe™***
- ***Highly stable temperature control system***
  Rapid and stable operation of attachments
- ***Improved functionality and unique design***
  Designed for ease of use with improved spectrometer functionality
- ***Compact design, high performance NMR spectrometer***

www.jeol.com

BRUKER

111 kHz probe

for ultra-fast magic angle spinning

Bruker developed the 111 kHz MAS probe for ultra-fast magic angle sample spinning, to provide a new tool for solid state NMR spectroscopists who want to improve their analytical capabilities with challenging samples. With a sample volume of 0.5 µl and unsurpassed sensitivity, this probe is ideal for studying structure and dynamics of biological samples as well as materials.

For more information please visit: www.bruker.com/MAS

Design by Mustard: www.mustardhot.com

Advantage West Midlands
www.advantagewm.co.uk

BBSRC
bioscience for the future

EPSRC
Engineering and Physical Sciences Research Council

investing in your future
European Regional Development Fund
European Union

Dr Dinu Iuga (Facility Manager)
Department of Physics
University of Warwick
Coventry CV4 7AL

T +44 (0) 24 761 50814
F +44 (0) 24 761 50897
E D.Iuga@warwick.ac.uk
W http://go.warwick.ac.uk/850mhz/

UNIVERSITY OF CAMBRIDGE
Durham University
University of Glasgow
The University of Nottingham
UNITED KINGDOM · CHINA · MALAYSIA
University of St Andrews
THE UNIVERSITY OF WARWICK